UCSF
UC San Francisco Electronic Theses and Dissertations

Title
High resolution measurements of kinesin-driven microtubule motility

Permalink
https://escholarship.org/uc/item/22h5964s

Author
Malik, Fady,

Publication Date
1993

Peer reviewed|Thesis/dissertation

eScholarship.org Powered by the California Digital Library
University of California

HIGH RESOLUTION MEASUREMENTS OF KINESIN-DRIVEN MICROTUBULE MOTILITY

by

FADY MALIK

DISSERTATION

Submitted in partial satisfaction of the requirements for the degree of

DOCTOR OF PHILOSOPHY

in

NEUROSCIENCE

in the

GRADUATE DIVISION

of the

UNIVERSITY OF CALIFORNIA

San Francisco



copyright 1993
by
FADY MALIK

To my wife, Karen and my parents, Ibrahim and Suhad

Acknowledgements

Although this thesis describes the work of an individual, namely myself, there are many others who helped make this work possible by providing advice, giving encouragement, participating in countless discussions, and of course supplying diversion to help keep my sanity and balance.

I am grateful to Ron Vale, my thesis advisor, mentor, and good friend. His advice and encouragement kept me focused and productive through some difficult times. His enthusiasm for science continues to be inspiring. Our many adventures together over the last 5 plus years contributed to what I know has been a unique experience.

I am grateful to members of the Vale lab, past and present, who were always interested in my work, sat through many a lab meeting discussing photodiodes, lasers, and vibrations, and who just were a good bunch.

I am especially grateful to Stephen J. Smith who got me started down the road of my thesis project with a beachside conversation in Monterey California.

I am grateful to all the members of the microtubule community at UCSF for their interest, conversation, and many Tuesday evenings with beer, chips, and cheese. I am especially grateful to Tim Mitchison for helpful discussions at all points in this project.

I am grateful to my thesis committee members and colleagues, Profs. Louis Reichardt, David Agard, Roger Cooke, Stephen Smith, and Ronald Vale for their interest and helpful discussions.

I am grateful to the Medical Scientist Training Program, directors David Cox and Tristam Parslow, and also, Jana Toutolmin whom everyone knows really holds things together. They provided me with an excellent framework within which to pursue a dual degree. It has been a pleasure to know my fellow MSTP students. They have been my peers and friends over the years.

I am grateful to Laszlo Bocskai, Orlando Teixeira, and Doug McVay of the UCSF machine shops for teaching me a bit of the art of being a machinist and providing many parts of the microscope.

I am grateful to my running partners over the years, David Drechsel, Mike Ignatius, Tony Hyman, and Paul Findell. They have helped to keep me sound in both mind and body.

I am grateful to my friends (they know who they are) for their support and encouragement, especially Ron Gallemore with whom many an hour was spent in both medical and graduate school toiling away together.

I am grateful to my parents for their tremendous support and love. They had faith that I knew what I was doing all these years (but I am sure they are as glad as I am that it is done!).

Finally, I am grateful to Karen, my wife and true love, whom I met just as I was beginning this project and who married me just as I finished. Her support, kind words, and company continue to be invaluable.

FUNDING

The work presented in the following pages was made possible by the following sources of financial support :

The Whitaker Foundation to Dr. Ronald Vale.

National Institutes of Health (GM38499) to Dr. Ronald Vale.

National Institutes of Health Medical Scientist Training Program Grant (GM07618) to Fady Malik.

The Lucille P. Markey Charitable Trust to the Program in Biological Sciences to UCSF.

Some equipment used in this study was donated by the Newport Corporation.

ABSTRACT

HIGH RESOLUTION MEASUREMENTS OF KINESIN-DRIVEN MICROTUBULE MOTILITY

by

Fady Malik

Recently developed in vitro assays allow one to measure the movement of single microtubules driven by a few or even a single kinesin motor. However, the mechanism by which cytoskeletal motors such as kinesin and myosin produce movement is unresolved. The most widely accepted theory states that during each ATPase cycle the motor undergoes a large conformational change (the power stroke) that alters its angle of attachment relative to the polymer. This model predicts that motors should produce stepwise movement, with the abrupt displacements corresponding to the size of a power stroke. To explore this issue, I constructed a microscope capable of tracking the movement of a microtubule with nanometer (nm) spatial and millisecond (msec) temporal resolution in attempt to observe "steps" if they exist.

The distance between kinesin binding sites on the microtubule is 8 nm. Although my system is capable of 1 nm resolution at a bandwidth of 200 Hz, the intrinsic noise of the kinesin-microtubule complex is about 4-10 nanometers, depending on how many kinesin molecules are attached to the microtubule. Under conditions in which 90% of moving microtubules are driven by a single kinesin molecule, the movement appears essentially smooth an overwhelming

majority

approx

reliable

look for

able to e

distribu

conditio

no indic

In

could de

have fou

conform

kinesin m

search a

the mot

majority of the time, although occasionally, abrupt displacements of approximately 8 nm were visible. Since visual inspection was not entirely reliable for detecting 8 nm steps, a Fourier spectral analysis was employed to look for any repetitive features in the traces. In modeled data, the analysis was able to easily detect regular 4 nanometer steps, and 8 nm steps when the distribution of time intervals had a coefficient of variation up to 20%. Under conditions in which single kinesin motors translocated microtubules, there was no indication consistent with any step size between 2 and 20 nanometers.

In conclusion, we have developed a microscope and analysis tools which could detect steps approximately the distance between kinesin binding sites. I have found no evidence for step-like behavior suggestive of a large and abrupt conformational change by the motor. Instead, I propose that the two-headed kinesin moves from one microtubule binding site to the next by a diffusional search and uses a small conformational change to provide a directional bias to the motion.



Louis F. Reichardt, Ph.D.
Committee Chairman

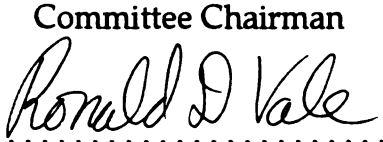

Ronald D. Vale, Ph.D.
Advisor

Chapter

Introduct
C
B
A
S
F

Chapter

Construct
nanoseco
O
D
C
D
Fi

Chapter

High reso
multiple
O
M
R
D
Fi

Chapter

High reso
single kin
O
M
R
D
Fi

Table of Contents

Copyright	ii
Dedication	iii
Acknowledgments	iv
Funding	vi
Abstract	vii
Table of Contents	ix
List of Figures	xi

Chapter 1 — *page*

Introduction
- Overview 1
- Background 2
- Approach 10
- Significance 11
- Figures 12

Chapter 2

Construction of a position detecting microscope with nanosecond spatial and millisecond temporal resolution
- Overview 15
- Design 16
- Calibration 25
- Demonstration 26
- Figures 29

Chapter 3

High resolution measurements of microtubules driven by multiple kinesin motors
- Overview 35
- Methods 36
- Results 38
- Discussion 43
- Figures 45

Chapter 4

High resolution measurements of microtubules driven by single kinesin motors
- Overview 53
- Methods 54
- Results 56
- Discussion 61
- Figures 63

Chapter

Spectral a
measurem
C
M
R
D
F

Chapter

Concludi
D
A
Fu
Fi

Reference

Appendix

Biochemic
Ki
Tu
La
La
La

Chapter 5 *page*

Spectral analysis of high resolution microtubule motility measurements
- Overview 69
- Methods 70
- Results 73
- Discussion 78
- Figures 81

Chapter 6

Concluding Remarks
- Discussion of Results 88
- A model for kinesin driven microtubule motility 90
- Future directions 97
- Figures 98

References 99

Appendix

Biochemical Methods
- Kinesin preparation 111
- Tubulin preparation 114
- Labeling tubulin with biotin 117
- Labeling latex microspheres with strepavidin 119
- Labeling microtubules with latex microspheres 121

List of Figures

Figure	Page
1-1	12
1-2	13
1-3	14
2-1	29
2-2	30
2-3	31
2-4	32
2-5	33
2-6	34
3-1	45
3-2	46
3-3	47
3-4	48
3-5	50
3-6	51
4-1	63
4-2	64
4-3	65
4-4	66
4-5	68
5-1	81
5-2	82
5-3	83
5-4	84
5-5	85
5-6	86
5-7	87
6-1	98

CHAPTER 1

INTRODUCTION

OVERVIEW

The process of how motor proteins transduce chemical energy into force and translocate along cytoskeletal filaments has long been a subject of intense study. The most widely accepted theory states that during each cycle of ATP hydrolysis the motor undergoes a large conformational change (the power stroke) that alters its angle of attachment relative to the polymer (Cooke, et al., 1984; Eisenberg and Greene, 1980; Eisenberg and Hill, 1985; Huxley and Simmons, 1971; Huxley, 1969; Lymn and Taylor, 1971). This model predicts that motors should produce stepwise movement, with the abrupt displacements corresponding to the size of a power stroke (Spudich, 1990). Despite concentrated effort, direct measurement of this power stroke has not been successful, and an understanding of the force generation mechanism is lacking. Part of the difficulty lies in the dearth of assays to study the actions of individual motor proteins rather than the averaged properties of an entire ensemble of motor proteins. In order to study the biophysical properties of this class of molecules, one must develop assays to measure the enzymatic properties, namely force production, ATP hydrolysis, and translocation, of individual molecules. The recent development of in vitro assays (Kron and Spudich, 1986; Vale, et al., 1985a), allows one to measure the movements of cytoskeletal

Chap

filamer

Howar

measur

tools w

kinesin

scale or

this mi

few and

trying t

to be so

cytoske

study a

morph

force

Schol

each

a mi

filaments driven by a few or even single motor molecules (Block, et al., 1990; Howard, et al., 1989; Uyeda, et al., 1991). Hence the opportunity arises to measure the properties of single motor molecules. What remains is to develop tools with sufficient resolution to make these measurements.

The following pages detail the development of a microscope to measure kinesin-driven microtubule translocation with a resolution appropriate to the scale on which this motor works, namely nanometers and milliseconds. Using this microscope, I have made measurements of microtubule motility driven by a few and even a single kinesin motor. My findings are presented in the light of trying to distinguish whether there exists a power stroke of sufficient magnitude to be solely responsible for movement from binding site to binding site along the cytoskeletal polymer. Finally, a model for kinesin movement consistent this study as well as others is presented.

BACKGROUND

The dynamic processes of muscle contraction, cell motility and morphogenesis, ciliary and flagellar beating, and axonal transport all rely upon force generating proteins that translocate on cytoskeletal filaments (Skoufias and Scholey, 1993; Titus, 1993). There are several classes of force generating proteins, each having unique motile properties. Myosin is an actin-based motor; dynein is a microtubule-based motor which translocates towards the minus end of the

microtubule; and kinesin is a microtubule-based motor, but it translocates towards the plus end of the microtubule.

While unique in their motile properties and cellular functions, motor proteins share several structural and enzymatic properties (for review see Vale, 1990a). Structurally, they are elongate molecules consisting of a stalk and a globular force generating domain (Fig. 1-1). The globular domain contains both ATPase and nucleotide dependent polymer binding activities and functions as the chemomechanical motor (Scholey, et al., 1989; Toyoshima, et al., 1987; Yang, et al. 1989; Yang, et al., 1990). The long stalk may serve to anchor the motor protein, either in a fixed position as with skeletal myosin (Kerwin and Bandman, 1991) or to an intracellular organelle that the motor is translocating along a cytoskeletal filament (Vale and Goldstein, 1990). Most importantly, these proteins are enzymes which catalyze three distinct "reactions", namely ATP hydrolysis, translocation, and force generation. These reactions are intimately coupled; the free energy changes associated with ATP binding and product release provide the energy for these motor proteins to do work (Cooke, 1986; Eisenberg and Hill, 1985). This work may be distributed as either force or velocity; the equation that describes this relationship is Work = Force*Velocity *time (F*V*t). For a given amount of energy derived from ATP hydrolysis in the time of an ATP hydrolysis (t), one can generate mostly force and move very slowly (isometric contraction of muscle) or one can generate very little force but move quickly (rapid shortening against no load). Thus, motor proteins are

mechanochemical transducers; they convert the energy of ATP hydrolysis into useful mechanical work, manifested as force production and translocation.

A full understanding of mechanochemical transduction involves appreciating how the motor protein hydrolyzes ATP, how the motor protein moves along the cytoskeletal filament, and how the these two processes are interrelated. A large body of work has provided information on the kinetic intermediates and actin binding constants of different states in the myosin ATPase cycle (shown in simplified form in Fig. 1-2a, for review see Goldman, 1987; Cooke, 1986; Taylor, 1992). In the absence of nucleotide, myosin binds strongly to the actin filament. Binding of ATP to myosin releases myosin from the filament. Nucleotide hydrolysis occurs and myosin rebinds to the filament weakly; binding to the filament accelerates the release of products (ADP and P_i), during which time the affinity of the actomyosin interaction increases. With the release of products, myosin returns to its original state, presumably having moved along the actin filament by some incremental distance. Since these biochemical studies are done in solution, it has not been possible to make any measurements of translocation or force generation in concert with the kinetics of the ATPase cycle. The kinesin ATPase cycle is similar to that of myosin (Hackney, 1988; Hackney, et al., 1989; Sadhu and Taylor, 1992) except that kinesin does not seem to detach from the microtubule after binding ATP; instead it detaches from the microtubule in an ADP bound state (Fig. 1-2b, Romberg and Vale, 1993).

Unfortunately, these biochemical studies do not provide any evidence for how a motor protein might move from one binding site to the next along a cytoskeletal filament. Investigation of muscle fiber contractile properties has led to several models attempting to relate the ATPase cycle to resulting movement along the actin filament. The models can be grouped together as either tightly coupled models or loosely coupled models.

In tightly coupled models (Eisenberg and Greene, 1980; Eisenberg and Hill, 1985; Huxley and Simmons, 1971; Huxley, 1969; Lymn and Taylor, 1971), the motor protein head binds to the polymer strongly, forming what is called a crossbridge. The head then undergoes a conformational change, probably involving a rotation of the head about a pivot point, that moves the polymer, and then detaches. Nucleotide binding, hydrolysis, and product release, establish the timing of this cycle. In such a model, the increment of forward movement for one ATP hydrolysis, known as the **step size**, cannot be greater than the distance through which the head is able to move, about 20 nm in the case of myosin. Although much effort has been expended in trying to measure such a conformational change, no one has been successful to date. Recently, the three dimensional structure of both actin (Holmes, et al., 1990; Kabsch, et al., 1990) and myosin (Rayment, et al., 1993b) has been solved. A model for how the two might bind to each other and how a conformational change might generate movement has been proposed (Rayment, et al., 1993a; Schroder, et al., 1993). In this model, ATP binding and release serve to open and close a cleft on the side of

the myosin head opposite the actin binding site. These small movements are amplified by a lever arm consisting of a long α-helical segment structurally stabilized by binding of the myosin light chains and the fulcrum for the lever is at the junction between the myosin head and tail. The total movement of the head is enough to account for at least a 50 angstrom movement, the distance between actomyosin binding sites. Validation of the model still awaits measurement of the predicted conformational change, or crystallization of the head in different nucleotide states.

In thermal ratchet models (Cordova, et al., 1992; Huxley, 1957; Oosawa and Hayashi, 1986; Vale and Oosawa, 1990; Yanagida, 1990), no large conformational change is postulated. The protein uses the energy of ATP hydrolysis to bias movement into directed translation down the filament. In loosely coupled versions of this model, the step size could be much larger than 20 nm, if the motor takes several steps during one ATP cycle.

In order to resolve the issue, there have been several attempts at measuring the step size of myosin (Huxley and Simmons, 1971; Ishijma, et al., 1991; Toyoshima, et al., 1990; Uyeda, et al., 1990; Yanagida, et al., 1985). Most of the studies have been done in muscle fibers, but the fiber's structural complexity greatly confounds measurements of myosin motility. The recent development of in vitro motility assays permits one to reconstitute translocation and force production in a simplified system using purified proteins (Kron and Spudich, 1986; Vale, et al., 1985a). In the motility assay, microtubules or actin filaments

glide over a glass surface coated with purified motor protein, or small beads coated with motor proteins move along fixed filaments (See Fig. 1-3). The translocation in this assay occurs under the condition of no load; the motor proteins have to generate very little force (as compared to maximal force output estimated from contracting muscle) to move the filament against the small viscous drag of the solution (Yanagida, et al., 1985; Howard, et al., 1989; Vale, et al.; 1989). One can measure the velocity of these translocating filaments easily using a video microscope (Allen, et al., 1981); introduction of a load on the filament and measurement of force production is also possible using a flexible glass needle (Ishijma, et al., 1991) or an optical trap (Kuo and Sheetz, 1993).

An accurate determination of step size is of fundamental importance in discriminating between loosely and tightly coupled models. The in vitro assays permit for the first time the measurement of motor protein action in a simplified system. Investigators have pursued basically two strategies to tackle the step size problem. The first method is indirect and consists of simultaneously measuring the velocity of filament transport, ATPase turnover rate, and the number of motors interacting with a filament in the in vitro assay (nm/ATP (step size) = nm/sec (velocity) X sec/ATP (hydrolysis rate)). Using this general approach, estimates for the step size of myosin have varied from 10 nm (Toyoshima, et al., 1990), 20 nm (Uyeda, et al., 1990), to >100 nm (Harada, et al., 1987). The difficulty with the above studies is that all parameters (velocity, ATPase activity and motor protein number) have not been measured

simultaneously in the same assay; hence, the accuracy of these measurements is suspect.

A second approach is to measure the "stepping" behavior of the motor by directly observing motor-induced translocation. For the kinesin motor, the only published report that utilizes this approach is from Gelles, et al. (1988). These investigators examined video tape records of kinesin-coated beads being transported along microtubules and performed a frame-by-frame centroid analysis of the bead to extract position information to a resolution of 2 nm with a time resolution of less than 33 ms (one video frame). In their assay, they observe fluctuations in microtubule velocity at low ATP concentrations, that is rapid translocation followed by periods of slow translocation. They interpret these fluctuations as steps, whose magnitude is 4 nm. However, in their assay several motors interact with the microtubule simultaneously. Thus, at low ATP concentrations (necessary because of their limited time resolution) rigor bond formation could constrain the forward translocation of the microtubule. In support of this hypothesis is the fact that at high kinesin densities, the velocity curve at low ATP deviates from the Michaelis-Menton relationship in contrast to the more ideal behavior at low kinesin densities (Howard, et al., 1989). Recent development of an assay in which it is possible to observe translocation of a microtubule by a single kinesin molecule makes it possible to overcome this difficulty (Howard, et al., 1989). For this reason, I chose to study the kinesin motor protein to explore issues of mechanochemical transduction.

What is known about how kinesin might move from one binding site to the next along the microtubule? Microtubules are hollow tubes whose walls are formed by 12 to 14 protofilaments which run the length of the microtubule (Mandelkow, et al., 1988). Several studies confirm that kinesin moves down the microtubule by following a single protofilament (Gelles, et al., 1988; Kamimura and Mandelkow, 1992; Ray, et al., 1993) to which it is able to maintain attachment for several microns and hundreds of translocation cycles (Block, et al., 1990; Howard, et al., 1989). The distance between successive binding sites is 8 nm as revealed by electron micrographs of microtubules decorated to saturation with the bacterially expressed head subfragment of the kinesin molecule (Harrison, et al., 1993; Song and Mandelkow, 1993). This dimension is the same size as the tubulin dimer. In fact, cross-linking studies suggest that kinesin binds to the β subunit, but not the α subunit, of the tubulin dimer (Song and Mandelkow, 1993). While these findings imply that kinesin must translocate a *minimum* distance of 8 nm per hydrolysis cycle, measurements of kinesin's microtubule-stimulated ATPase activity (~20 ATP/sec) and the velocity of transport (~0.6 μm/sec) suggest that the net distance moved per ATP (~30 nm) may be greater than one tubulin dimer (Howard, et al., 1989).

The dimensions of the kinesin head are quite a bit smaller than that of myosin. The head is an oblate spheroid about 9 nm in length and 3 nm in width (Hirokawa, et al., 1989). Although it is possible to imagine that the kinesin head

might span the distance between successive microtubule binding sites by a conformational change, it is not likely that a tightly coupled motility model could account for a step size larger than 8 nm. Hence, a measurement of the kinesin step size might distinguish between tightly and loosely coupled models of force generation.

APPROACH

To resolve how kinesin moves from one binding site to the next along a microtubule, motility must be measured directly with high spatial and temporal resolution. The centroid analysis technique for position measurement has its drawbacks; its time resolution (33 msec) is too slow to discern features of the mechanochemical cycle at physiological ATP concentrations and the analysis is very time consuming. Thus, I decided to build a high resolution microscope to measure microtubule motility with sufficient resolution to detect steps if they might exist. This darkfield microscope uses a quadrant photodiode array to track two-dimensional movements with nanometer spatial and millisecond temporal resolution in real time. Silicon photodiode detectors provided an excellent solution to the problem of position detection, since they can detect an object's position with nanometer precision and at 10-100 fold faster rates than those achieved by video. Although this strategy has never before been implemented to study motor proteins in vitro, it has been applied in other biological settings. Howard and Hudspeth (1987) utilized this technique to

measure small and rapid displacements of hair cell bundles in their study of mechanically-gated ion channels. Kamiya and Kamimura (1989) have also utilized this technology to examine small ATP-dependent vibrations in isolated axonemes from Chlamydomonas. However, these investigators were imaging objects 10 to 1000 times larger than the microtubule, thus the challenge is to develop a way to do position detection on objects much smaller than before.

SIGNIFICANCE

Elucidating the mechanism of mechanochemical transduction has been perhaps one of the most extensively pursued subjects in biophysics in the last forty years. The experiments detailed in the following pages address fundamental question of the motor protein step size. In a broad sense, an understanding of mechanochemical transduction contributes to our understanding of a number of essential biological events, such as mitosis, cytokinesis, cell migration, organelle transport, and muscle contraction. The high resolution position detecting microscope developed for this study may also have more general use in biology for researchers who are interested in tracking extremely small objects in vitro or within cells. For example, these techniques could also be applied directly to study dynein-based motility.

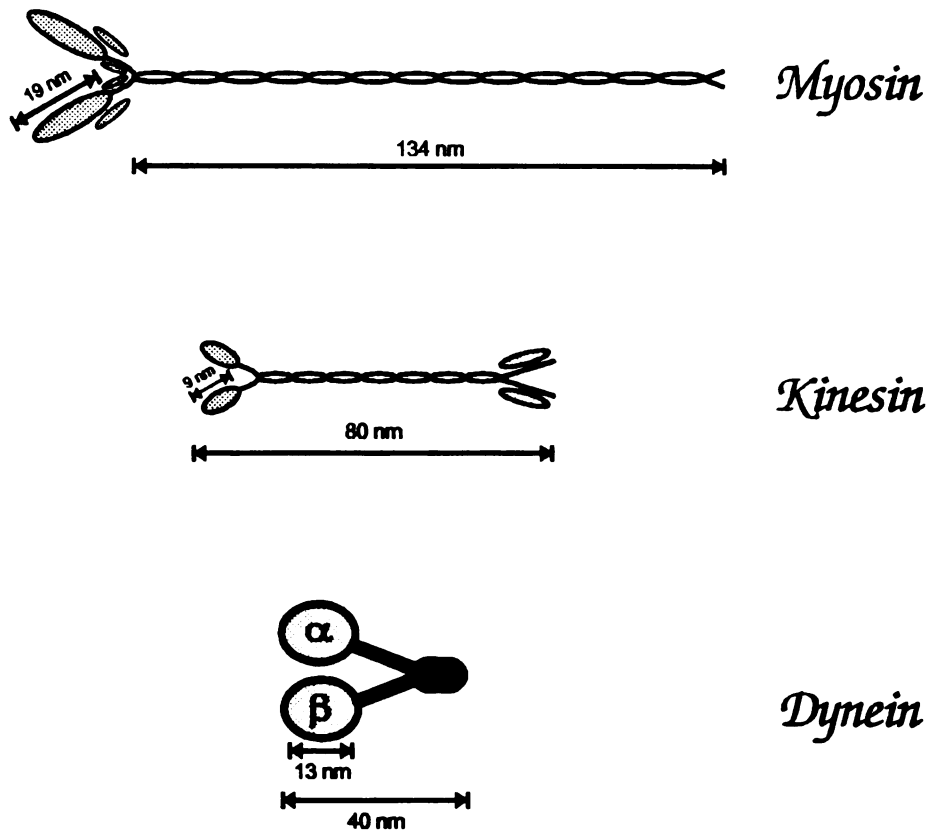

Fig. 1-1. Cartoon drawings of three different cytoskeletal motors. In all cases, the force generating domain of the motor lies at the left of drawing. The myosin motor moves along actin; it is a dimer of a heavy chain (M_r ~220 kD) with two bound light chains (M_r ~ 15 and 22 kD). The kinesin motor moves towards the plus end of a microtubule; it is a dimer of a heavy chain (M_r ~110 kD) with a single bound light chain (M_r ~60 kD). Kinesin differs from myosin in that the light chains are not bound to the force generating domains. The dynein motor moves towards the minus end of a microtubule; the outer arm axonemal motor shown here is a complex polypeptide consisting of two different heavy chains, called α and β (M_r ~500 kD each), and several different smaller polypeptides. The sizes indicated on the drawing are taken from electron microscopic pictures of these proteins.

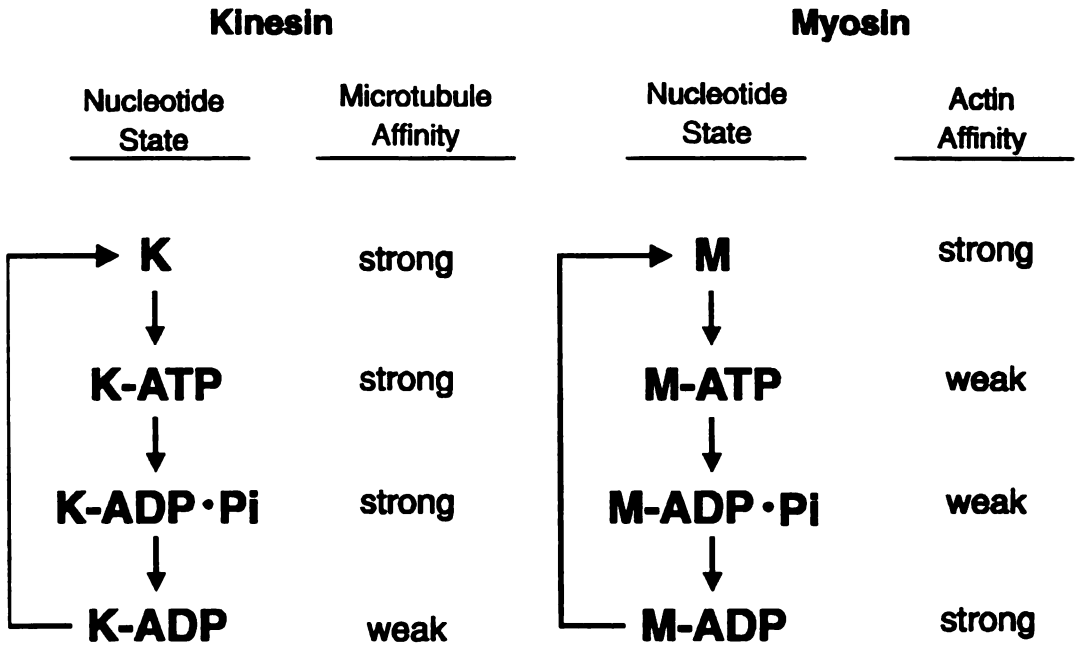

Fig 1-2. Simplified scheme of ATP hydrolysis and filament binding for myosin and kinesin. The kinesin scheme is a provisional model based upon the work of Romberg and Vale (1993). The major difference between the two motor proteins lies in the binding affinity for the filament during different states of the ATP hydrolysis cycle. The kinesin motor seems adapted for maintaining it's grasp on the microtubule throughout its hydrolysis cycle, while myosin has a prolonged period of weak binding to an actin filament. This difference may reflect the relative numbers of motors working in vivo. Relatively few or even a single kinesin motor may be responsible for moving intracellular organelles, while countless myosin motors are assembled into a muscle fiber where they are responsible for muscle contraction.

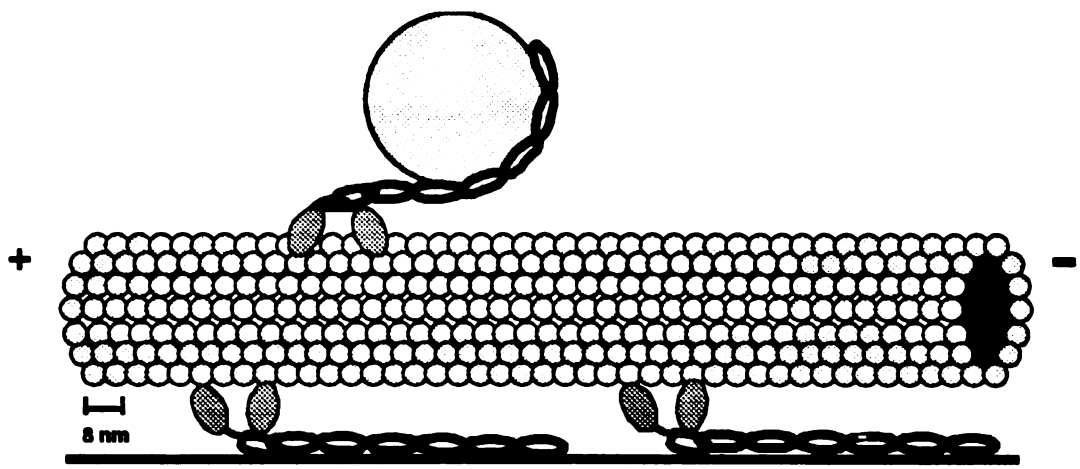

Fig. 1-3. Diagram depicting the various configurations of the in vitro motility assay. The filament in this case is a microtubule. Above, a bead with an attached kinesin molecule moves down the stationary microtubule. On the other hand, with kinesin molecules attached to the glass surface, the microtubule moves over the glass surface.

CHAPTER 2

CONSTRUCTION OF A POSITION DETECTING MICROSCOPE WITH NANOSECOND SPATIAL AND MILLISECOND TEMPORAL RESOLUTION

OVERVIEW

This chapter describes the principle of operation and design of a custom built inverted darkfield microscope which could measure the position of the microtubule with high resolution in real time. Using darkfield microscopy, it is quite easy to image single microtubules. However, the amount of light they scatter is not sufficient to make high resolution measurements of their position. The microscope uses an argon laser as a secondary light source to illuminate a 100 nm strepavidin coated latex bead attached to a biotin labeled microtubule. Now, the amount of light scattered by the microtubule is greatly increased, and furthermore, neither the microtubule nor kinesin is affected by the argon laser light. The laser illuminated image of the microtubule-bead complex is relayed to a quadrant photodiode detector array which acts as two dimensional position detector. The microscope is capable of simultaneously imaging the microtubule onto a silicon intensified target (SIT) camera so that the image can be seen on a television monitor. A motorized stage is used to position the specimen onto the photodetector so that I could avoid introducing vibration into the microscope during an experiment. The photodetector converts the light into an electrical voltage; appropriate signal processing of these voltages yields two signals whose

value is proportional to the X and Y positions of the spot on the detector. A two dimensional piezoelectric translator could move the microscope stage in nanometer displacements and provide a periodic calibration signal. Ultimately, the resolution of the microscope for a firmly fixed object was 1 nm at a bandwidth of 200 Hz.

DESIGN

Light Path and Microscope

The microscope must be optimized for stability, vibration immunity, and maximal light transmission. These properties are all essential for nanometer scale measurements. The reason for vibration immunity is obvious, at this scale even loud air borne sounds can shake the stage sufficiently to move it several nanometers. Stability means the specimen will stay in one spot for several seconds and not drift. Although seemingly trivial to achieve, at this scale temperature changes in the room can cause sufficient thermal expansion to move the specimen a considerable amount. Finally, light is the signal by which the position measurement will be made; the greatest signal to noise ratio is achieved by maximizing the amount of light available for the measurement. It is difficult to stabilize commercially sold microscopes to the degree necessary to achieve consistent nanometer scale measurements. It is also difficult to easily modify the light path of these microscopes to introduce dichroic mirrors and sliding filters. In addition, commercial microscopes frequently contain an abundance of optical

components in the light path which may provide the user with some convenience and a better image but also decrease the amount of light put through. For these reasons, I chose to design and build a custom microscope optimized for the desirable properties to make nanometer scale measurements.

The microscope is an inverted darkfield microscope made from optical mounting components and custom fabricated parts. A schematic drawing is shown in Fig. 2-1 and the numbers in parentheses refer to this figure. The microscope is anchored firmly to a vibration isolation table (Newport Inc., Irvine CA), which is ballasted with an additional one thousand pounds of lead bricks. A vertically mounted four inch thick vibration damped breadboard supports components of the light path. Illumination from a 100 W mercury arc lamp (1) and a 100 mW argon ion laser (2) (Model 5490A, Ion Laser Technology, Salt Lake City, Utah) were combined by a dichroic filter (3) (525 longpass, Omega Optical, Brattleboro, VT). The arc lamp provides field illumination for imaging purposes, while the laser, which is focused onto a spot in the specimen plane (4) coincident with the image plane of the position detector (5), illuminates the latex microsphere on the microtubule. This approach greatly augments the amount of light scattered by the microtubule, generating a sufficient signal to make high resolution measurements. Radiation pressure on the 100 nm beads was negligible (< 1 femtonewton) because free beads in solution were not displaced or trapped by the beam. During uncaging experiments (described in Chapter 4), a 530 nm long pass filter on a movable slide (6) is positioned in front of the arc

lamp. The light from the combined sources now enters the rear of a 1.2-1.33 numerical aperture reflecting ball type darkfield field condenser (7) (Olympus; Lake Success, NY) and is focused onto the specimen. An Olympus 40x 1.0 NA DPlanApoUV collects the darkfield image. The image from the arc lamp illumination passes through a second 525 longpass dichroic mirror (9) and is directed to either a binocular head or to a SIT camera (10) (Hamamatsu Photonics, Bridgewater, NJ) which sends the image to a television monitor and a sVHS video tape recorder. The second dichroic mirror (9) also reflects the laser signal and directs it to the position detector (5).

The microscope body (Fig. 2-2a) is a rectangular box made of machined aluminum on top of which is mounted an objective nosepiece and filter cube holder (Nikon, Garden City, NY). Inside the microscope body is a tight fitting aluminum cylinder which serves to align the optical axis (Fig. 2-2b). At the base of the microscope and at the bottom of this cylinder is a rotating platform supporting a prism table (Klinger Scientific, Garden City, NY) allowing for precise positioning of a silvered right angle prism (Melles Griot, Irvine, CA). The prism serves to bend the light path and with rotation of the entire assembly direct it to either a binocular microscope head or a viewport for the silicon intensified target camera.

The optical design of the microscope is very simple. The image is collected by the objective and focused at infinity by a telen lens contained within the nosepiece assembly. Conversion to an infinity focus system allows for more

flexibility in the positioning of optical components, since the light can more easily be refocused at any point back into a real image. The image going to the SIT camera passes through the second dichroic mirror and reflects off the directing prism; the infinity focused light is then formed into a real image by using a two lens telescope. The first lens of the telescope is a 160 mm focal length achromatic doublet (actually the tube lens from a Zeiss binocular head) which focuses the light onto the back focal plane of a 15X ocular eyepiece (Nikon). The telescope is made of a tube within a tube; by sliding the two tubes together and apart one can focus the image onto the camera faceplate. Variable magnification without much image degradation is achieved by moving the camera closer or further from the ocular and refocusing. The ocular and camera are coupled by a flexible rubber bellows (BMW; Bavaria, Germany) which facilitates moving the ocular relative to the camera while maintaining a closed light path.

The dichroic mirror mounted in the Nikon filter cube holder reflects the laser light towards the position detector. A 160 mm achromat (Melles Griot) and a 25x ocular (Zeiss, Oberkochen, Germany) are used to focus the image onto the position detector again using a two lens telescope to form an image on the detector. This telescope is more compact than the one used to project an image to the SIT camera to allow for mounting onto the filter cube holder.

Stage Subassembly

Perhaps the most important and most difficult to design part of the microscope is the microscope stage. The stage must function both as a stable yet mobile platform on which the specimen sits. After much trial and error the following design proved to fulfill those needs.

In order to achieve stability relative to the imaging components, the stage is coupled directly to the microscope (Fig. 2-3a). A platform attached at one end to the microscope body supports the stage assembly at the level of the objective lens. A pair of one inch diameter steel rods anchor the other end of the platform to the vibration isolation table. On this platform sits a three axis stage constructed of a heavily spring loaded X-Y steel translation stage, an aluminum block, and a single axis translation stage mounted vertically on the face of the aluminum block. The vertical stage is modified slightly so that the micrometer is mounted to the side of the translation stage rather than the end. This combination proved to be exceptionally drift free once the room had reached an equilibrium temperature.

To prevent vibrations from being introduced into the microscope during measurements, the stage was moved via remote control in X and Y with two motorized drives that were geared to a ratio of 1:1650 (Newport Inc., Irvine CA); a joystick plugged into the motor control unit was used for manipulation. While the motors were capable of moving slowly enough to permit fine positioning of the specimen, the joystick control was too coarse to control the motors

effectively. A simple modification of the joystick provided two ranges of motor speed, fast and slow. An operational amplifier divided the voltage signal the joystick was sending to the motor controller by 5 fold when switched into the signal path. Hence, by flipping a switch, I could reduce the motor speed by five fold while maintaining the full range of joystick motion. This fine control was necessary because the size of the laser illuminated area in the field was only about one micron in diameter; microtubules had to be placed directly in this region to make a measurement. Focusing the microscope was done with the vertically mounted stage and a manual micrometer.

While the motorized drives allowed the field to be scanned over a range of several millimeters, they are not capable of very small movements on the order of nanometers. Moving the specimen is the single best way of calibrating the position detector. This calibration must be performed repeatedly because the sensitivity of the position detector varies with the brightness of the object which changes continuously as the object moves through the laser spot. Hence, a way of constantly moving the stage in nanometer increments was required.

Piezoelectric devices are ideal for this purpose. Piezoelectric crystals expand a small amount (nanometers per volt) when a voltage is applied across the crystal. The specimen holder was mounted to a small stage incorporating piezoelectric elements (Fig. 2-3b) (Physik Instruments; Waldbraun, Germany) which was attached directly to the vertically mounted translation stage. By minimizing the mass of the specimen holder, rapid nanometer scale translations

of the specimen are possible. A custom built low noise amplifier using OPA 2111 operational amplifiers (Burr-Brown; Tuscon, Arizona) as output stages drove the piezoelectric stage with a 50 msec voltage pulse (sensitivity is about 70 nm/volt) so that the specimen would move 50 nm every 500 msec. This movement provided a reference signal on each record of microtubule translocation so that each record could be converted into units of nanometers. A calibration procedure for determining the magnitude of the voltage pulse to achieve a 50 nm translation will be described in a subsequent section. In conclusion, the stage assembly just described permits one to scan the microscope slide looking for microtubules, to carefully position them in the laser spot, and to calibrate the position detector dynamically during the course of an experiment.

The Position Detector

Silicon photodiodes are simple, inexpensive devices which convert light energy into an electrical current. While easy to use, their drawback is that they are not very sensitive; it takes thousands to millions of photons per second falling on the detector to get an appreciable signal (as opposed to photomultiplier detectors which are sensitive to as little as 5-10 photons). However, silicon photodiodes are readily available in a variety of detector geometries, some of which can act as exquisitely sensitive position detectors. A common way to measure the position of an object is to use a segmented detector

such as a bi-cell or quadrant photodiode. I chose a quadrant photodetector, since it is capable of giving two dimensional positional information.

The quadrant photodiode is basically a circular disk divided into four quarters (Fig. 2-4a); each quarter has its own separate current lead. When a bright object is centered on the photodiode, the light signal is equal on all four quadrants. As the image moves, then some quadrants show an increase in light signal while others show a decrease (Fig. 2-4a). By doing the proper algebraic sums, a voltage signal proportional to the X and Y position of the bright spot can be derived. A strength of this approach is that the position signal is formed by taking differences between the photodiode quadrants; thus noise in the light source which is common to all the quadrants gets canceled out.

Great care was taken to minimize the noise in the detector, because the amount of light scattered by the 100 nm bead under laser illumination is still only on the order of 100 - 500 picowatts. The detector chosen was a small area (~ 1 mm diameter) quadrant photodiode (Hamamatsu, S-1557) with a low noise equivalent power (4.5×10^{-15} W/Hz$^{1/2}$). The amplifiers needed to transduce the picoamp level photocurrents into voltages are similar to patch clamp amplifiers and use a very large feedback resistor (10 gigaohms). Special circuitry is built-in to these high impedance amplifiers to maintain the frequency response. A commercially available computer controlled eight channel instrumentation amplifier (Cyberamp 380, Axon Instruments; Foster City, CA) and four low

noise, high bandwidth picoamp to voltage converters (AI-403, Axon Instruments) were used to transduce the photocurrents into position signals.

The picoamp to voltage converters were connected directly (less than 1 inch lead length) to each of the four photodiode quadrants (Fig. 2-4b). The four headstages as well as the photodetector were housed in a shielded box, mounted onto a XYZ translation stage and coupled to the microscope via a flexible rubber bellows (BMW; Bavaria, Germany). The four headstages were connected to the Cyberamp and each channel was filtered at 2000 Hz with the built in four pole Bessel filter. The remaining four channels of the Cyberamp were used to process the voltage signals (Fig. 2-4a) to give two voltage signals proportional to X and Y movements of the spot on the detector. At the final stage, the signals were filtered with a 200 Hz four pole Bessel filter.

Data Acquisition and Software

The X and Y voltage signals as well as the signals from each individual quadrant of the photodetector were sampled at 0.5 msec intervals using an A/D board (ATDIO16-F5, National Instruments; Austin, Texas) residing in a PC compatible computer (33 MHz, 386 processor). Custom software developed using Labwindows (National Instruments) was designed to store up to 6 seconds of sampled data in memory after a keyboard trigger. The data could be displayed on the computer screen and rapidly scanned. Successful experiments

(when the microtubule had traveled near the center of photodetector) were saved to disk with a filename encoding date and time.

A video capture board in the computer allowed for display of the microscope image on the computer screen and was used to line up the microtubule-bead complex with the detector. A computer program to simply measure microtubule velocity from videotaped experiments also utilized this capture board as well as computer controlled videotape recorder with a time base reader (Panasonic AG1950; Selectra, Walnut Creek, CA).

CALIBRATION

The X and Y signals are approximately linearly proportional to the displacement of the spot on the detector for small displacements away from the center of the detector. The linear range corresponds to approximately 400 nm of travel in the specimen plane. A calculation of the photodetector output function for a simple Gaussian shaped bar of light swept across the photodiode is shown in Fig. 2-5. However, one cannot rely on an absolute calibration of the detector because the sensitivity changes with the brightness of the spot and the exact position of the spot on the detector. Thus, a method of continuously calibrating the detector during a position measurement is necessary. The piezoelectric stage incorporated into the stage subassembly was used for this purpose, because it allows for extremely small and rapid movements of the specimen.

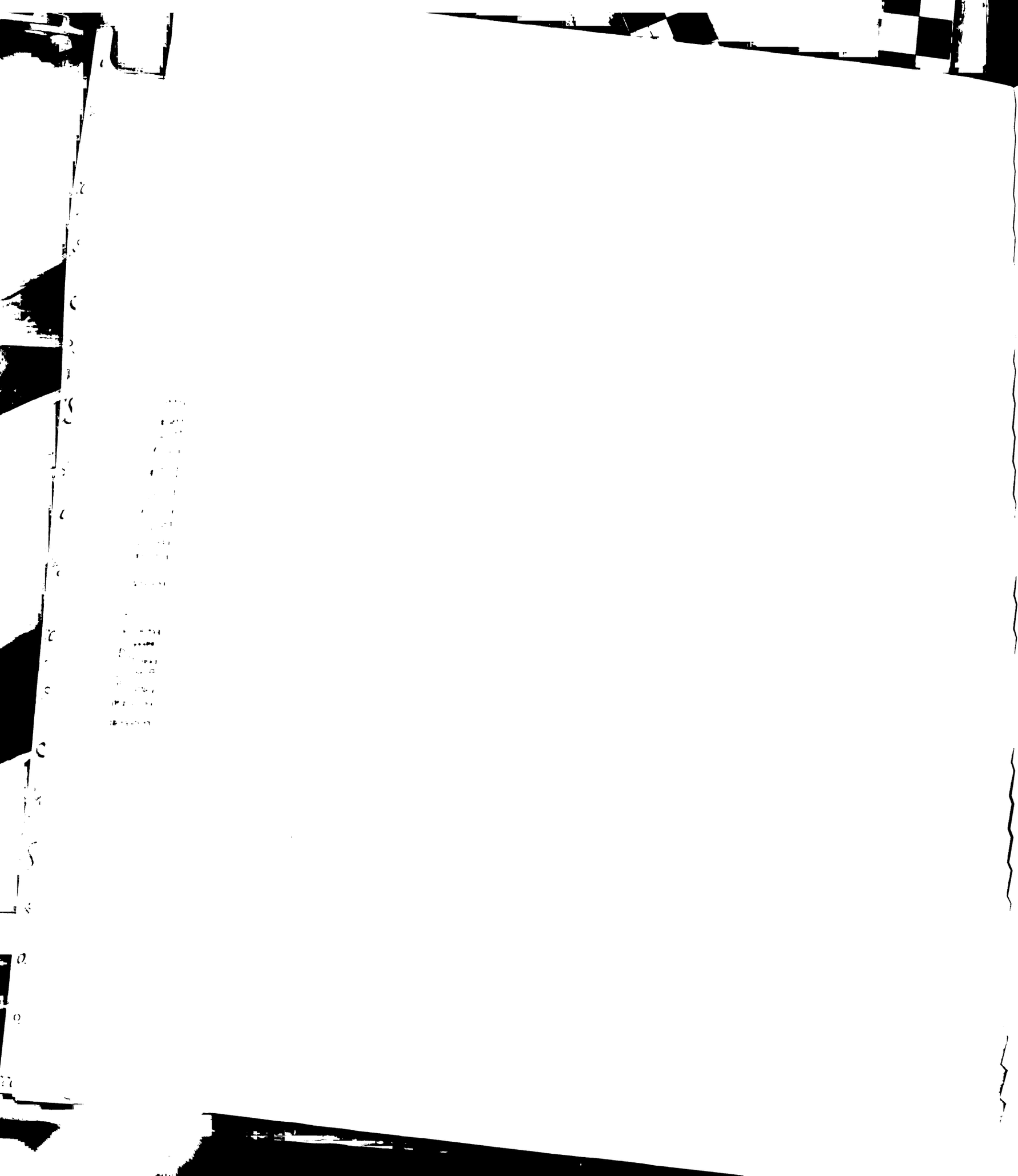

In order to calibrate the piezoelectric stage, a voltage pulse was applied to the stage to move a test spot which was focused onto the position detector. By measuring the displacement at the detector required to exactly counterbalance the stage translation the magnitude of the piezoelectric driven movement was determined. The microscope magnification (330x) translates a 50 nm movement of the specimen into a 16.5 μm movement of the spot on the detector. Thus, it is possible with a high resolution manual micrometer to measure the movement of the detector needed to counterbalance the stage movement. The voltages driving the piezoelectric stage were adjusted to give a 50 nm displacement in both the X and Y direction. The stage calibration was stable from day to day for several weeks. This calibrated stage translation could then be used dynamically to calibrate the position detector during an experiment since the stage could be moved a 50 nm increment every 500 msec.

Each individual record was calibrated by measuring the height of the calibration pulse on the record and calculating a conversion factor by dividing the height of the pulse into 50 nm. The values making up the rest of the record were then divided by this conversion factor. The resulting values of the record were now in nanometers.

DEMONSTRATION

To prepare for an experiment, the laser was carefully aligned at the start of the day with the target marked onto the video image. The raw laser beam



was directed into the back of the dark field condenser using beam steering mirrors. With all the dichroic filters in place, very little laser light would bleed through to the camera; however, enough was present to see the position of the beam. The beam was positioned empirically to achieve maximal brightness. The etched bars of a stage micrometer (Nikon) were used to find the location of the position detector in the field. The detector was then moved to the center of the field coincident with the laser beam.

To demonstrate the resolution of the detector, a small fixed bright defect in the glass slide was positioned in the target area. The amount of light scattered is similar to the light scattered by the 100 nm latex beads used in experiments. However, by its very nature, the defect is firmly attached to the glass surface and thus measurements of its position reflect purely the resolution of the microscope. Figure 2-6 is a measurement of the position of a representative particle. The r.m.s. noise of this particle is ~1 nm at a 200 Hz bandwidth. The pulse on the records is an example of the piezoelectric 50 nm calibration. Note the rapid rise time of the pulse reflecting the rapid stage translation. In fact, the speed of translation was limited to a rise time of about 4 msec by filtering the driving square pulse in order to prevent the stage from ringing with each translating pulse. Also, note the stability of the baseline of the record. There is a slightly greater amount of noise in the X channel; this noise is probably due to a vibrating resonance in the stage whose source has been very difficult to track down and remove.

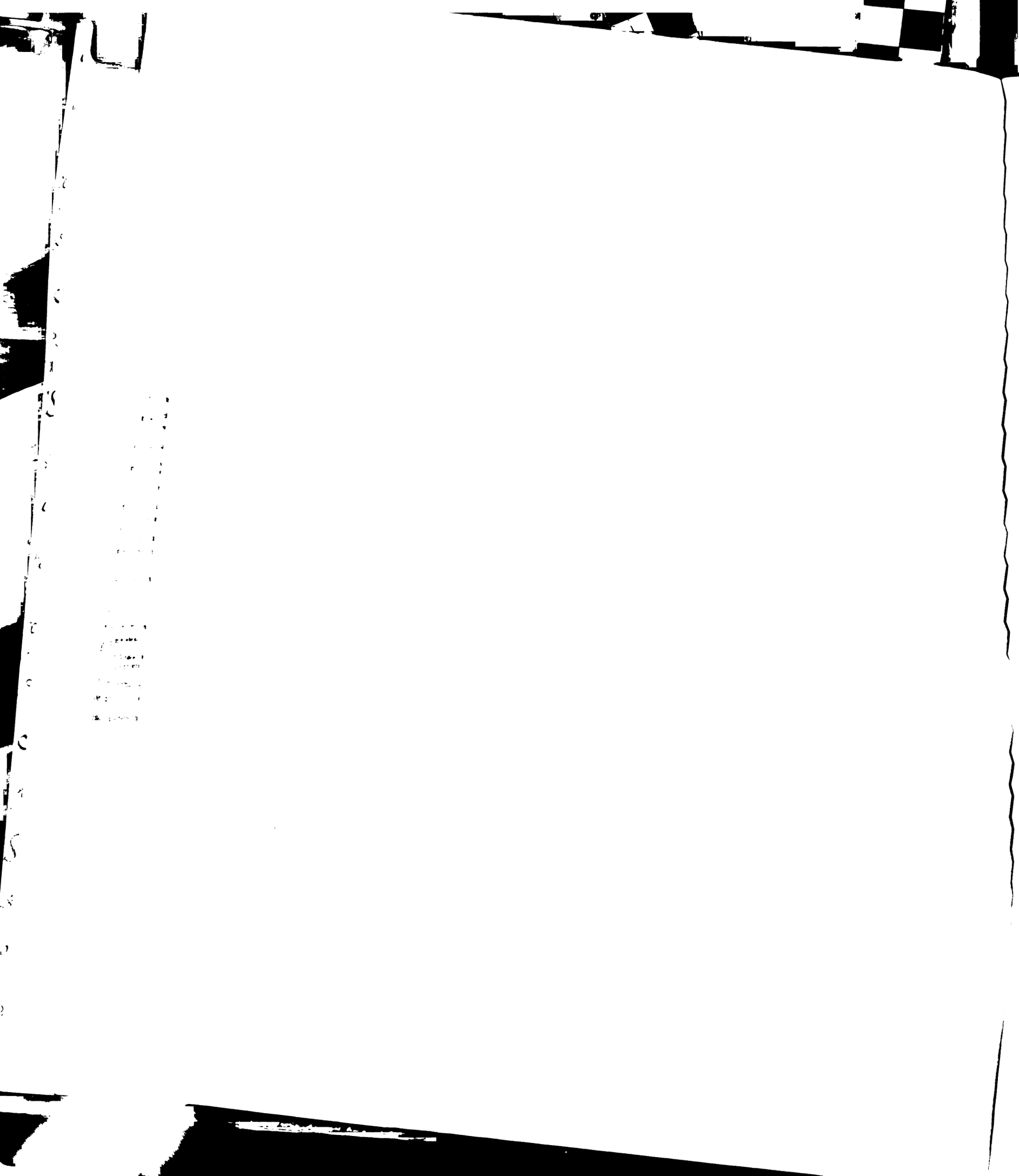

In conclusion, this microscope is capable of measuring the position of an extremely small object (a 100 nm latex bead) with a resolution near to 1 nanometer at a bandwidth of 200 Hz.

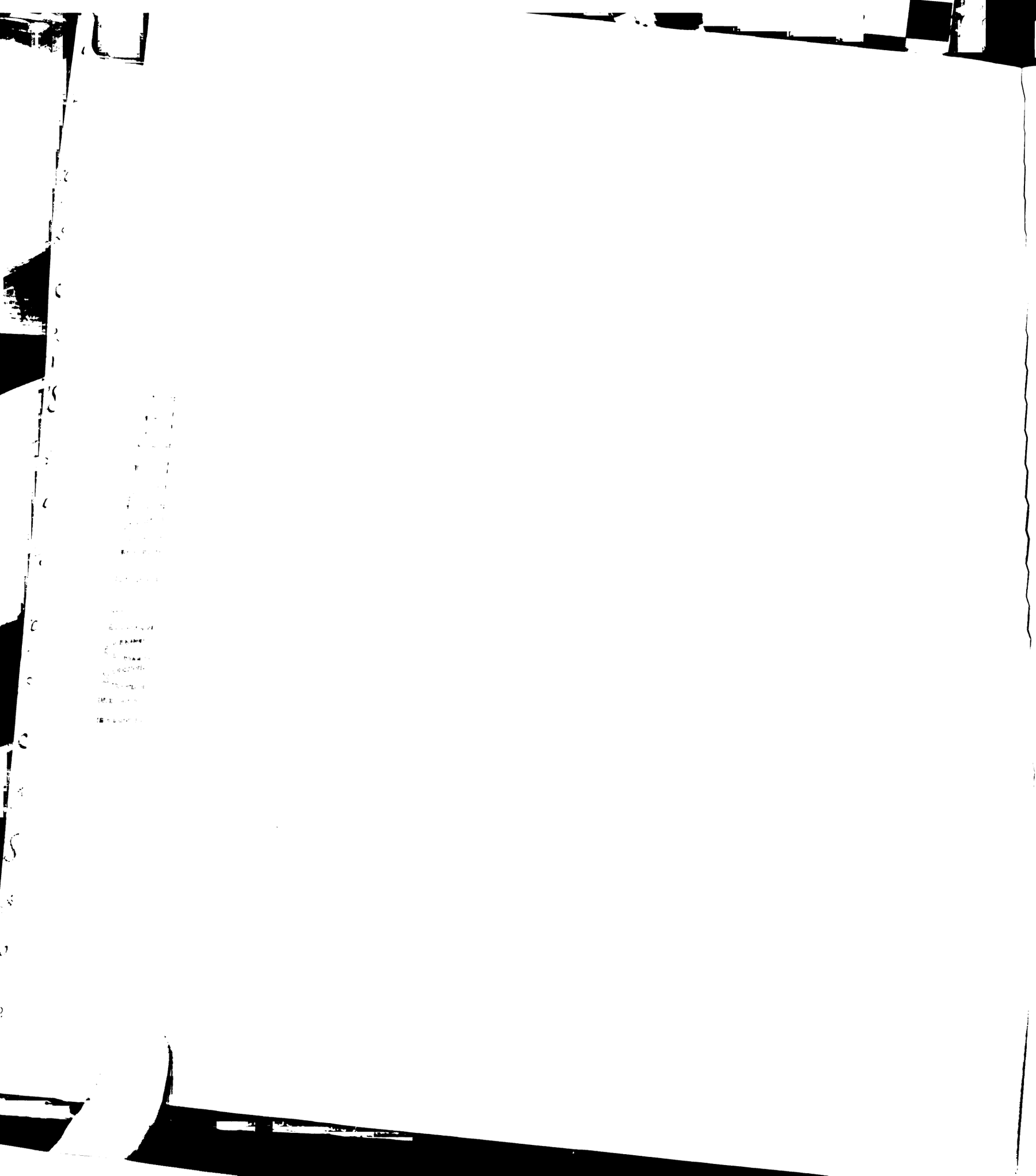

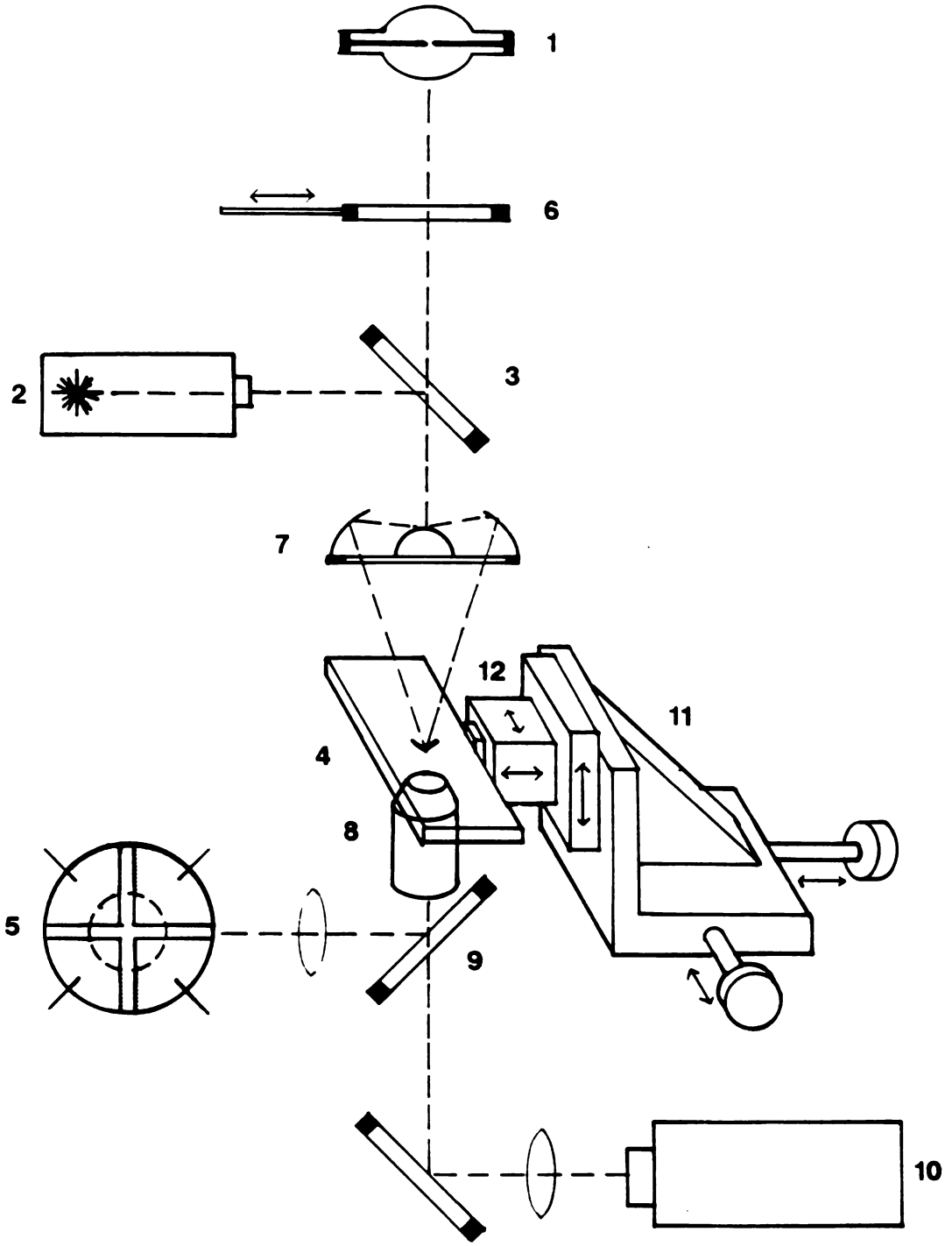

Fig. 2-1. Schematic of the nanometer spatial and millisecond temporal resolution microscope used for measurements of kinesin driven microtubule motility. A full description of the principle of operation is contained within the text of this chapter.

a)

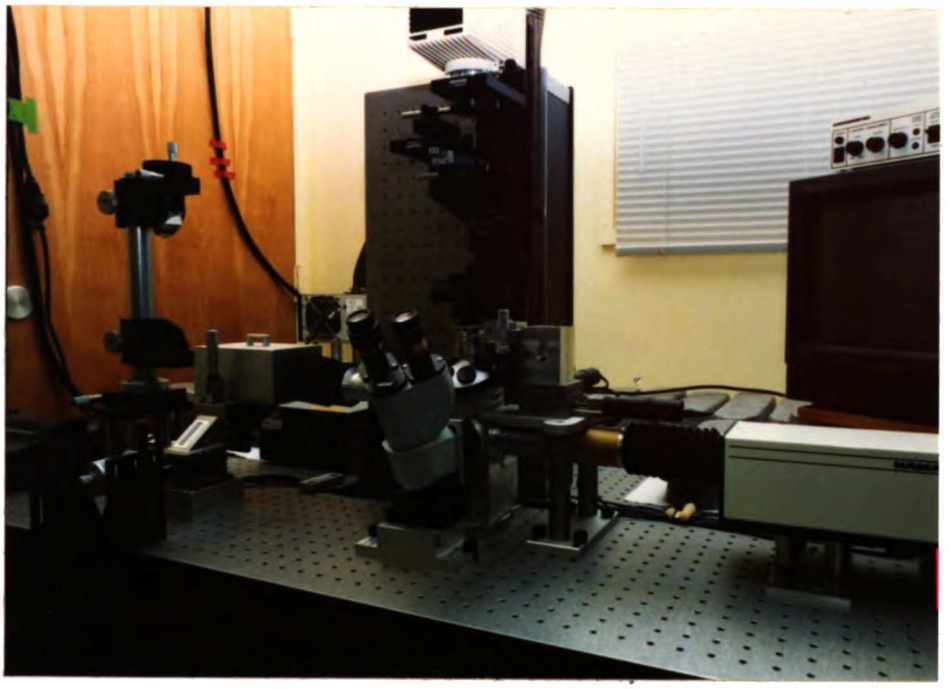

b)

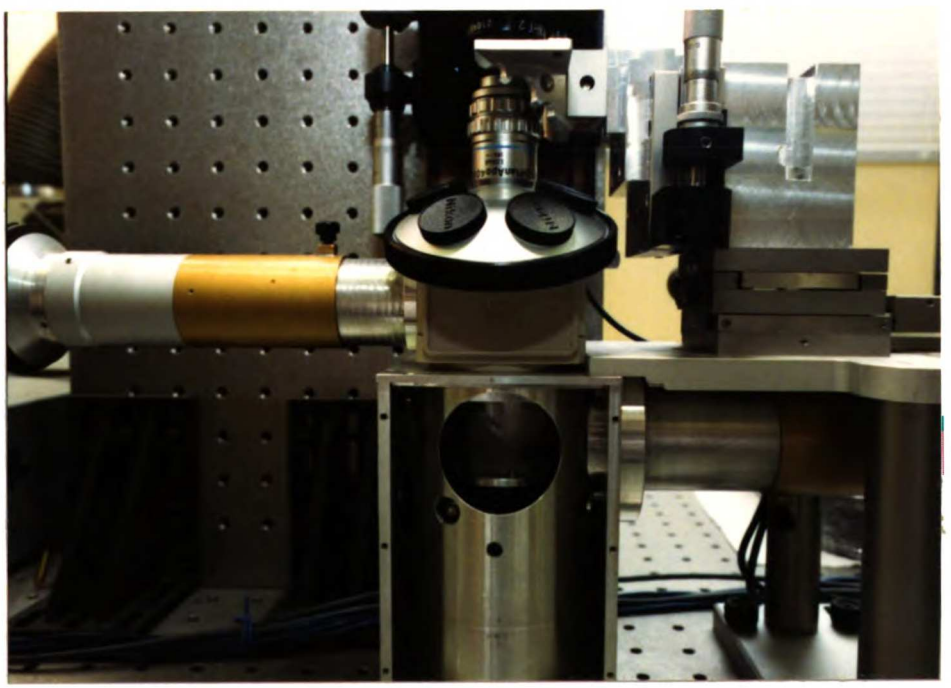

Fig. 2-2. Photograph of the microscope body. In (a) the microscope body is shown intact. In (b) the cover has been removed to expose the inner mechanism.

a)

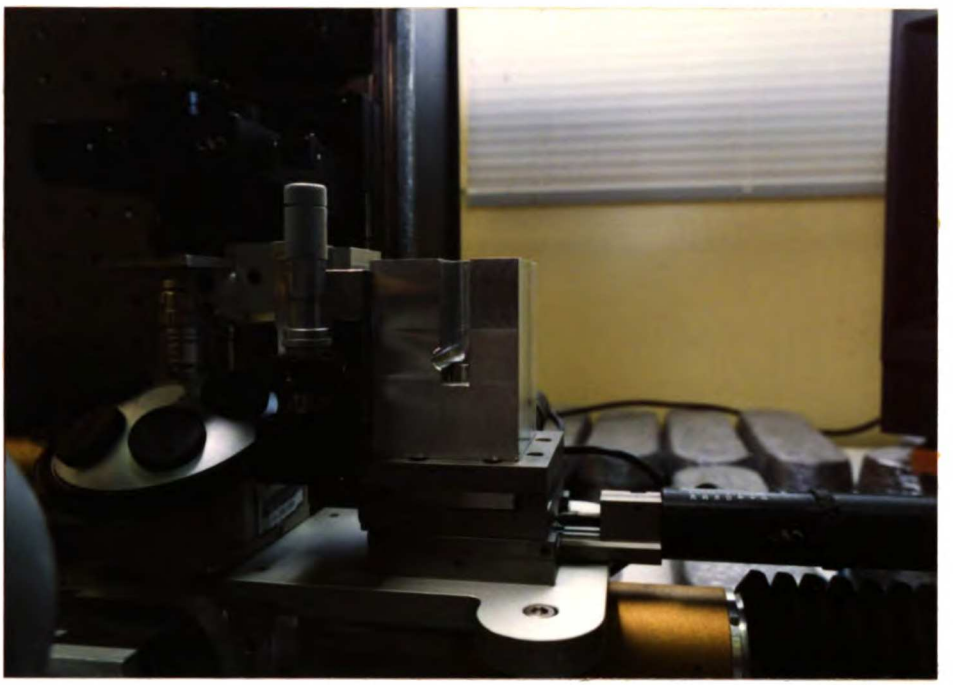

b)

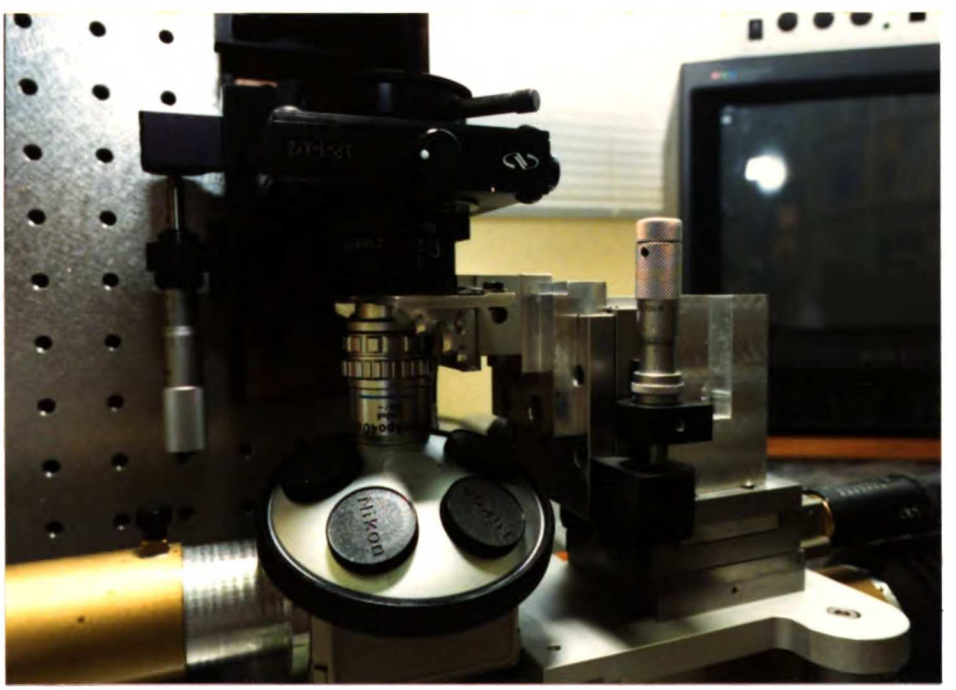

Fig. 2-3. Photograph of the stage assembly. The overall construction of the stage is shown in (a). In (b), a close-up of the stage and piezoelectric translator used for calibration.

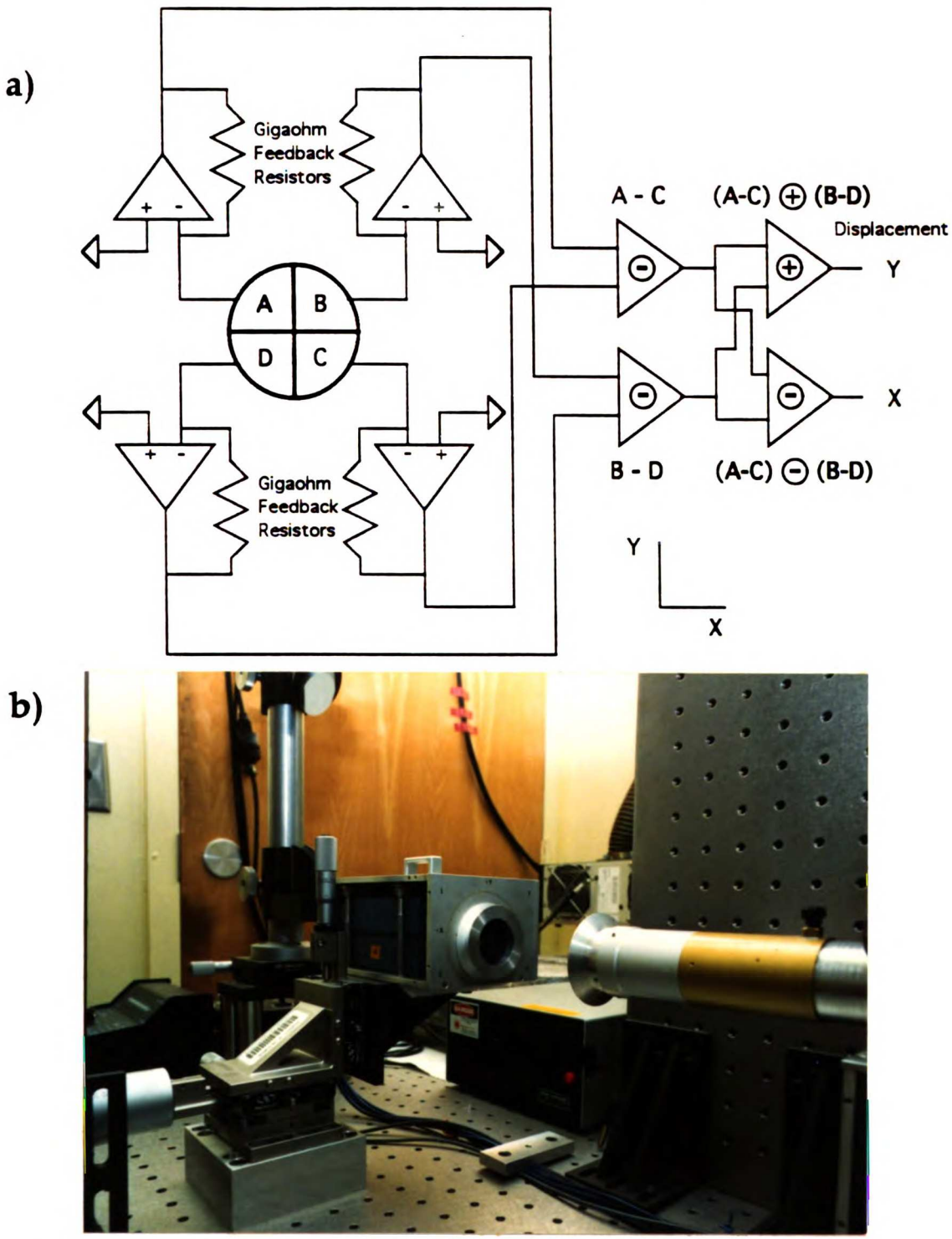

Fig. 2-4. The position sensitive detector. A schematic of the signal processing required to convert the photodiode currents into position sensitive signals is shown in (a). In (b) is a photograph of the quadrant photodiode in a housing which also contains the current to voltage amplifiers.

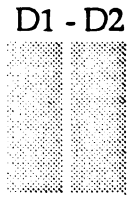

The output function of a bicell detector is simply a Gaussian shaped bar described by the constants

$\sigma := 0.2$

$x := -1, -0.95 .. 1$

$u := 0$

and the equation $\dfrac{e^{-0.5\cdot\left(\frac{x-u}{\sigma}\right)^2}}{\sqrt{2\cdot\pi\cdot\sigma}}$

gives the following profile

$\dfrac{e^{-0.5\cdot\left(\frac{x-u}{\sigma}\right)^2}}{\sqrt{2\cdot\pi\cdot\sigma}}$

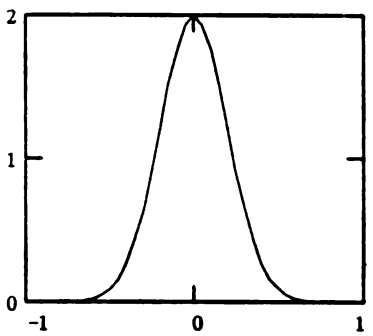

As the bar sweeps across the bicell detector, to calculate D1-D2 for any position, u of the bar.

$$D1 - D2 = \int_{-1}^{0} \frac{e^{-0.5\cdot\left(\frac{x-u}{\sigma}\right)^2}}{\sqrt{2\cdot\pi\cdot\sigma}}\,dx - \int_{0}^{1} \frac{e^{-0.5\cdot\left(\frac{x-u}{\sigma}\right)^2}}{\sqrt{2\cdot\pi\cdot\sigma}}\,dx$$

Let u vary... $u := -0.5, -0.45 .. 0.5$ then

$$\int_{0}^{1} \frac{e^{-0.5\cdot\left(\frac{x-u}{\sigma}\right)^2}}{\sqrt{2\cdot\pi\cdot\sigma}}\,dx - \int_{-1}^{0} \frac{e^{-0.5\cdot\left(\frac{x-u}{\sigma}\right)^2}}{\sqrt{2\cdot\pi\cdot\sigma}}\,dx$$

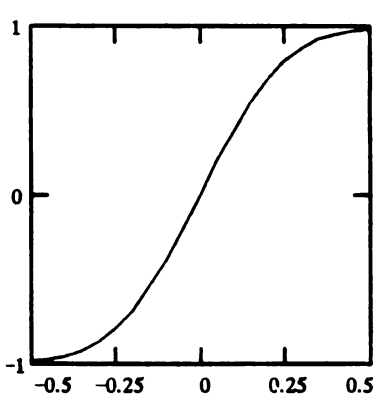

The linear range stretches from about -0.2 to 0.2, roughly equal to the standard deviation of the Gaussian curve.

Fig. 2-5. Demonstrating the linear range of a bi-cell position detector.

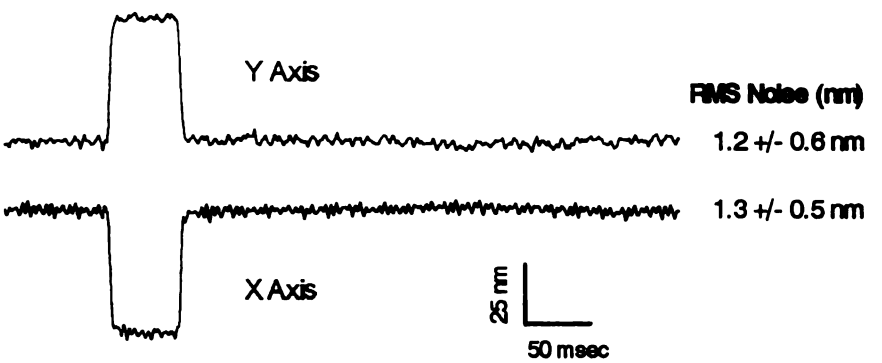

Fig. 2-6. Noise of a stationary spot on the glass surface. The records show the position of a bright defect in the glass surface. The radiant power of the spot was approximately matched to that of a 100 nm latex microsphere by varying the laser power. The upper record is the positional noise in the Y axis of the position detector while the bottom record is the noise in the X axis. The rectangular pulses on the records (upgoing in the top and downgoing in the bottom record) are the calibration pulses produced by the piezoelectric stage. They are 50 nm in magnitude. Note the rapidity with which the movement takes place. The noise magnitude is approximately equal in the two axes although the frequency distribution is somewhat different for each axis (data not shown). The average noise value of 10 different stationary spots is shown to the right of the record.

CHAPTER 3

HIGH RESOLUTION MEASUREMENTS OF MICROTUBULES DRIVEN BY MULTIPLE KINESIN MOTORS

OVERVIEW

In the motility assay used for these studies, microtubules glide over a casein coated glass surface onto which purified kinesin is absorbed. The kinesin can be diluted to low enough surface densities where only a single kinesin motor is propelling the microtubule (Howard, et al., 1989; Romberg and Vale, 1993). At these densities, microtubules move no further than their length before detaching from the glass surface. At higher motor densities, microtubules move smoothly for long distances. For this reason, I chose to first characterize the movement of microtubules at a kinesin density where ~3-5 kinesin motors would be interacting with the microtubule. The standard motility assay was modified by using microtubules with a 100 nm bead attached (Fig. 3-1) to function as a marker for the position detector and by using a lower ionic strength buffer than usual to promote tighter binding of the kinesin to the glass surface.

I made high resolution measurements of microtubules traveling at either high (200 μM) or low (50 μM) ATP. Examination of the data showed that the microtubules moved in a smooth and continuous manner for the overwhelming proportion of the time with an average resolution of about 4 nm. Although occasional abrupt displacements occurred, there was no consistent pattern of

step-wise movement. Even at ATP concentrations of 10 μM and velocities as low as 60 nm/sec, when one might expect the occasional formation of rigor kinesin-microtubule bonds, microtubule translocation was exceedingly smooth. Either, the step-like behavior of individual motors is damped by having several motors attached to the same microtubule, or the kinesin molecule itself has some intrinsic mechanism to smooth out forward translocation. To resolve these issues, in the next chapter I will describe efforts to measure microtubule movement driven by a single kinesin motor.

METHODS

Motility Assay

The multiple motor assay was performed in a perfusion chamber of simple construction. To make the perfusion chamber, two parallel strips of grease (Lubriseal; Thomas Scientific, Swedesboro, NJ) were extruded through a 20 gauge needle and placed about 15 mm apart on the slide surface. The grease was impregnated with 15 μm glass beads (Duke Scientific; Palo Alto, CA) to act as spacers for a coverslip (18x18 mm, number 1; Clay Adams, Lincoln Park, NJ) which was lightly placed on top of the grease strips; the chamber was sealed by gently applying pressure. The chamber volume was approximately 5 microliters; fluid could be exchanged through the flow cell by applying it at one

end with a pipetteman and wicking it through using number 4 Whatman filter paper (Whatman, Maidstone, England) at the other end.

For the multiple motor motility assay, one chamber volume of casein (see Appendix) was perfused into the chamber and allowed to adsorb to the surface for two minutes. The chamber was then rinsed with 3 volumes of low ionic strength motility buffer (LIB, 10 mM Tris HCl pH 7.0, 3 mM $MgCl_2$, 1 mM EGTA, 0.1 mM EDTA). A stock squid kinesin aliquot (25 μg/ml), thawed fresh for each day's experiments, was diluted 150-fold into LIB and mixed. Five microliters of the diluted kinesin were perfused into the chamber and allowed to adsorb to the casein coated surface for 2 minutes. Five microliters of microtubules with 100 nm latex beads attached (see Appendix for details) were diluted 1:50 in LIB with 16 μm taxol, introduced into the flow cell, and allowed to attach to the kinesin molecules on the surface for two minutes. To remove any unattached microtubules and beads in solution, the perfusion chamber was then rinsed with three volumes of LIB containing 16 μM taxol. Finally, two volumes of LIB containing 16 μM taxol, 0.1% methylcellulose, and either 200 μM ATP or 50 μM ATP were rinsed through the chamber to initiate motility. The methylcellulose is a non-Newtonian viscosity agent (Uyeda, et al., 1991) which prevents microtubules from diffusing away from the glass surface when they detach from a kinesin molecule but provides little resistance to movement parallel to the microtubule axis. Since I have rinsed out all the free microtubules

in solution to prevent light scatter (which hinders the position measurement), this agent is needed to prevent rapid depletion of microtubules from the glass surface as actively moving microtubules detach from kinesin and diffuse away.

RESULTS

Characterization of the Assay

At the dilution of kinesin used (0.17 μg/ml) there were approximately 4 kinesin molecules/μm^2 on the glass surface. Although it is impossible to know the exact number of motors attached to a given microtubule (unless it is just a single motor), it is possible to estimate the number of kinesin molecules per microtubule on average in two ways. First, if a microtubule is traveling along a single kinesin motor, it will detach from the surface of the glass when the kinesin molecule reaches the end of the microtubule. In the presence of methylcellulose, the microtubule usually diffuses near the glass surface and quickly attaches to another nearby kinesin motor. Only the shorter microtubules frequently exhibit this behavior; the longer microtubules travel smoothly. In this assay, microtubules < 2 μm would frequently detach before traveling further than their length. This observation provides a rough estimate of the average length of microtubule per kinesin motor; in this case, on average, there is about 1 kinesin motor per 2 μm of microtubule length. For the typical microtubule length of 5 μm, this equates to about 3 motors per microtubule. The second way to estimate

the number of kinesins per microtubule is to determine the limiting concentration at which nearly all microtubules are attached to single motors. For the kinesin stock used for these experiments this concentration is 0.011 μg/ml (data is shown in Chapter 4). Since the linear density of kinesin along the microtubule increases with the square root of concentration; then for this experiment, $\sqrt{2200/150} = 3.8$, and thus there are about 4 motors per microtubule.

The low ionic strength buffer (LIB) used in these assays reduced the noise in the linkage between kinesin and microtubule. There might be two reasons for this effect. The first is that this buffer might increase the affinity of kinesin for the glass surface. The evidence for this point is that lower dilutions (1:2200 vs. 1:800) of kinesin could be used for single motor movement than could be used in the standard motility buffer (BRB80, 80 mM KPipes pH 6.8, etc.) which might reflect better attachment of kinesin to the glass. The second reason is that the bond between the kinesin and the microtubule might be stronger. Evidence for this point lies in examination of the velocity ATPase curve. In LIB, the curve is shifted to the right as compared to the curve in BRB80 (Fig. 3-2). Both curves deviate from a Michaelis-Menton relationship indicating a drag on the microtubule, but the deviation is greater in LIB. The K_m (the ATP concentration for half maximal velocity) in LIB is about 100 μM ATP while in BRB80 the K_m is about 25 μM ATP. If motility is viewed as a simple chemical reaction, in LIB the

energy of a rigor bond maybe higher than in BRB80; a greater concentration of reactant (ATP) might required a to overcome the energy of activation for release of the microtubule, hence, the higher K_m. A second piece of evidence for a tighter rigor bond lies in the unusual behavior of the velocity vs. ATP curve at ATP concentrations less than 10 μM. At this concentration the microtubules simply stop moving. This behavior is not observed at concentrations as low as 100 nM ATP (personal observation) in BRB80. Again this phenomenon might be explained by a stronger rigor bond. As ATP concentration decreases, rigor bond formation is favored, and in LIB the rigor bonds are strong enough to prevent active kinesin molecules from advancing the microtubule. In BRB80, the rigor bonds are not sufficiently strong to prevent active kinesin motors from breaking them and advancing the microtubule. However, a single rigor bond is not enough to stop a microtubule; at lower densities of motors on the glass, microtubules move at ATP concentrations less than 10 μM (see Fig. 4-2 in Chapter 4).

High Resolution Measurements of Kinesin Driven Microtubules

As mentioned earlier, 100 nm latex beads coated with strepavidin and coupled to biotin labeled microtubules were used in the assay to make high resolution measurements. The latex bead marked the microtubule's position for the high resolution position detector. The r.m.s. noise of the bead-microtubule

complex held to the glass surface by a kinesin motors in the absence of ATP is shown in Fig. 3-3. The noise was 4-fold greater than that of a bead firmly fixed to the glass surface, reflecting the flexibility in the attachment between the bead and microtubule and the microtubule with the surface-bound kinesin. Interestingly, the component of the bead noise perpendicular to the microtubule axis was larger than the parallel component ($p < 0.05$). In other words, the bead appears to be able to rock side to side on top of the microtubule; movement parallel to the microtubule axis is more difficult either because the bead is tethered fore and aft by strepavidin-biotin bonds or the kinesin head is less flexible in this direction. This side to side rocking motion suggests that the bead was not stuck to or being dragged along the surface in the motility measurements described below.

Measurements of moving microtubules were made by introducing ATP into the perfusion chamber before placing it under the microscope. A typical microscope field would have 4-6 microtubules moving with one or two of these labeled with a latex bead. Using the joystick to control the motors moving the stage, a bead-labeled microtubule was situated so that its trajectory would cross the spot in the field coincident with the laser and the position detector. Data acquisition was started, and if the microtubule traversed near the center of the position detector, a nanometer spatial and millisecond temporal resolution record of its motion was obtained.

In the first set of experiments, an ATP concentration of 200 μM was used. Some 100 hundred examples of microtubule movement were obtained; a set of 14 examples are shown in Fig. 3-4. The average velocity of this group of microtubules is 360 ± 90 nm/sec. Close inspection of these as well as the other examples of microtubule movement show that they move in a smooth and continuous manner for the overwhelming majority of the time. Occasionally, abrupt displacements did occur and infrequently a string of two or three abrupt steps separated by a motionless pause were seen. Two examples are shown in Fig. 3-5. The size of the steps was variable as was the timing between steps; furthermore, the same microtubule can subsequently exhibit completely smooth translocation.

Since lowering the concentration of ATP increases the lifetime of the rigor kinesin-microtubule bond, one might reason that steps would become more prominent because the microtubule would spend longer in a non-moving state. Thus, some 100 examples of microtubule movement at an ATP concentration of 50 μM were obtained; a set of 14 examples are shown in Fig. 3-6. The average velocity of this slower group of microtubules is 170 ± 60 nm/sec. Even at these reduced velocities, in some cases corresponding to a maximum of 15 steps per second (assuming an 8 nm spacing of binding sites), there was still no step-wise translocation of the microtubule. Although some variations in velocity do occur, overall the movement was still remarkably smooth and continuous.

Finally, many records of translocating microtubules in the BRB80 motility buffer at different concentrations of ATP were taken; the results were the same as those in the LIB motility buffer (data not shown).

DISCUSSION

In high resolution position measurements of dozens of translocating microtubules powered by 3-5 kinesin motors, the only consistent finding by visual inspection is smooth and continuous motion. Although, occasional sequences of step-like episodes do occur, they are rare and frequently followed by completely smooth translocation. Manipulations of ATP concentration have no effect on the character of the records other than the resulting lower velocity of translocation. With a background noise of 4 nm, step movements of the kinesin motors spanning the 8 nm distance between microtubule binding sites should be readily apparent to visual inspection of the records.

How can one explain the apparent smooth translocation of microtubules at a variety of velocities? It is possible that the step-like behavior of individual motors might be damped by having several motors attached to the same microtubule. Thus, a motor undergoing its power stroke would be resisted by the other motors attached to the microtubule. Its power stroke might not be completed in a single, fast movement, but would instead apply a steady forward force which would dissipate as other motors released their grasp on the microtubule. Indeed, a computer model of in vitro translocation (Pate and

Cooke, 1991) shows that as the number of motors interacting with the filament grows, the average step becomes smaller.

The ATP versus velocity curves in the low ionic strength motility buffer suggest that rigor kinesin-microtubule bonds produce a drag on the microtubule. In fact, at low enough ATP this drag is sufficient to stop the microtubule from moving at all. In a higher ionic strength motility buffer (BRB80), the effect of the rigor kinesin-microtubule bonds is hinted at by a deviation of the ATP versus velocity curve from simple Michaelis-Menton kinetics at low ATP. However, in the case of a single motor, the shape of the ATP versus velocity curve follows Michaelis-Menton kinetics almost exactly in both BRB80 and in LIB (Fig. 4-2 in Chapter 4). This finding implies that the strength of a single rigor kinesin-microtubule bond (even a single kinesin has two heads and thus two force generating domains) is not enough to alter the kinetics at low ATP and may not impose a significant drag on the microtubule during translocation.

Even as few as 3-5 motors per microtubule are enough to complicate the interpretation of the position measurements of translocating microtubules. The logical next step is to measure microtubule movement produced by a single kinesin motor. The following chapter details these experiments and their results.

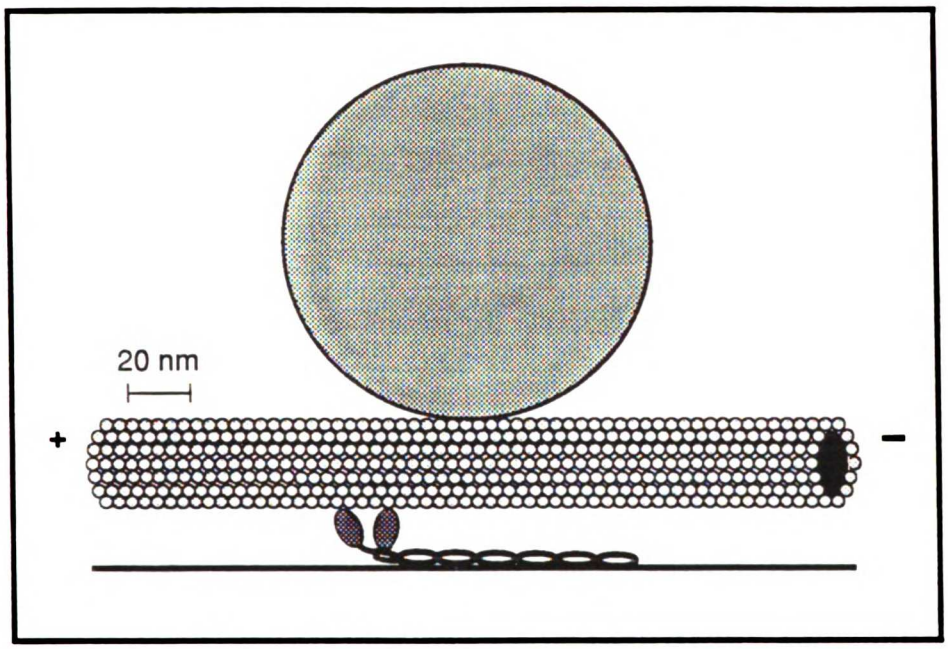

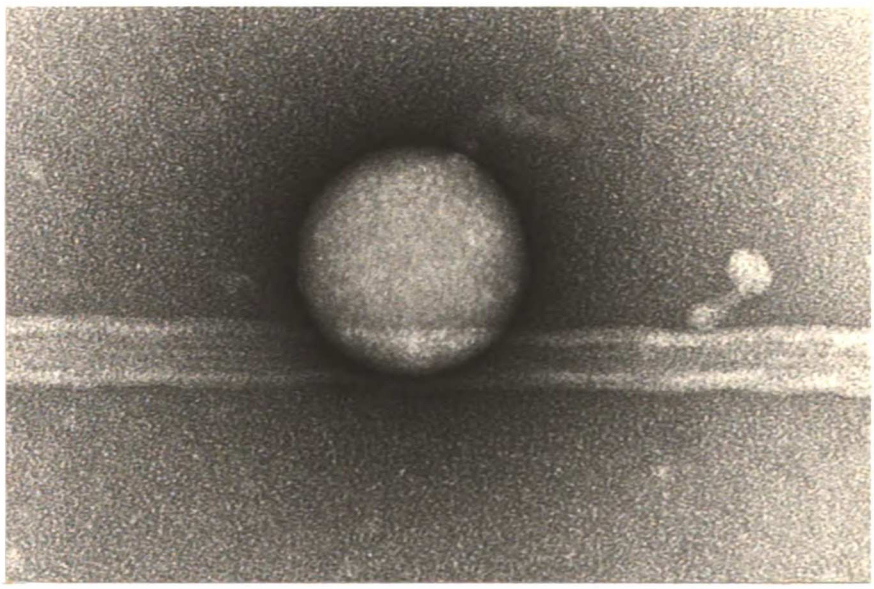

Fig. 3-1. Schematic of the motility assay in which surface-absorbed kinesin powers the transport of a microtubule. A single 100 nm strepavidin coated latex microsphere bound to a biotinylated microtubule (see electron micrograph below) serves as a bright marker to determine accurately the microtubule's position.

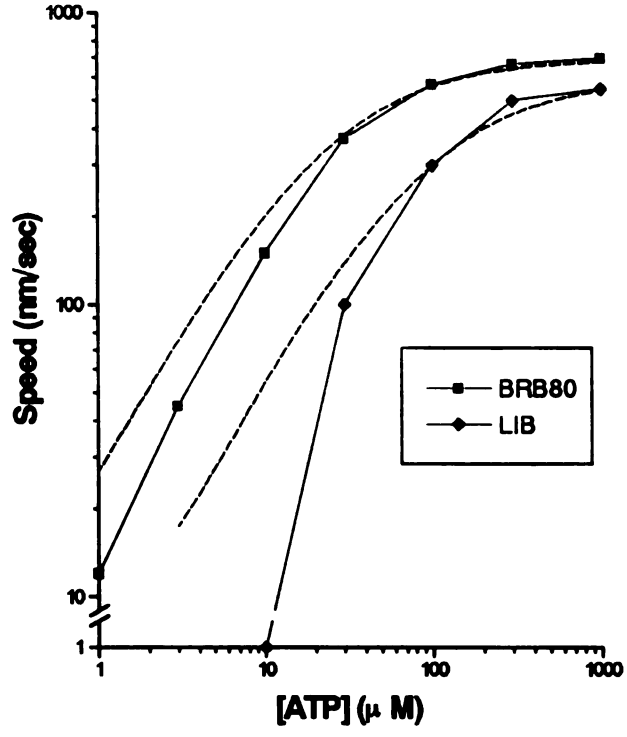

Fig. 3-2. Dependence of microtubule speed on ATP concentration at multiple motor densities. The velocities of 25 microtubules at each ATP concentration were averaged together to obtain each data point. The dashed lines are plots of the Michaelis-Menten relationship under each condition (Km = 25 μM ATP in BRB80 and 100 μM ATP in LIB). In LIB, the data deviate rapidly from Michaelis-Menton kinetics. The 10 μM ATP point in LIB represents approximately the lower limit of the velocity measurement; there was no actual movement detected at this ATP concentration. Data in BRB80 taken from Howard, et al., 1989.

MIT LIBRARIES

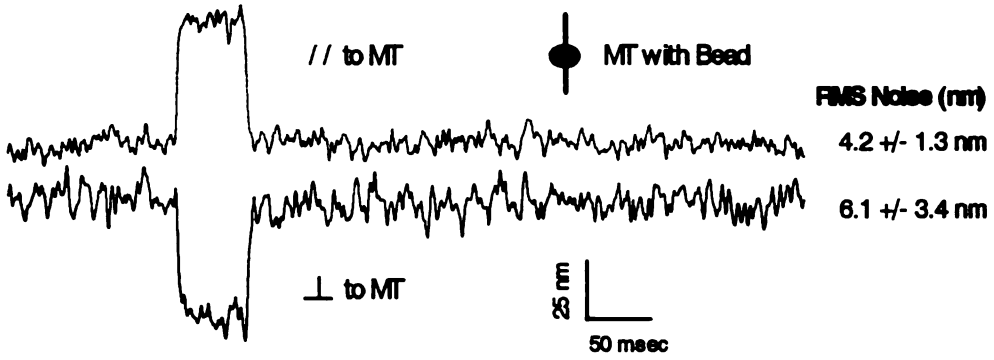

Fig. 3-3. Noise of a stationary kinesin-bead-microtubule complex at multiple motor densities. The records show the position of the bead which labels the microtubule. The upper record is the positional noise in a direction parallel to the microtubule while the lower record is the noise perpendicular to the microtubule. The rectangular pulses on the records (upgoing in the top and downgoing in the bottom record) are the calibration pulses produced by the piezoelectric stage. They are 50 nm in magnitude. Note the rapidity with which the movement takes place. As described in the text, the noise in the perpendicular direction is greater than that in the parallel direction. The average noise value of 15 different kinesin-microtubule complexes is shown to the right of the record.

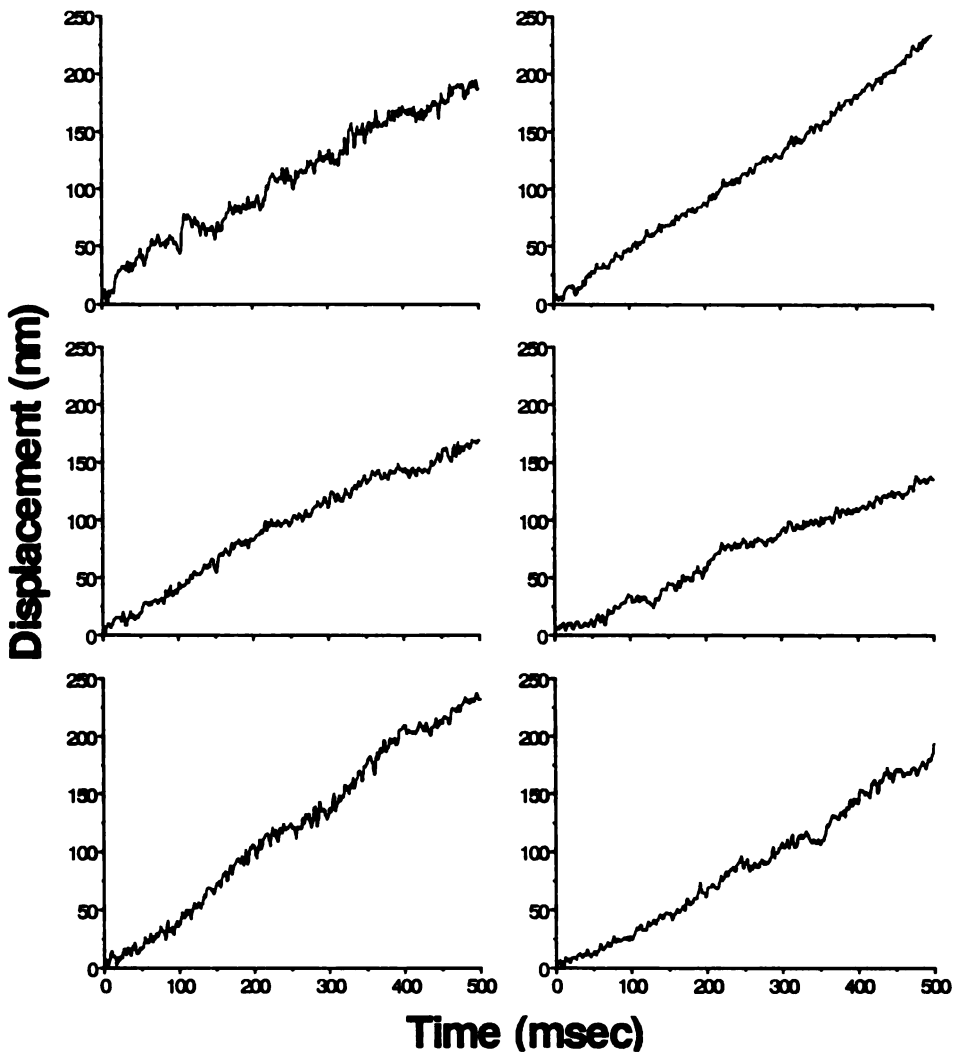

Fig. 3-4. High resolution displacement records of microtubules driven by multiple kinesin motors at an ATP concentration of 200 μM. These 14 records (figure is continued on the next page) represent movement along an axis parallel to the microtubule axis. Each record represents a different translocating microtubule. Although some changes in speed do occur, the displacements are smooth overall. Occasionally, abrupt displacements do occur (see boxed regions on next page; these are enlarged in the next figure).

UCSF LIBRARY

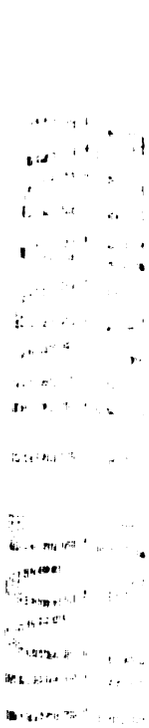

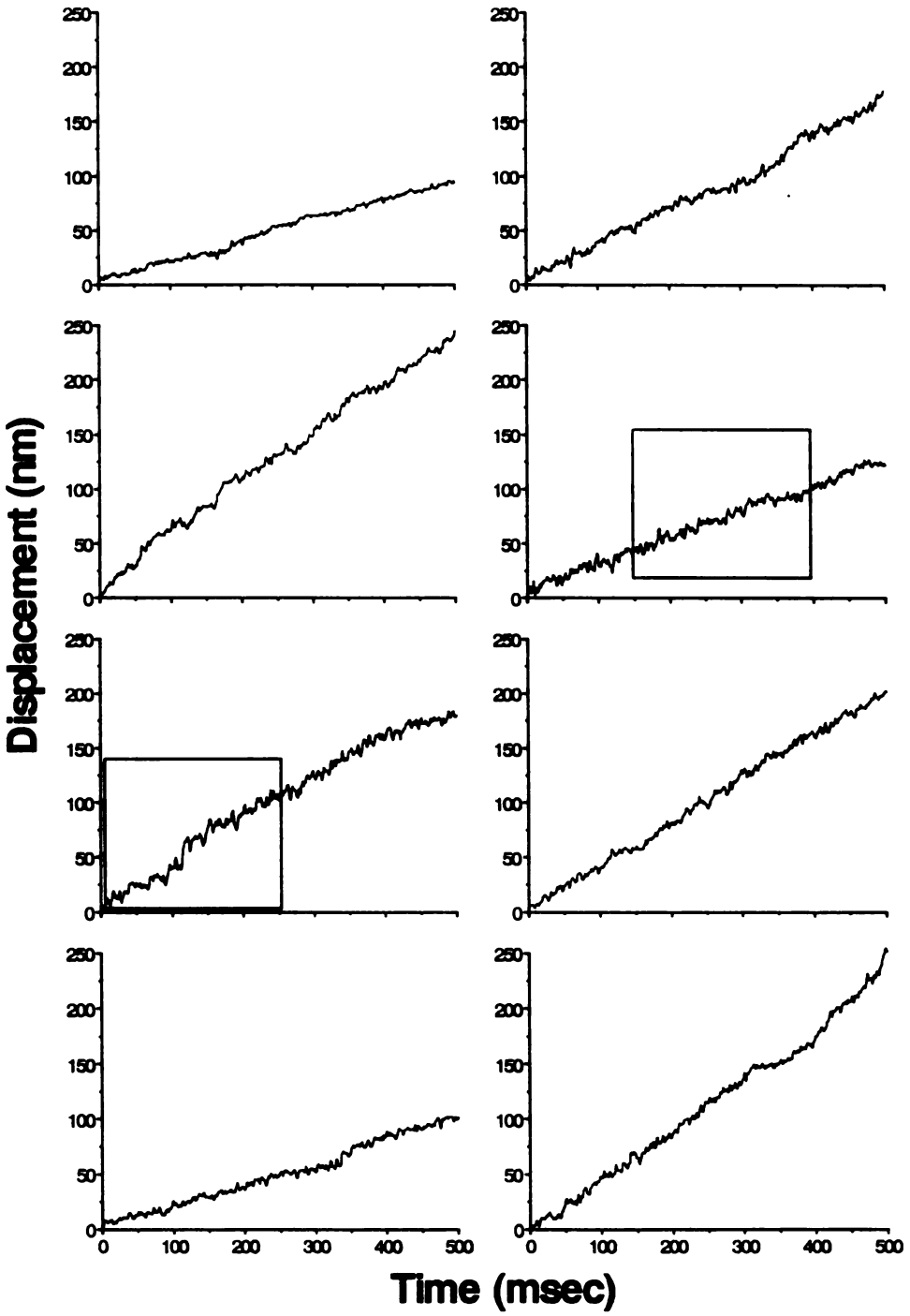

Fig. 3-4 cont.

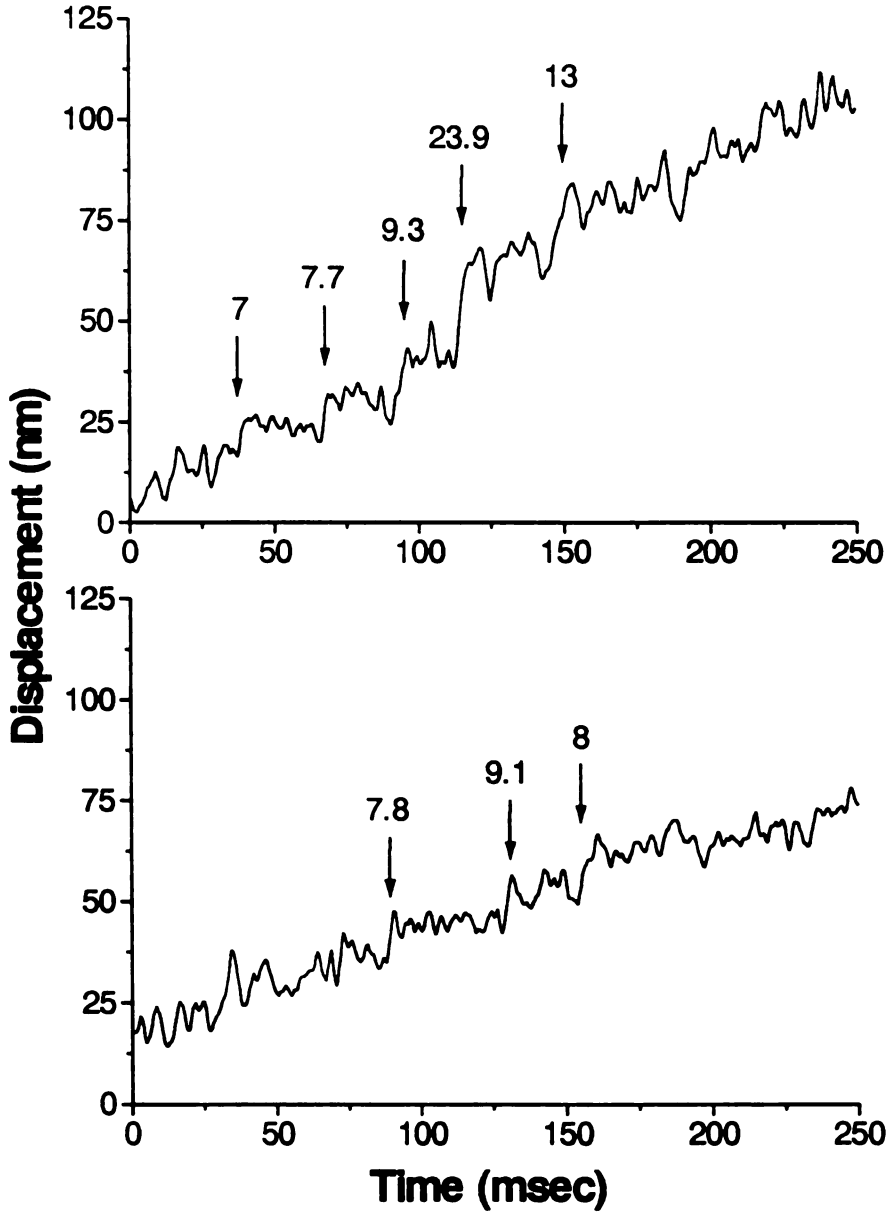

Fig. 3-5. Step-like displacements found in records of microtubule translocation shown in previous figure. Sections correspond to boxed regions on previous page. The arrows indicate abrupt displacements corresponding to "steps". The numbers above the arrows are the magnitudes of the displacements. Such displacements are rare and occur briefly in records of otherwise smooth movement, making these steps difficult to distinguish from random Brownian noise.



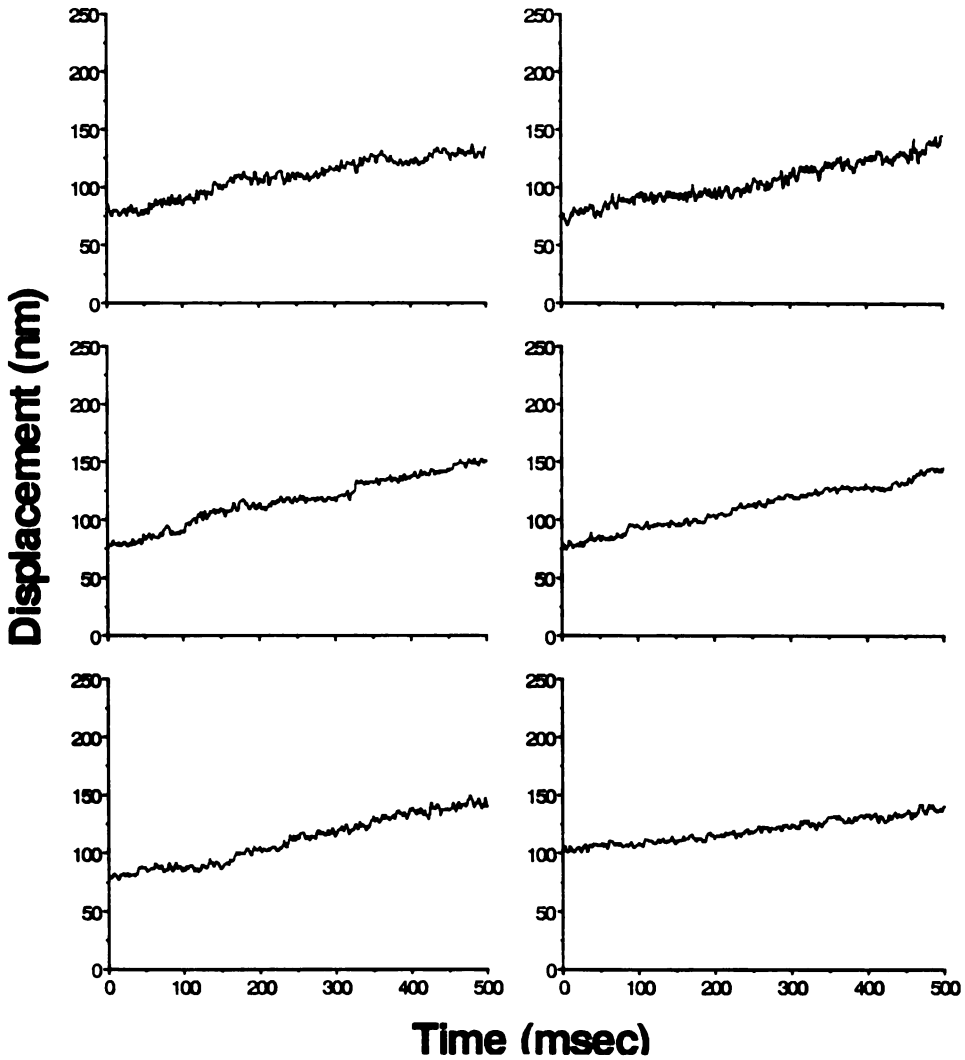

Fig. 3-6. High resolution displacement records of microtubules driven by multiple kinesin motors at an ATP concentration of 50 μM. These 14 records (figure is continued on the next page) represent movement along an axis parallel to the microtubule axis. Each record represents a different translocating microtubule. Again, although the records are somewhat more discontinuous than high ATP, the displacements are smooth overall.

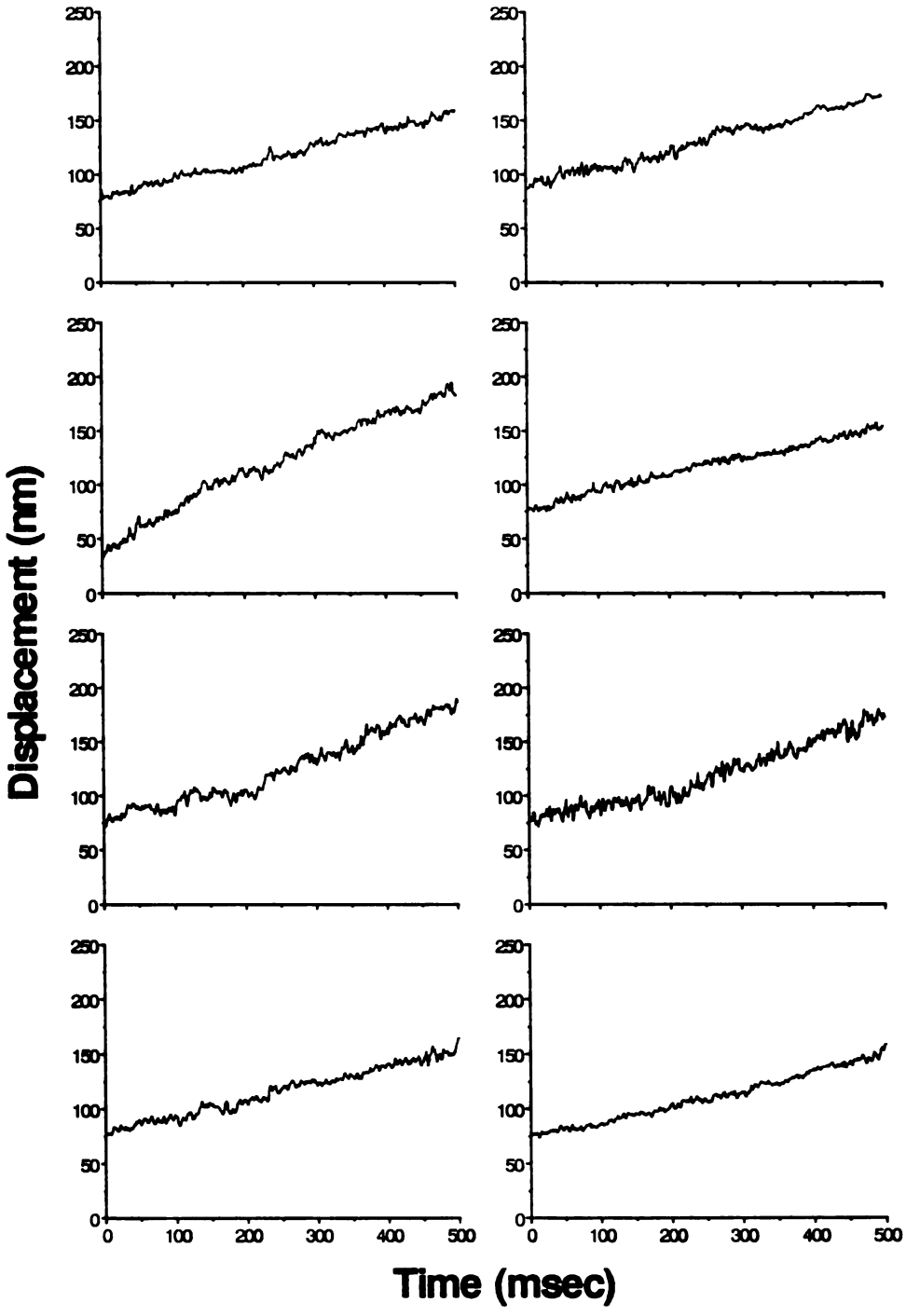

Fig. 3-6 cont.

CHAPTER 4

HIGH RESOLUTION MEASUREMENTS OF MICROTUBULES DRIVEN BY SINGLE KINESIN MOTORS

OVERVIEW

The main difficulty with previous measurements of the step size of various motor proteins is that the preparations used typically consisted of a filament interacting with multiple motors. The range is from million of motors in a skinned muscle fiber to only a few motors in the in vitro motility assay. The estimate for the length of the step size likewise ranges anywhere from 4 nm to 100 nm in the actomyosin system (Toyoshima, et al., 1990; Uyeda, et al., 1990; Harada, et al., 1987). Furthermore, these measurements were indirect, resulting from a calculation based on parameters measured under several different conditions (see Chapter 1 for details). The direct high resolution measurements of kinesin-driven microtubule motility described in the previous chapter poignantly demonstrate the difficulties of measuring the step-size in a system that involves multiple motors.

In the kinesin-microtubule system, it is possible to observe the translocation of a microtubule driven by a single kinesin motor. I was able to modify the usual single motor assay to allow high resolution measurements of microtubule movement. In the conventional single motor assay, a large number of microtubules are free in solution. These microtubules scatter light and

UVVI LIBRARY

obscure the position detector. In my modified assay, microtubules are bound to kinesin on the glass surface in the absence of ATP, free microtubules are rinsed out of the perfusion chamber and caged ATP is introduced. After the image of the bead-labeled microtubule is aligned on the photodiode, motility is initiated by releasing ATP with UV illumination.

Using this assay it was possible to measure microtubule movement produced by a single kinesin. The noise of the rigor kinesin-microtubule complex was greater in the single motor case (~7 nm) than in the multiple motor case (~4 nm). This increase in noise reduces the certainty of ruling out 8 nm steps by visual inspection of the motility records. However, as in experiments when multiple motors interacted with a microtubule, the overall movement was smooth and no consistent step-like behavior was observed. The movement was smooth regardless of the velocity of translocation. Although, again occasional abrupt displacements occurred, there was no consistent pattern of step-wise movement.

METHODS

Motility Assay

The single motor assay was performed in a manner similar to the multiple motor assay. One chamber volume of casein was perfused into the chamber and allowed to adsorb to the surface for two minutes. The chamber was rinsed with

3 volumes of LIB. In these experiments, the stock kinesin aliquot (25 μg/ml) was diluted 2200-fold into LIB and mixed. Five microliters of the diluted kinesin were perfused into the chamber and allowed to adsorb to the casein coated surface for 2 minutes. Then, five microliters of bead-labeled microtubules were diluted 1:25 in LIB with 16 μm taxol, introduced into the flow cell, and allowed to attach to the kinesin molecules on the surface for five minutes instead of two minutes as in the multiple motor assay. To remove free microtubules and beads in solution, the perfusion chamber was then rinsed with three volumes of LIB containing 16 μM taxol. Finally, two volumes of LIB containing 16 μM taxol, 0.1% methylcellulose, an O_2 radical scavenger enzymatic system, and 200 μM 3-O-(1-(2-nitrophenyl)ethyl)ester ATP (NPE caged ATP; Molecular Probes Inc., Eugene Ore.) were used instead of ATP. The scavenger system consisted of 0.1 mg/ml catalase, 0.03 mg/ml glucose oxidase, 10 mM glucose, and 0.3% 2-mercaptoethanol. A UV cutoff filter (535 longpass filter, Oriel, Stratford, CT) was placed on a sliding mount in the light path of the mercury arc lamp. ATP was uncaged by briefly manually sliding the filter out of the light path; the UV light would travel through the darkfield condenser and uncage ATP in the illuminated microscope field (~20 μm in diameter). Microtubules would immediately begin moving and soon detach as its trailing end moves past the kinesin molecule to which it is attached. The uncaged ATP would be rapidly diluted as it diffused away from the center of activation. Thus, microtubules in

adjacent microscope fields would still be motionless, and the same slide was able to be used for many activations.

RESULTS

Characterization of the Assay

A slight modification of the previously developed single motor assay allowed me to make high resolution measurements of microtubules being driven by single kinesin molecules. In the standard single motor assay, pretreating the glass surface with a blocking protein, such as casein, allows kinesin to be absorbed in an active form at very low densities. Under such conditions, many of the microtubules (which range from 1 to 10 μm in length) are translocated by single kinesin molecules. There are two visual cues that indicate microtubules are being moved by single kinesin motors. First, when the kinesin molecule reaches the end of the microtubule and a second motor has not been found, the microtubule detaches from the glass and diffuses into solution. Thus, the microtubule can only travel a distance less than or equal to its length. Second, sometimes the microtubule will pivot about a nodal point, indicating where the kinesin motor is located; just as often though, it will move for some distance without exhibiting any pivoting motion. The release of a microtubule from the surface before traveling a distance greater than its length, and the pivoting motion are two visual cues that a single motor is driving motility. While these

visual clues are convincing evidence for single motor translocation, it is also possible to measure the probability of microtubule attachment to kinesin molecules on the glass surface and show statistically that a single motor is capable of translocating a microtubule (Howard, et al., 1989).

The primary change in my modified assay was the substitution of caged ATP for ATP. Microtubules in solution could be rinsed away and microtubules attached to the glass remained motionless until exposed to UV light which released ATP and activated motility (Goldman, et al., 1984). Removal of free microtubules in solution eliminated the problem of random scattered light obscuring the position detector. If caged ATP was not used, the microtubules attached to the surface would translocate to their ends and detach from the surface in a matter of seconds, quickly leaving the surface devoid of moving microtubules.

The low density of surface bound kinesin, the observation of pivoting motion during translocation, and the translocation of a microtubule no further than its length served to confirm that measurements were of single motor driven microtubules. At the dilution of kinesin used for these single motor assays, there were approximately 0.25 kinesin molecules/μm^2 on the glass surface. At this kinesin density, greater than 90% of the microtubules less than 6 μm long were moved by single motors. The distribution of single motor movements relative to microtubule length is shown in the histogram of Fig. 4-1. Also, during the

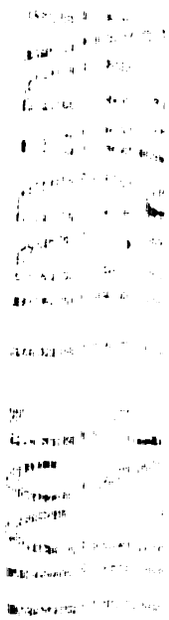

course of an experiment, microtubules analyzed by the position detector were simultaneously recorded onto videotape. The visual record of the microtubule movement was later reviewed and judged to be caused by a single motor if microtubules traveled for a distance less than their length or displayed pivoting behavior at some time before they detached.

The relationship of ATP concentration to velocity was examined in a separate series of experiments. At low densities in the low ionic strength buffer, the ATP concentration versus velocity curve (Fig. 4-2) is fitted well by a Michaelis-Menton relationship (K_m = 125). Although, there are still two force generating domains interacting with the microtubule, apparently a single kinesin head is not sufficient to cause a deviation of the ATP versus velocity curve from a Michaelis-Menton relationship in contrast to the multiple motor case (see Fig. 3-2, Chap. 3). This result suggests that the second head does not pose a significant drag on the microtubule and does not interfere with the active force generating head.

High Resolution Measurements of Microtubules Driven by Single Kinesins

The r.m.s. noise of a microtubule-bead complex held to the glass by a single kinesin motor is shown in Fig. 4-3. The noise is 7-fold greater than that of a bead firmly fixed to the glass surface, and 2-fold greater than the noise in the case of multiple motors, probably reflecting the fact that the microtubule is tethered to the glass at only a single point rather than at multiple points.

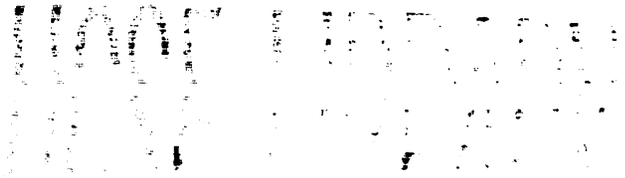

Rigor-attached microtubules were confirmed to be tethered to a single motor by uncaging ATP and observing detachment before traveling greater than their length. The microtubule-bead noise did not change significantly after uncaging. Again, the component of the bead noise perpendicular to the microtubule axis was larger than the parallel component ($p < 0.05$) although the difference was not as pronounced. The noise from a single motor is still quite low considering the 80 nm length of kinesin, suggesting that the majority of a kinesin molecule is well attached to the surface and is not just bound at one end. The increase in stationary noise with decreasing motor number suggests that the kinesin molecule is a significant elastic element under these assay conditions. A measure of this elastic element is the spring constant (K) of the kinesin molecule which can be calculated by equating the energy of a simple spring ($1/2Kx^2$, where x is the rms noise displacement) to the driving energy of thermal motion (kT, where k is Boltzmann's constant). In this assay, the kinesin spring constant is 1.7×10^{-4} N/m, comparable to the myosin spring constant of 2.5×10^{-4} N/m (Huxley and Simmons, 1971). The pivoting behavior a moving microtubule sometimes displays also indicates that the kinesin head has a great deal of intrinsic flexibility. In fact, microtubules have been seen to pivot by greater than 180 degrees about the nodal point where the kinesin molecule is located (personal observation).

Measurements of moving microtubules were made by searching the field for bead-labeled microtubules. The UV filter was then removed from the light

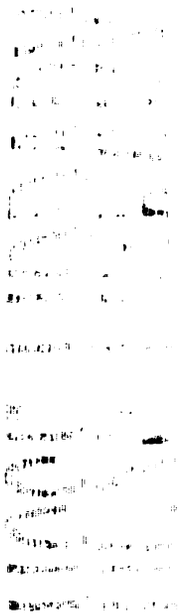

path very briefly (<0.5 sec). Enough caged ATP was liberated so that the microtubule would move for a very short distance (often less than a micron) and then stop; this allowed the direction of movement to be ascertained. The microtubule was then positioned so that its motion would carry it through the spot in the field coincident with the laser and position detector. The video recorder and data acquisition were started, and another longer (~1-2 sec) exposure to UV light was delivered to reinitiate motility. This time sufficient ATP was liberated so that the microtubule traveled through the detector spot and eventually detached from the glass. The uncaged ATP quickly diffused away from the 20 μm diameter activation area; thus in other areas of the perfusion chamber, microtubules would still be motionless.

The amount of caged ATP released by the UV flash was variable because removal of the sliding filter was manual. Thus, instead of varying ATP concentration to look at different velocities, it was possible to merely vary the uncaging time to release more or less ATP. Microtubule records were then grouped based on velocity. In all, some 300 records of microtubule movement were collected at this kinesin density. About half of the records were confirmed to be single motor movements by inspecting videotape. Since microtubules have the ability to pivot when undergoing single motor movement, many of these records are quite noisy and difficult to interpret. However, a number of the records were of sufficient quality to analyze further and are discussed below.



A set of 14 records of fast moving microtubules driven by single kinesin motors is shown in Fig. 4-4. These are relatively low noise records of single motor motility. The average velocity was 275 ± 60 nm/sec. Once again, close inspection of these as well as the other examples showed that the microtubules move overall in a smooth and continuous manner for the majority of the time. If one looked for possible 8 nm steps, occasional examples could be found but were infrequent (data not shown). The size of the steps was difficult to measure owing to the Brownian noise of the system but did not seem consistent. Again as in the multiple motor case, there were sections of records which were completely smooth with no evident stepping behavior.

A smaller set of slow moving microtubules is shown in Fig. 4-5. The average velocity of this slower group of microtubules was 175 ± 40 nm/sec. Once again, the movement appeared smooth and no different from the faster moving microtubules except for the decrease in velocity.

DISCUSSION

Reducing the number of motors interacting with the microtubule to a single kinesin molecule overcomes the complication of having several asynchronous motors moving the microtubule at the same time. These measurements represent the first high resolution measurements of a single motor protein moving its complementary filament. Visual inspection of the records

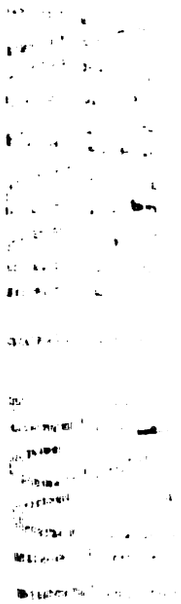

shows that a single kinesin produces nearly smooth movement. There are no consistent abrupt step-like movements of the microtubule.

The magnitude of the background noise in the records makes it difficult to rule out the existence of the smallest probable step size by visible inspection of the data. The noise of the single motor records is on the order of 8 nm, the minimum distance between kinesin binding sites, and makes reliable detection of 8 nm steps difficult. On the other hand, the next probable increment of the step size would be the distance between two binding sites which is 16 nm. Steps of this magnitude or larger would easily be observable on top of the background noise (see next chapter). To detect steps smaller than visual inspection would allow, a Fourier spectral analysis was employed to look for repetitive features in the records; this approach is discussed in the next chapter.

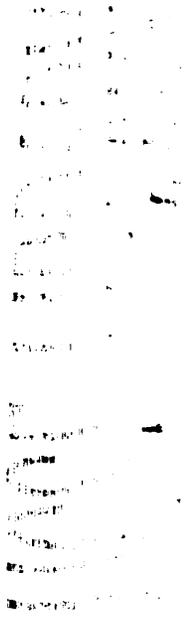

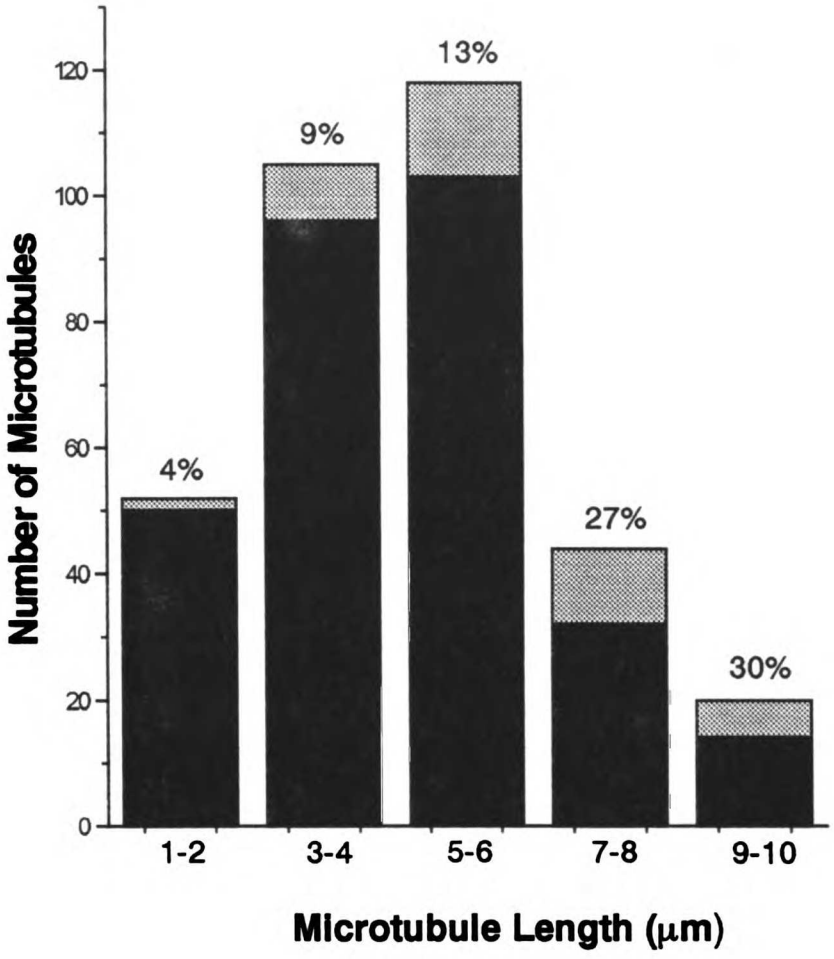

Fig 4-1. Histogram of single motor microtubule movements in the low density assay. A total of 340 microtubules were scored. Microtubules were judged to be moved by single motors if they traveled less than their length and/or displayed pivoting movement. The dark bars are the number of single motor movements at each microtubule length. The gray bars represent multiple motor movements. The percentages above the bars are the proportion of multiple motor movements at each microtubule length.

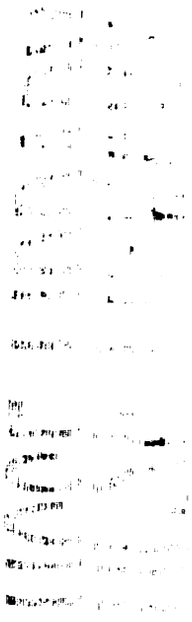

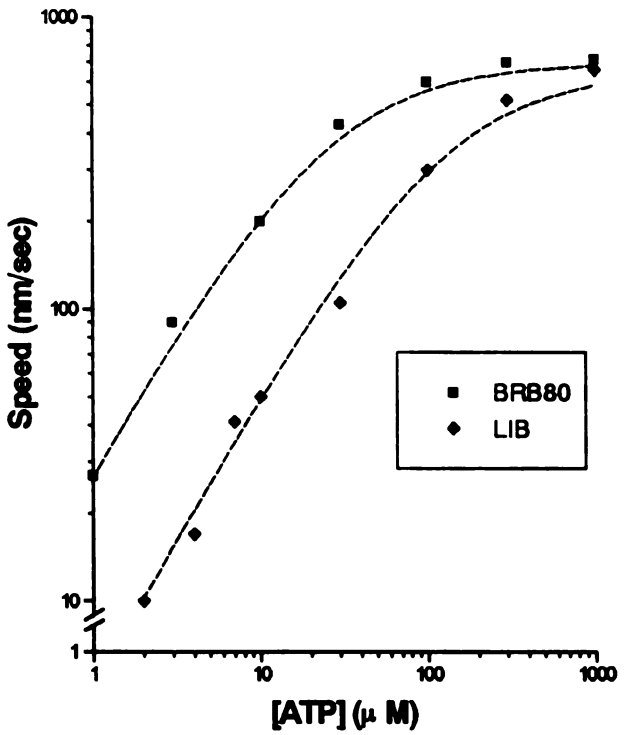

Fig. 4-2. Dependence of microtubule speed on ATP concentration at single motor densities. The velocities of 25 microtubules at each ATP concentration were averaged together to obtain each data point. The dashed lines are plots of the Michaelis-Menten relationship under each condition (Km = 25 μM ATP in BRB80 and 125 μM ATP in LIB). At this motor density, the data follow Michaelis-Menton kinetics closely.

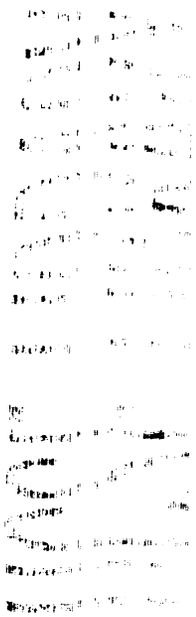

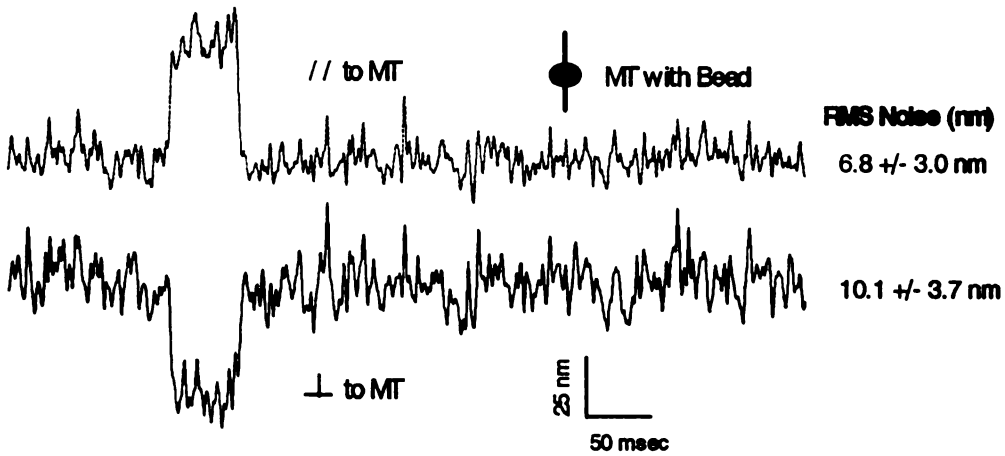

Fig. 4-3. Noise of a stationary kinesin-bead-microtubule complex at single motor densities. The records show the position of the bead which labels the microtubule. The upper record is the positional noise in a direction parallel to the microtubule while the lower record is the noise perpendicular to the microtubule. The rectangular pulses on the records (upgoing in the top and downgoing in the bottom record) are the calibration pulses produced by the piezoelectric stage. They are 50 nm in magnitude. Note the rapidity with which the movement takes place. As described in the text, the noise in the perpendicular direction is greater than that in the parallel direction. The average noise value of 15 different kinesin-microtubule complexes is shown to the right of the record.

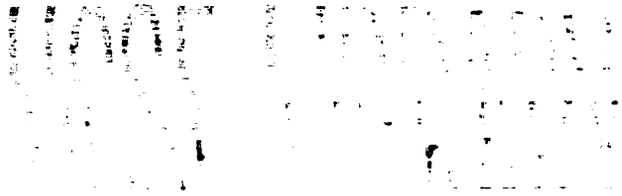

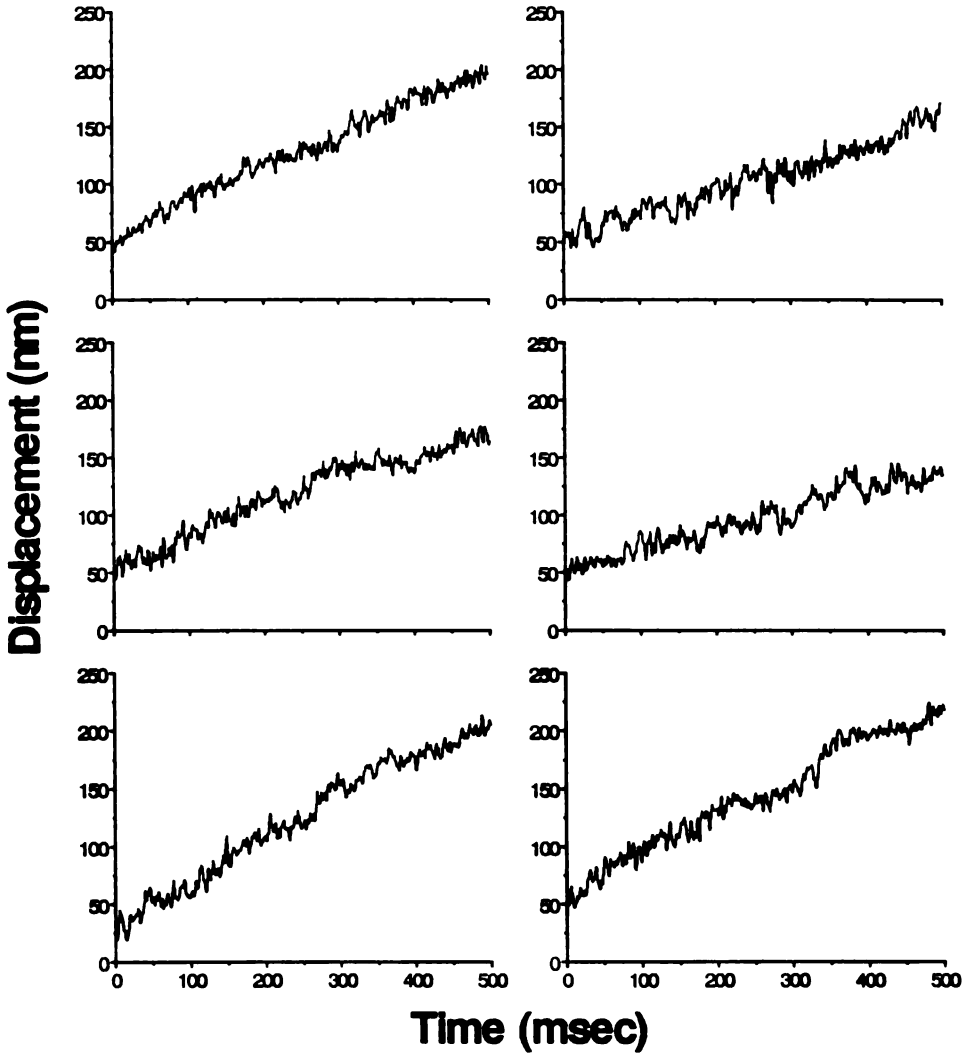

Fig. 4-4. High resolution displacement records of microtubules driven by single kinesin motors. The concentration of ATP uncaged is near saturating as judged from the microtubule velocities. These 14 records (figure is continued on the next page) represent movement along an axis parallel to the microtubule axis. Each record represents a different translocating microtubule. Although some changes in speed do occur, step-wise displacement is not evident.

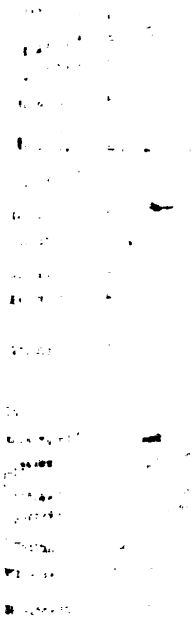

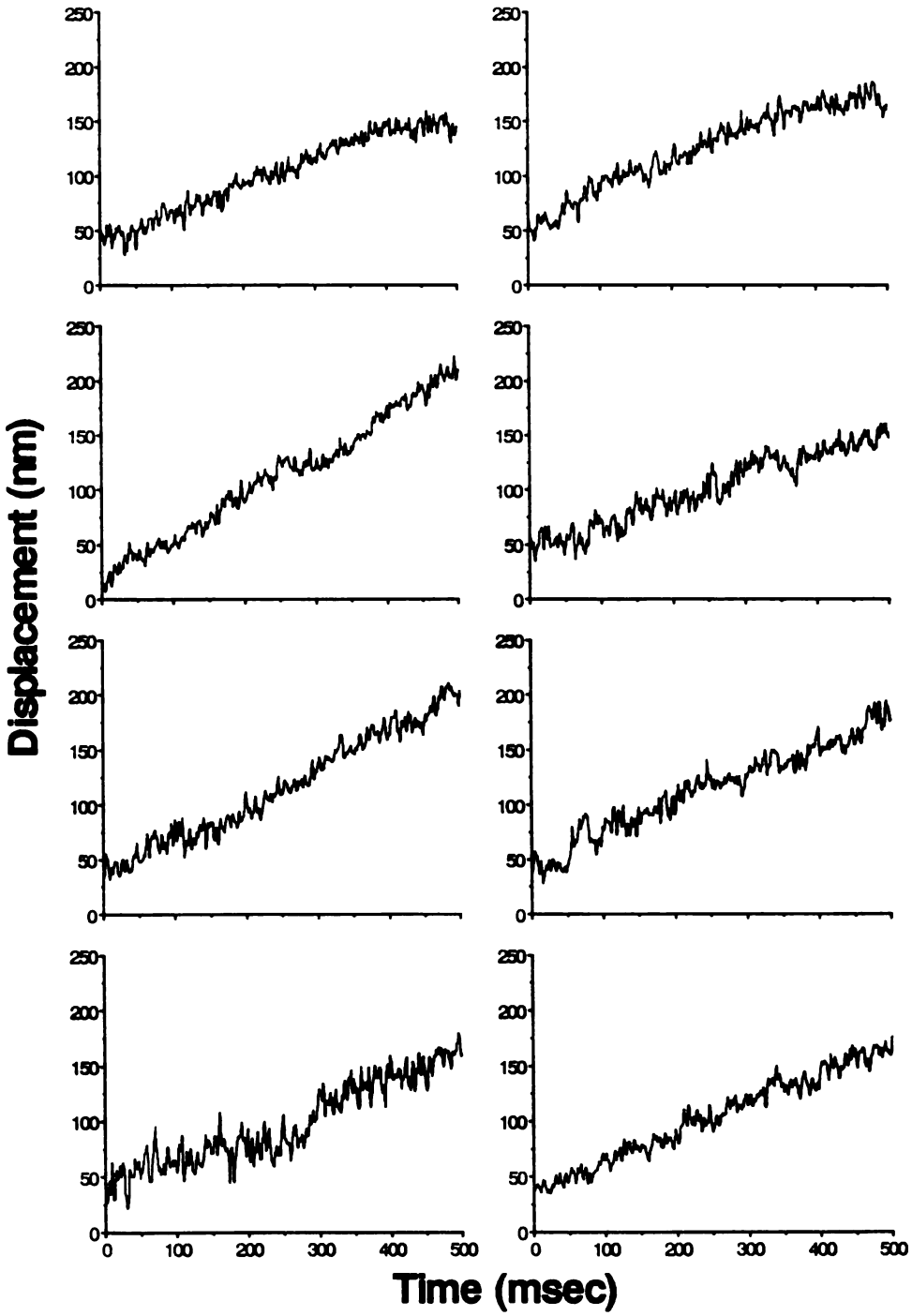

Fig. 4-4 cont.

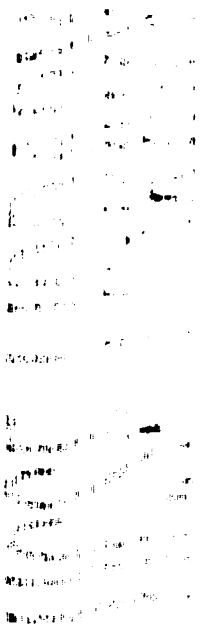

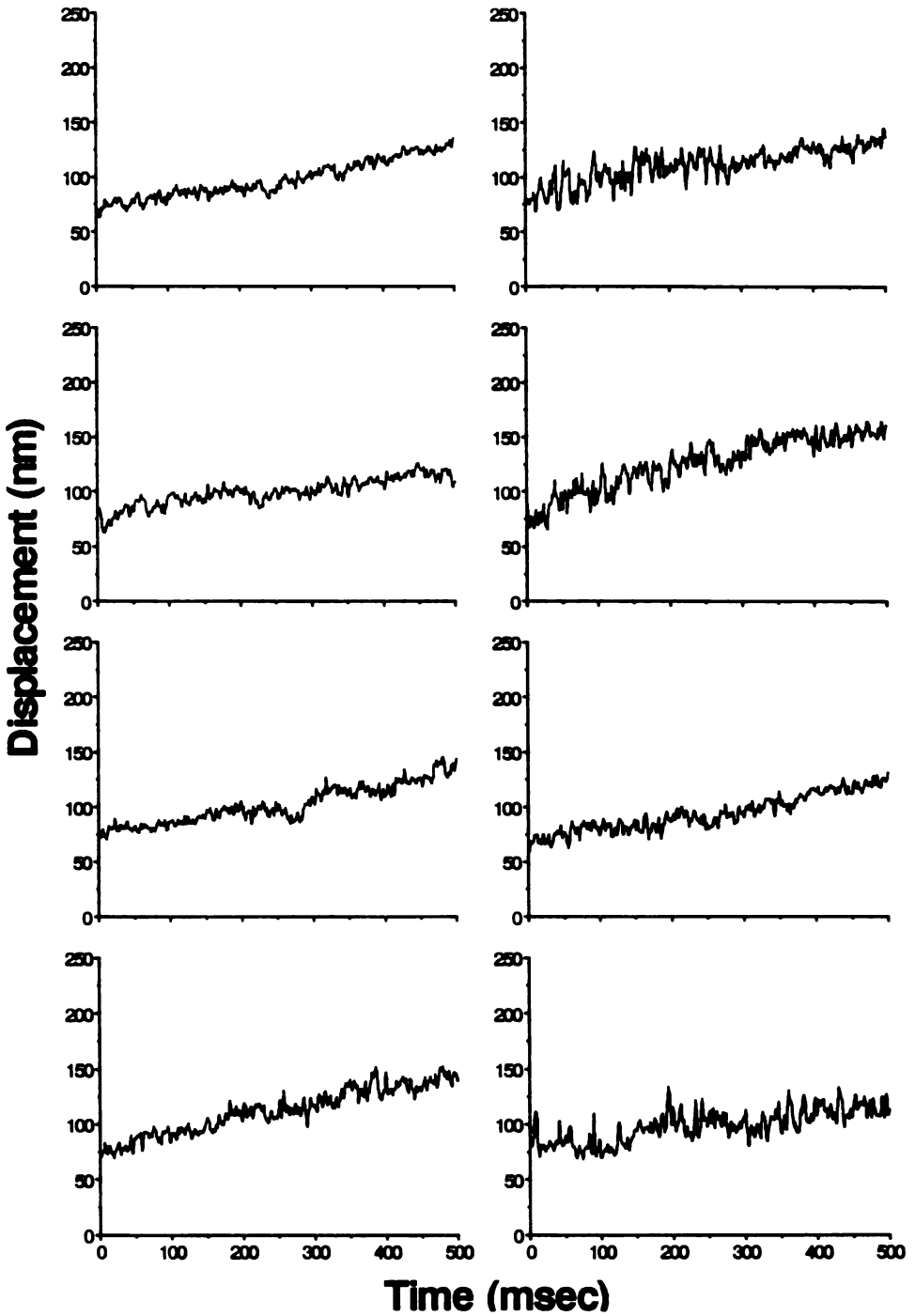

Fig. 4-5. High resolution displacement records of microtubules driven by single kinesin motors at lower ATP concentrations. Each record represents a measurement of a different microtubule.

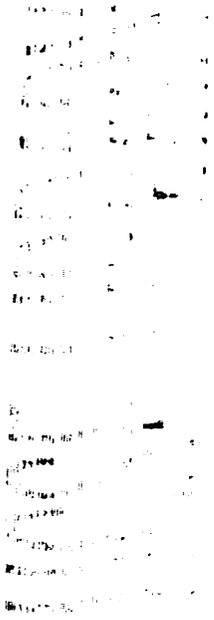

CHAPTER 5

SPECTRAL ANALYSIS OF HIGH RESOLUTION MICROTUBULE MOTILITY MEASUREMENTS

OVERVIEW

Since visual inspection of the single motor or multiple motor records did not reveal any repetitive features, an analysis algorithm was developed to look for periodic features in the records. A method of applying Fourier spectral analysis to detect small steps was tested using a set of modeled data created by adding a series of steps to records of stationary kinesin-microtubule rigor data. The modeled data also served to test the size of step detectable by visual inspection of the traces. In modeled records using single motor rigor data, steps on the order of 12 nm were easily detectable to naive observers. Steps 8 nm in size were much more subtle and not reliably detectable by visual scanning of the traces (Fig. 5-1).

The spectral analysis consisted of obtaining the power spectrum of a data segment, normalizing with respect to microtubule velocity, and averaging the spectrum of different microtubules together. This analysis could easily detect a regular pattern of 4 nm or greater sized steps added to the single motor rigor data. Since power strokes of motors may not occur at entirely regular intervals, a set of modeled records were created in which the time interval between 8 nm steps randomly varied. With a time interval coefficient of variation up to 0.2, a significant peak at the expected frequency was still obtained. Stochastic steps

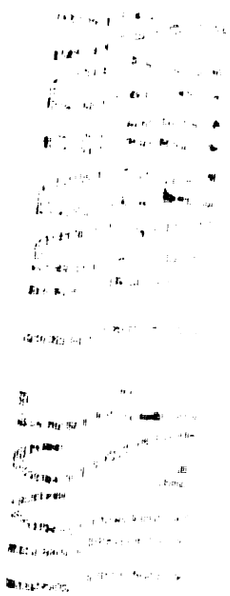

could not be resolved, although model records containing stochastic 8 nm steps did not resemble the data collected in that the velocity in a record varied much more than was observed (Fig. 5-1).

The analysis was applied to four sets of data from multiple and single motor experiments. A set of rigor data was also analyzed to serve as a control. When the analysis was applied to the rigor traces, as expected, there were no significant peaks. Similarly, analysis of the single motor data revealed no significant peaks that might represent periodic motor activity. In the multiple motor traces, there were significant peaks associated with high frequency events. The lower background noise of the multiple motor traces may have allowed these peaks to be detected, or they simply may only be present when several motors are interacting with the microtubule simultaneously. Interpretation of these peaks is complicated by the presence of several motors and will be more fully discussed at the end of this chapter. The work done in this chapter was done in collaboration with David Brillinger, Professor of Statistics, UC Berkeley.

METHODS

Creating Model Traces

A computer program was written to add a series of regularly spaced steps to records of stationary single motor rigor microtubule complexes. A constant velocity of 200 nm/sec was modeled and the time interval between steps was

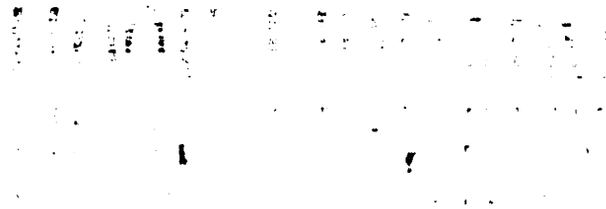

varied to achieve this velocity when modeling different sized steps. One second of sampled data consisted of 2000 points (0.5 msec sampling time). An array of 2000 points starting at zero and incremented by the chosen step size every 1000/(200/stepsize) msec was created and then filtered using a 4 pole lowpass digital Butterworth filter to simulate the effects of the analog filtering of the position detector signals. The array was then added to a record of a rigor microtubule to create the model record. Using a set of 15 records of different rigor single kinesin microtubule complexes, model sets of data with 4 nm, 6 nm, 8 nm, and 16 nm steps were made to test the spectral analysis and the limits of visual inspection. In addition, as a control, a flat line of slope 200 nm/sec was added to the rigor records. This data would represent completely smooth translocation of the microtubule.

As well as the regularly spaced steps, a model data set of 8 nm steps occurring at non-uniform time intervals was created. The time intervals were distributed according to a Gamma probability function with an average value of 40 msec (to achieve a velocity of 200 nm/sec). Distributions with different coefficients of variation (i.e. the spread in the values about the mean value) were tested with the analysis method. Some records in which the time interval between steps occurred at completely random times were created using a random number generator. Steps were assigned to the times given by the random number generator.

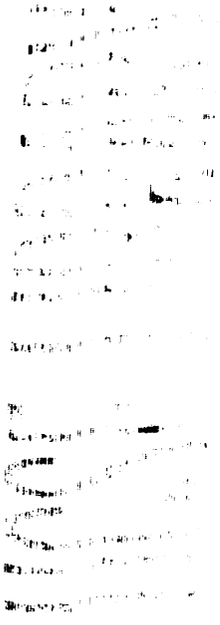

Fourier Spectral Analysis

The reference frame of the microtubule's translocation was translated from that of the position detector's X and Y axes to axes parallel and perpendicular to the microtubule long axis. Using calibrated records of microtubule displacement, a section of data between the calibration pulses 512 msec in length (1024 sampled points) was selected. The displacement parallel to the microtubule's long axis was calculated by projecting the X and Y components from the position detector along a unit vector parallel the direction of microtubule travel. This unit vector, $\hat{\mathbf{u}} = V_x / \sqrt{V_x + V_y}\,\hat{\mathbf{i}} + V_y / \sqrt{V_x + V_y}\,\hat{\mathbf{j}}$ was calculated from the magnitudes of the velocity in the X and Y directions. The projection along this vector was carried out by calculating $\hat{\mathbf{u}} \bullet \hat{\mathbf{v}}$, where $\hat{\mathbf{v}} = X\hat{\mathbf{i}} + Y\hat{\mathbf{j}}$. The displacement perpendicular to the microtubule's long axis was calculated by taking a similar dot product but using the unit vector perpendicular to the one parallel to the microtubule axis.

A line was robustly fitted (Becker, et al., 1989) to the displacement record, and residual values were calculated by subtracting the fitted line from the displacement record. A Fourier transform was performed on this data, and the modulus determined. In preparation for averaging the data from several microtubules to try to enhance a small signal present in all the data, the spectra were prewhitened by subtracting a robustly fitted line to the log spectral values at low frequencies, which resulted in flat spectra. Since the individual microtubules were traveling at somewhat different velocities, the periodic

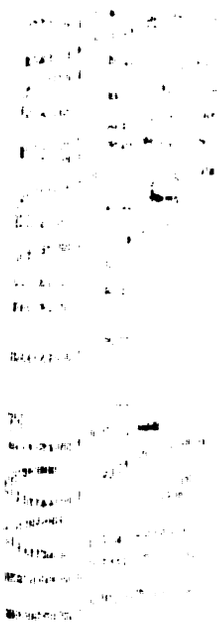

behavior of the motors would appear at different frequencies. Thus, the spectra were normalized by transforming frequency into displacement by the following relationship, nm = velocity/frequency. For example at a velocity of 200 nm/sec, a 25 Hz peak becomes a peak at 8 nm. Similarly, at a velocity of 400 nm/sec, a 50 Hz peak also appropriately becomes a 8 nm peak. The normalized spectra of each data set were then averaged together to obtain a composite average spectrum. The spectra were converted back to a frequency axis by using the average velocity of the data set. The significance of the largest peak in the spectrum was tested using a X^2 analysis applied to the values in the average spectrum as well as the underlying values in the individual spectra.

RESULTS

Inspection of Model Records

In order to ascertain the acuity of visually inspecting high resolution motility records for evidence of steps, a set of model data were created. The model data were based on stationary rigor microtubules at single motor density. A staircase of abrupt steps simulating the hypothesized power stroke were added to these records. The resulting records were now similar to those of moving microtubules. When a step size of 16 nm was used, the steps were readily apparent on top of the background noise (see Fig. 5-1). However, when a series of 8 or 4 nm steps were added to the rigor records, the records were difficult to distinguish from records in which a smooth line was added to the

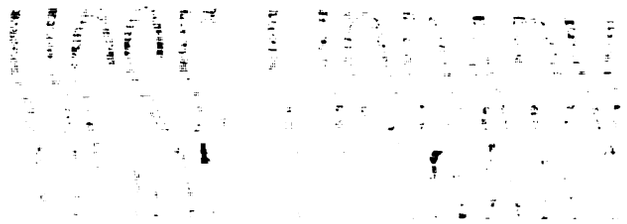

data (Fig. 5-1). Since a 8 nm step size is possible because this distance probably is the minimum distance between microtubule binding sites, more powerful means than visual inspection of the data were sought to try to detect the smaller step sizes.

Demonstration of the Analysis Method

The data were first subjected to several statistical tests looking at the distribution of displacements within the data to determine if there might exist an increased number of displacements at any particular magnitude. For example, a histogram of the distances between different points in each record was compiled to look for a preponderance of any particular magnitude of displacement. No difference between rigor and moving microtubules was found. Furthermore, the tests were not particularly sensitive since they were not able to successfully find steps in the modeled data. The reason for this failure is that the noise in the records is of comparable magnitude to an 8 nm displacement; since the noise contains already many 8 nm displacements, a few more contributed by a stepping motor does not produce a significant signal.

Based on the rationale that step displacements might be separated by an average time interval, an analysis method was developed that attempts to uncover periodic features that lie in the records. Since any repetitive feature might be smaller than the level of noise in the records, a signal averaging approach was employed to increase the power of the analysis. As a substrate for

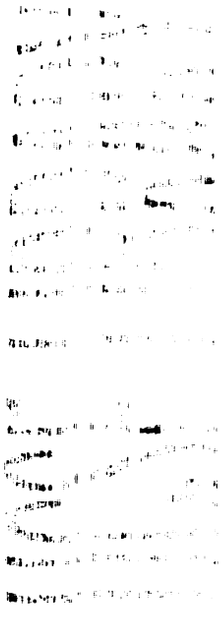

the analysis method, a set of 14 different single motor rigor microtubules (which have the same rms noise as moving microtubules) with either a smooth line, or 4, 6, and 8 nm steps added to them were used.

The analysis algorithm consisted essentially of calculating the power spectrum of a record, normalizing the spectrum with respect to velocity, and then adding the spectra of different microtubules together to obtain an average. The significance of the largest peak was calculated using a X^2 analysis applied to the aggregate spectral data.

This analysis could easily detect a regular pattern of 4 nm or greater steps in the modeled data (see Fig. 5-2). In the modeled data of 8 nm steps, a large peak occurs at 25 Hz which is the expected frequency for a velocity of 200 nm/sec; a smaller harmonic peak occurs at 50 Hz. The peak is significant to a p value $< 10^{-19}$ (please note that the vertical scale in Fig. 5-2 is log scale). A significant peak began to appear after as few as four records were averaged together (data not shown). Significant peaks also occur at the expected frequencies with 6 nm ($p < 10^{-19}$) and 4 nm ($p < 0.003$) steps. However, in the control data set in which a smooth line is added, none of the peaks are significant. Thus, we feel confident that this analytical method is a powerful tool for finding steps in the data even when they are not visible.

In the analysis presented above, the modeled steps were regular, that is separated by equal time intervals. Real enzymes of which motor proteins are a class, are not likely to be perfectly regular in their actions. Thus, we strove to

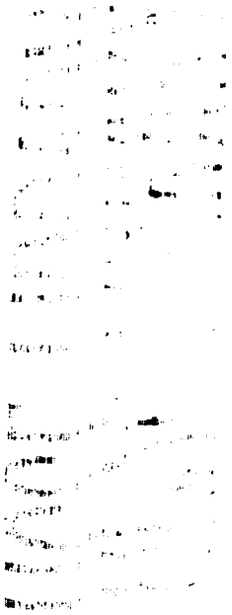

test the analysis method against a set of modeled data in which the time interval between steps were allowed to vary.

An enzyme will catalyze a reaction in an amount of time related to the inverse of the reaction rate constant. However, individual forward reactions will occur in different amounts of time, those time intervals being distributed about a mean time interval. If one considers a small ensemble of individual motor proteins, the probability P of observing x number of enzymatic events in a short time interval t is a Poisson distribution given by $P = e^{-t/\tau}\frac{1}{x!}(\frac{t}{\tau})^x$ where τ is the mean time interval between events. To get the distribution of time intervals for a single catalysis, you can set x =1, giving the relationship $P = (\frac{t}{\tau})e^{-t/\tau}$. This distribution is known as a Gamma probability function. A more general form of the Gamma function is $P = \frac{k}{\tau}(\frac{kt}{\tau})^{k-1}e^{-kt/\tau}$ where the coefficient of variation is $1/\sqrt{k}$. The function is shown in Fig. 5-3a. This probability distribution was used to select the variable time interval between the 8 nm steps. The width of the distribution (described by the coefficient of variation, analogous to the standard deviation for a Gaussian distribution) was increased to get more and more variable time intervals.

Creating modeled data of 8 nm steps with variable time intervals, we tested the analysis method using successively increasing coefficients of variation. A significant peak (and also the largest peak in the averaged spectrum) at the appropriate frequency was found as long as the coefficient of variation was less than or equal to 0.2 (see Fig. 5-3c). Thus, this analysis technique is capable of

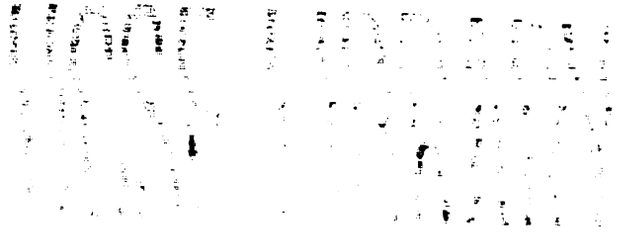

detecting 8 nm steps with a moderate variability in the time interval between events. However, for steps occurring with much greater variability, such as when the coefficient of variation approaches 1 (i.e. when the standard deviation is equal to the mean value), this technique is not capable of resolving 8 nm steps.

Analysis of Single Motor Microtubule Motility

The Fourier spectral analysis was applied to data sets of obtained from moving microtubules transported by single kinesin motors. The set of fourteen records (shown in Fig. 4-4, Chapter 4) were used for the analysis of fast moving microtubules. Both displacement parallel to the long axis of the microtubule as well as perpendicular to it were analyzed. The perpendicular displacement analysis served as an internal control; since periodic movements associated with forward translocation would most likely appear only in the analysis of parallel motion or at least be of much greater magnitude than in the perpendicular direction.

The results of the analysis are shown in Fig. 5-4. None of the peaks in the average spectrum are significant ($p > 0.1$). A set of slow moving microtubules (see Fig. 4-5, Chapter 4) were also analyzed. The results are shown in Fig. 5-5. Once again, there are no significant peaks in the average spectrum ($p > 0.1$).

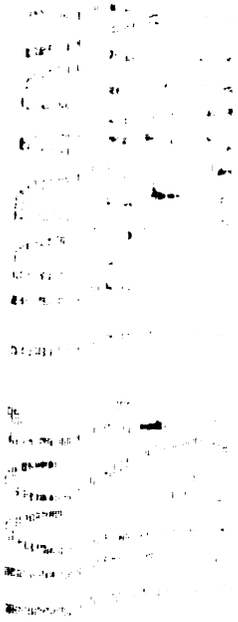

Analysis of Multiple Motor Microtubule Motility

Data from microtubules driven by 3-5 kinesin motors as described in Chapter 3 were also analyzed. The results from a set of fourteen microtubules moving in 200 μM ATP (see Fig. 3-4, Chap. 3) are shown in Figure 5-6. In the averaged spectrum, there are significant peaks associated with higher frequency events (75 and 95 Hz, $p < 0.003$). However, the peak at 75 Hz is also present in the average spectrum of movement perpendicular to the direction of travel, suggesting that it may not be entirely related to forward movement.

A set of fourteen microtubules moving in 50 μM ATP were also analyzed. Unlike the higher ATP results, there are no significant peaks in the data under these conditions (Fig. 5-7).

DISCUSSION

The analysis technique developed here allows for the detection of features in the records not readily discernible by visual inspection of the records. While the model data indicates that it is possible to easily find 12 nm steps, it also demonstrates that 8 nm or smaller steps are not distinguishable by eye in the single motor data. The spectral analysis on the other hand easily detects regular steps as small as 4 nm in the background of 8 nm single motor noise. Steps that occur at variable time intervals are more difficult to detect, but the analysis technique is still able to detect 8 nm steps occurring at time intervals varied with a 20% coefficient of variation.

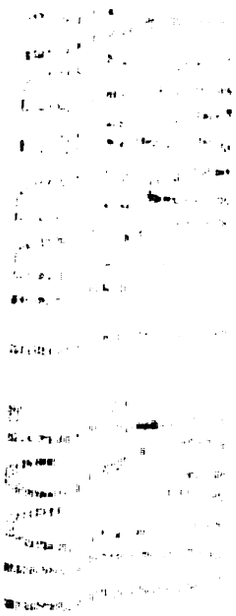

In the analysis of single motor data, no significant peaks were found. This result is consistent with the absence of a moderately regular power stroke with sufficient magnitude to entirely account for the 8 nm spacing between binding sites on the microtubule. However, it is possible that the time interval between power strokes might vary randomly about the mean time interval and that this would not be picked up by the data analysis. If this were the case though, one might expect to see lengthy pauses with zero movement in the records of microtubule translocation at times when there was a lag between successive power strokes. Such pauses are not evident in the records of microtubule movement.

There are significant peaks in the multiple motor data at 200 μM ATP. These peaks may have appeared in this data as opposed to the single motor data because the background noise is about half that in the single motor case. It is uncertain how to interpret this data because of the possibility that the motors may interact through their binding to the microtubule. However, these high frequency peaks may be related to motor generated events, possibly a small conformational change in the motor. The disappearance of the peaks at lower ATP levels might be explained by the increased duration of the rigor kinesin bonds. These rigor bonds might serve to damp out the motion present at higher ATP.

While these results do not rule out all the various incarnations of the power stroke, they do put some new limits its size. From previous





measurements of the single motor kinesin velocity and of its ATPase rate, step size estimates ranged from 20 to 30 nm. Analysis of the data virtually rules out the existence of a power stroke of 16 nm or greater. Assuming a distance of 8 nm between binding sites that leaves only one possible step size, that of 8 nm. It is more difficult to entirely rule out steps of this size. Certainly, 8 nm steps occurring with any semblance of uniformity would be detectable by the means employed here. This leaves 8 nm steps in which the time interval between steps varies with a coefficient of variation greater than 0.2. Finally, the scenario of a variable sized step (with an 8 nm mean) and with a variable time interval between steps is also possible. An attempt to analyze modeled data of this sort (using a computer simulation described by Pate and Cooke, 1991) was made, however the analysis could not detect steps of this nature.

In conclusion, I find that any step sizes greater than 8 nm would be highly unlikely. A step size of 8 nm is still possible, although there is no evidence for a 8 nm step in this analysis. A smaller conformational change that may carry the kinesin head part way to the next binding site is still possible and may be reflected in the high frequency peaks of the multiple motor data. A model of how kinesin might utilize a small conformational change to generate unidirectional movement is presented in the next chapter.

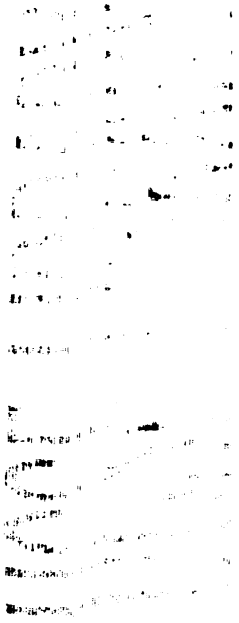

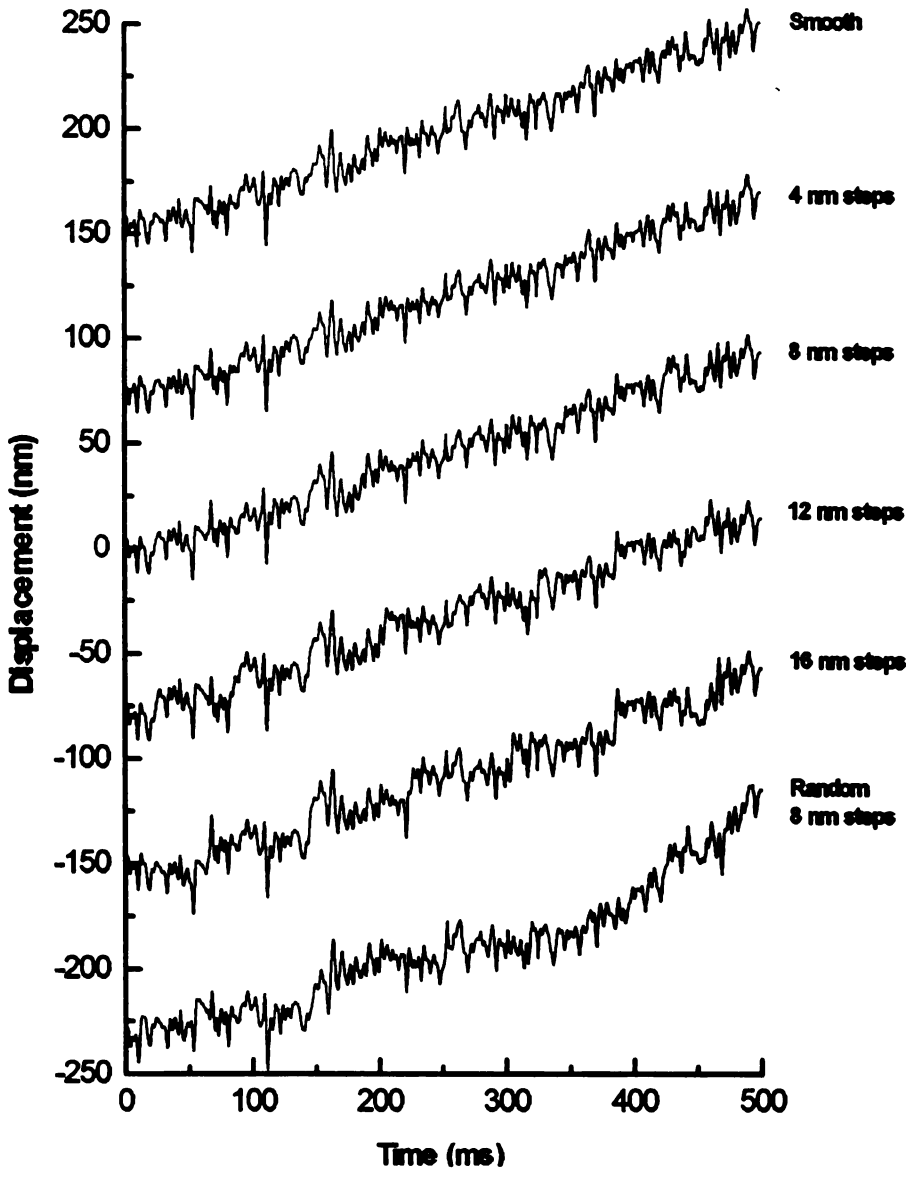

Fig. 5-1. A typical rigor single motor record with r.m.s. noise comparable to the average value of the data sets has steps added to simulate a power stroke. The same rigor record has either a smooth line or staircase ramps of regularly spaced 4, 8, 12, or 16 nm steps added to it. Steps only start to become evident at 12 nm. The bottom record has 8 nm steps with a random time interval between the steps added to it. Compared to the single motor records shown in Chapter 4, it displays a greater variation in velocity.

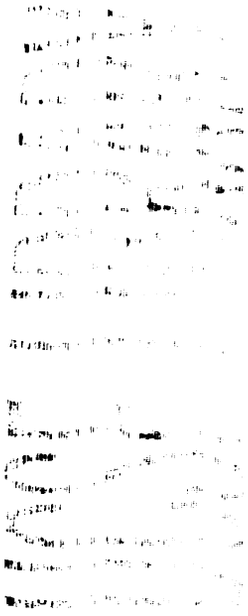

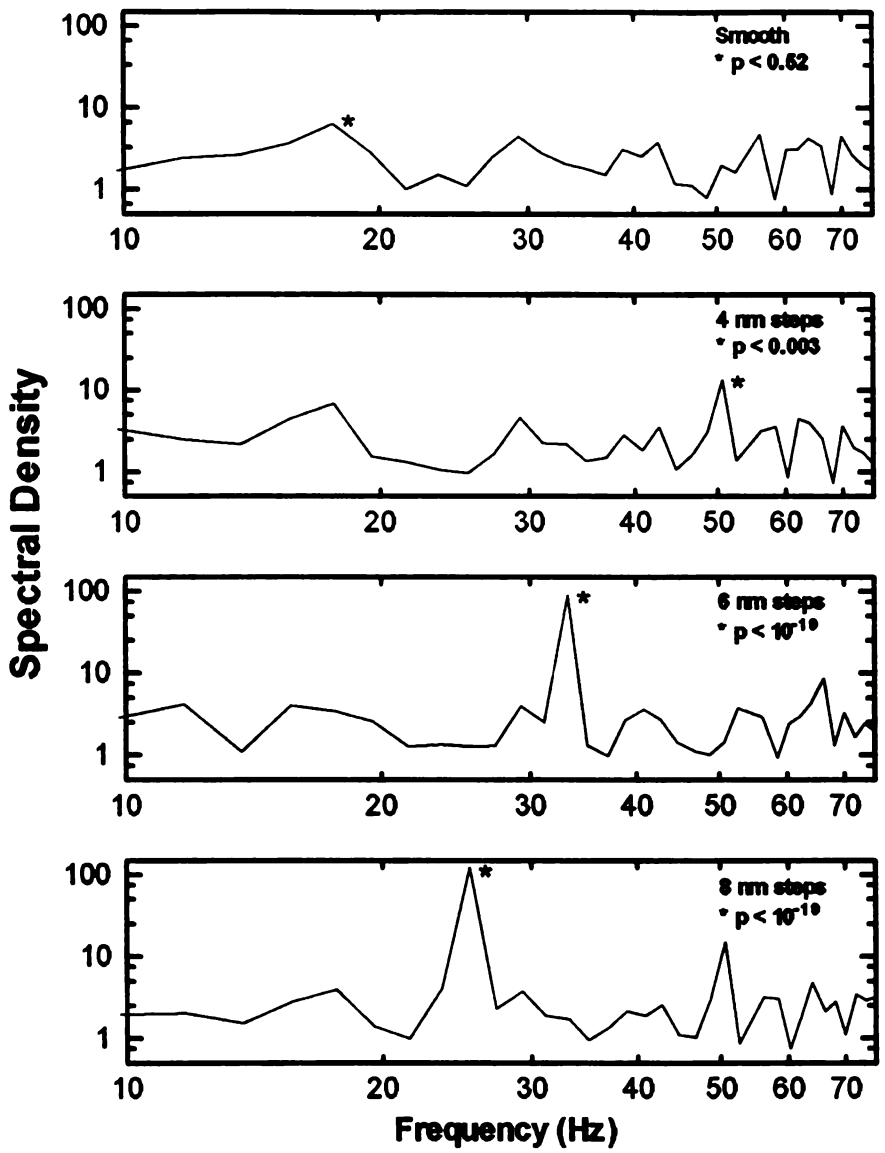

Fig. 5-2. Spectral analysis of model sets consisting of 15 rigor single motor records with a staircase of regularly spaced steps added to them. The step magnitude is indicated in the upper right of each box. The starred peak is the largest peak in the spectrum; the p value indicating its significance is shown in the upper right of each box. When a smooth line is added to the rigor records, none of the peaks in the spectrum are significant. The significant peaks in the other spectra occur at the proper frequencies for the 200 nm velocity modeled here (step frequency = velocity/step size). Please note the logarithmic axes.

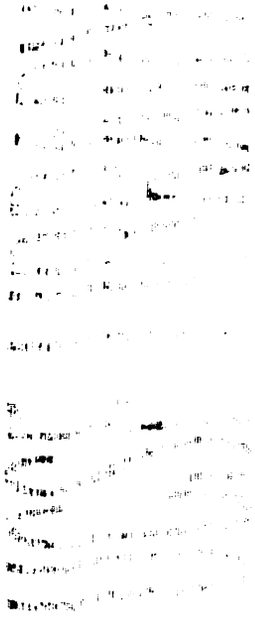

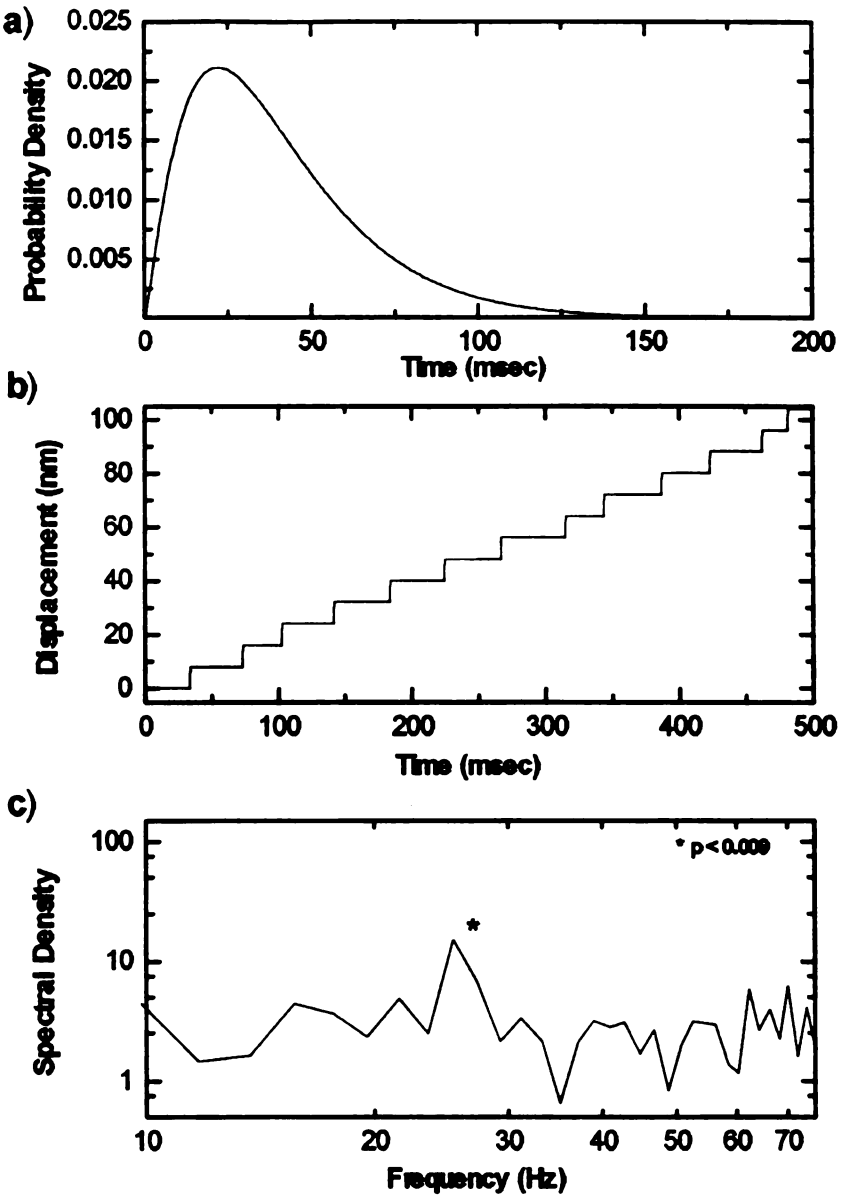

Fig. 5-3. Analysis of rigor single motor records with 8 nm steps occurring at varying time intervals. *a*) A Gamma probability distribution with a coefficient of variation of 0.2 used to generate varying time intervals. *b*) A sample staircase of 8 nm steps with time intervals varying according to the Gamma function in *a*. *c*) Analysis of a model set of 15 records created by adding the step functions as in b to rigor single motor records. The significant peak (designated by *) is at the appropriate frequency for 8 nm steps.

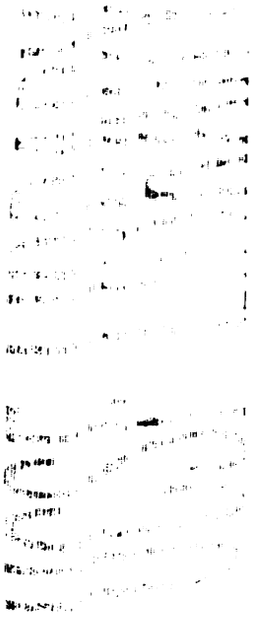

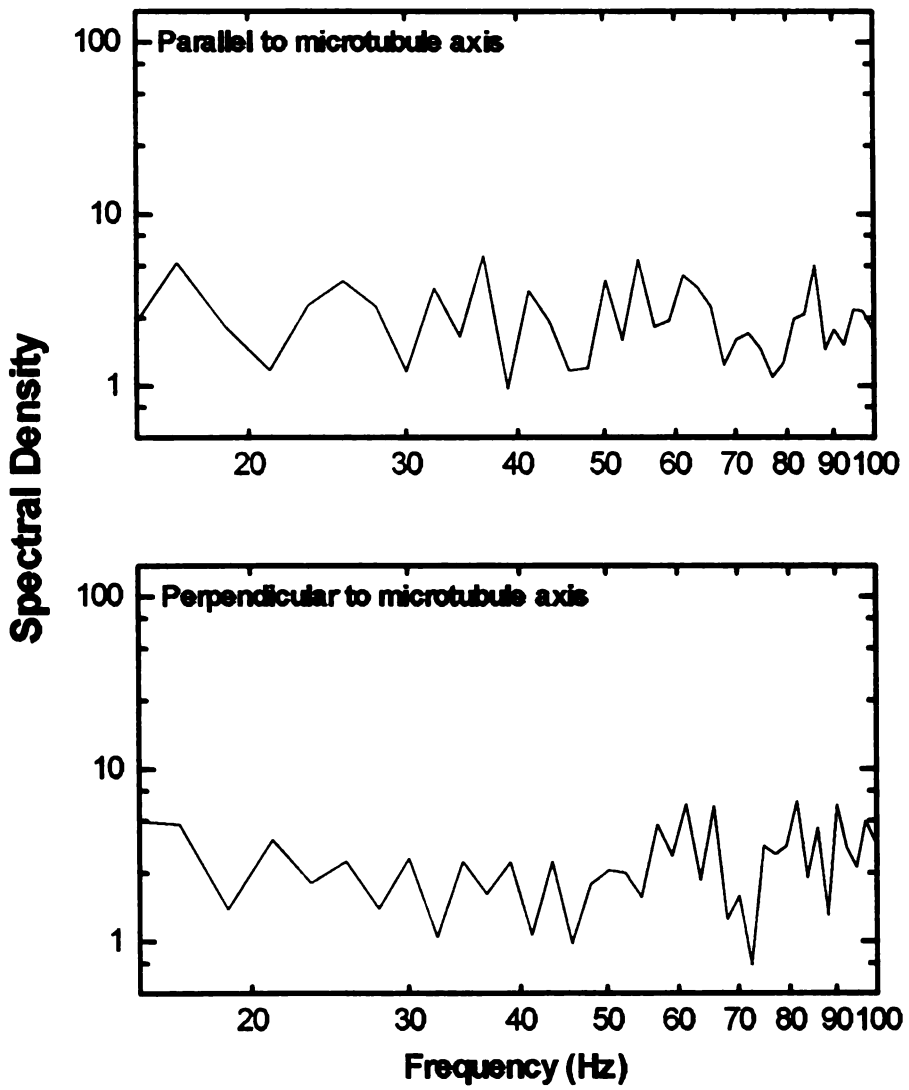

Fig. 5-4. Analysis of 14 microtubules driven by single kinesin motors. The concentration of ATP uncaged is near saturating as judged from the microtubule velocities. These microtubules correspond to those shown in Fig. 4-4. Motion parallel to the microtubule axis as well as perpendicular to it are shown. There are no significant peaks in either axis.

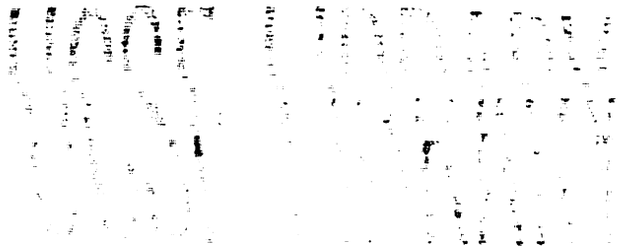

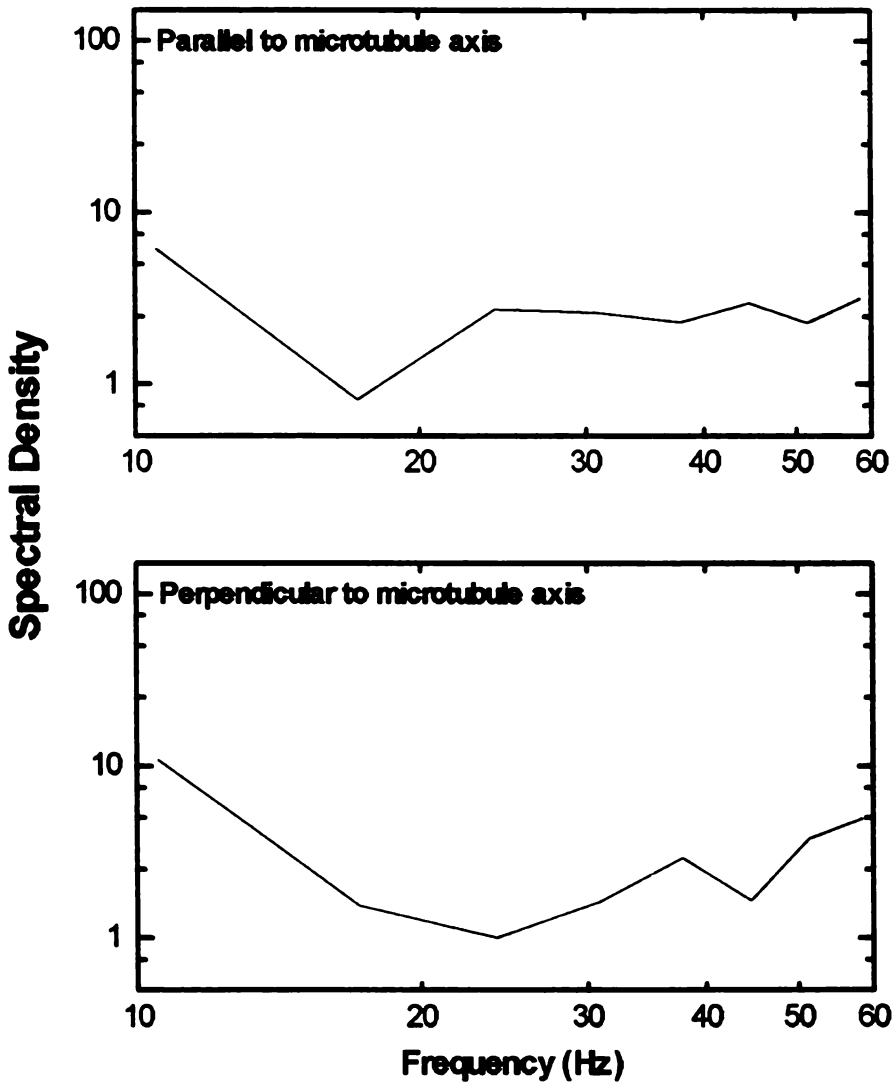

Fig. 5-5. Analysis of 8 microtubules driven by single kinesin motors. These microtubules are moving at lower ATP concentrations than the previous figure and correspond to those shown in Fig. 4-5. Motion parallel to the microtubule axis as well as perpendicular to it are shown. There are no significant peaks in either axis.

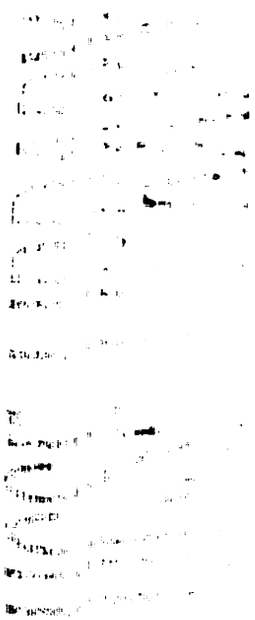

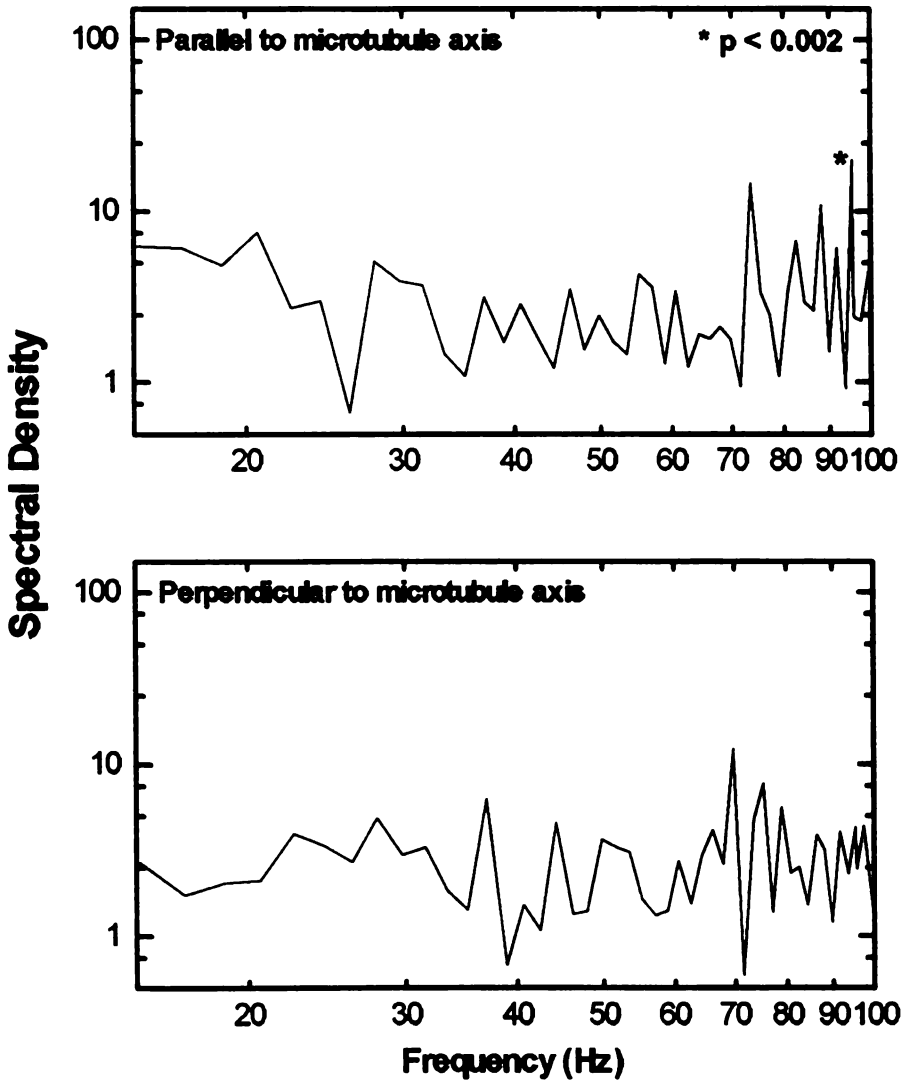

Fig. 5-6. Analysis of 14 microtubules driven by multiple kinesin motors. These microtubules are moving in the presence of 200 μM ATP and correspond to those shown in Fig. 3-4. Motion parallel to the microtubule axis as well as perpendicular to it are shown. In the direction parallel to the microtubule axis there is one unique significant peak at a frequency of 95 Hz (designated by *). Another peak at about 75 Hz is also seen, although there is a large peak in the direction perpendicular to the microtubule axis at approximately the same frequency.

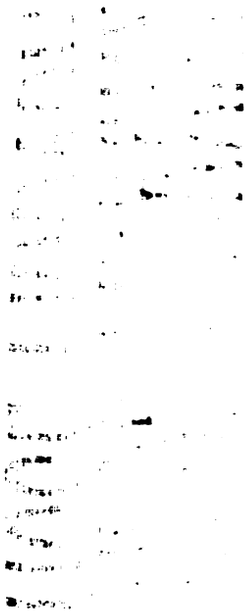

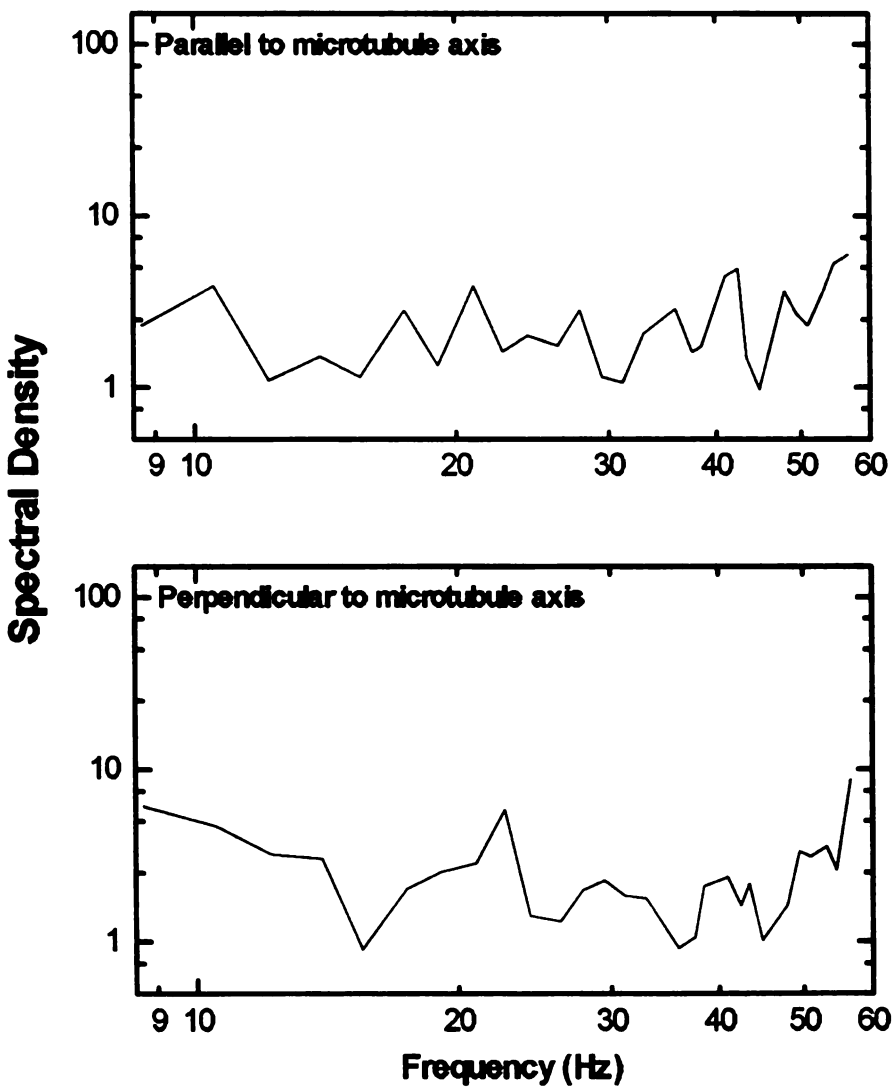

Fig. 5-7. Analysis of 14 microtubules driven by multiple kinesin motors. These microtubules are moving in the presence of 50 μM ATP and correspond to those shown in Fig. 3-6. Motion parallel to the microtubule axis as well as perpendicular to it are shown. At these slower velocities, the 95 Hz peak found at the higher ATP concentration should appear at about 47 Hz. There is not a significant peak near that frequency nor any others at this lower ATP concentration.

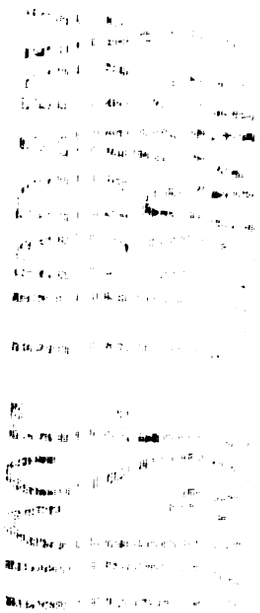

CHAPTER 6

CONCLUDING REMARKS

DISCUSSION OF RESULTS

Under a variety of conditions and motor densities, kinesin driven microtubule translocation appears essentially smooth when the only load on the microtubule is the viscous drag of the surrounding aqueous solution. There are no step-like features evident in records of microtubules driven by single kinesin motors, although it is still possible that steps spanning the minimum 8 nm distance between binding sites on the microtubule might exist. The analysis of the previous chapter sets some boundary limits on the nature of these 8 nm steps, namely that they occur at time intervals which are not completely stochastic but have a coefficient of variation greater than 0.2. The traces also contain almost no backward translations greater than the background diffusional noise. The absence of steps in the data would argue against models that incorporate steps larger than 8 nm or models in which kinesin rapidly moves forward several tubulin subunits during a single ATP hydrolysis. Purely diffusional models in which kinesin undergoes a random walk along the microtubule biased in one direction by the hydrolysis of ATP are also unlikely since few if any backward translations occur in the data.

What might be other explanations besides insufficient resolution for the lack of detectable step like movements in the data? Although, some of the

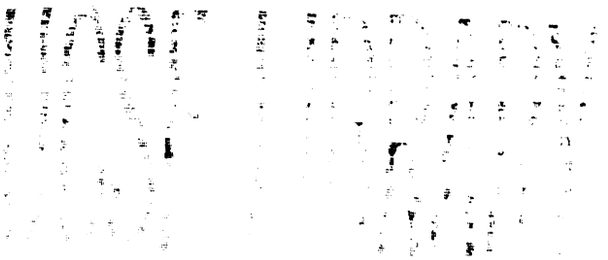

measurements represent the actions of a single kinesin molecule, the native molecule is made up of two identical heavy chains which each have a microtubule binding domains. In essence, one kinesin molecule contains two motors. It is possible that these two motor domains could interact to damp a large conformational change; however, the ATP concentration versus velocity curve suggests that the two heads do not interfere with one another. One would expect to observe steps at least a good portion of the time, which is not the case.

In addition to damping by a second kinesin head, the coupling between a power stroke and microtubule movement might be damped by elasticity in either the kinesin-microtubule-bead complex or tubulin bonds within the microtubule. Since strepavidin is small and the microtubule has a stiffness comparable to Plexiglas (Gittes, et al., 1993), the kinesin molecule itself probably represents the most elastic component in the system. This notion is supported by the finding that noise increases with decreasing numbers of motors attached to the microtubule. However, this flexibility may be an inherent property of motor proteins and required for motility. The myosin head also displays a similar flexibility in vitro (Toyoshima, 1991). The flexibility in the kinesin head might account for most of the increase in noise (~3-4 nm) when going from multiple motors to a single motor. While it is conceivable that this flexibility might mask 8 nm steps, it seems unlikely that it would mask steps larger than 8 nm.

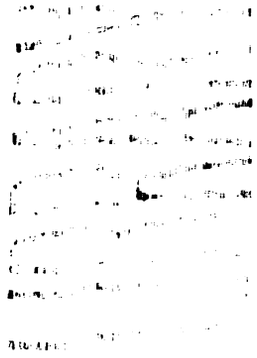

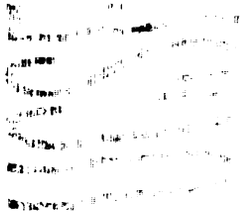

Another possibility, is that the power stroke occurs gradually over many milliseconds and is not at all abrupt. These slow power strokes would be difficult to distinguish on the traces from the random variation in velocity that occurs naturally. However, it is thought that the conformational changes occurring in proteins happen very rapidly, in the sub-millisecond time range (Levitt and Sharon, 1988). Movements occurring this time scale would appear virtually instantaneous with the data filtering used in these experiments.

Models of kinesin movement must account for the major features found in the records of kinesin driven movement, namely that the traces are relatively smooth, have no steps greater than 8 nm, and contain almost no backward translations greater than the background diffusional noise. A model for how two mechanically coordinated kinesin heads could move smoothly forward by biased diffusion is presented in the next section.

A MODEL FOR KINESIN DRIVEN MICROTUBULE MOTILITY

Besides accounting for the features found in high resolution measurements of kinesin driven motility, a model of kinesin movement must account for the following properties.

1) Kinesin moves along the microtubule in only one direction (Vale, et al., 1985b).

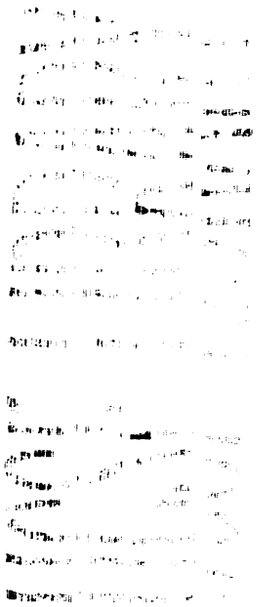

2) A single kinesin molecule can remain attached to a microtubule for 99.99% of the time, yet each head must detach in order to move forward (Block, et al., 1990; Howard, et al., 1989).

3) The velocity of microtubule translocation is constant regardless of the number of motors acting on the microtubule (Howard, et al., 1989).

4) A 45 kD proteolytic fragment containing the kinesin head has a 5 fold increased ATPase as well as a ten fold increased microtubule affinity (Kuznetsov, et al., 1989).

5) An E. Coli expressed motor fragment has an ATPase rate comparable to the native molecule in BRB80, yet in this buffer release from the microtubule is minimal in contrast to the native molecule. Optimal release requires upwards of 300 mM salt in addition to ATP (J. Kull, personal communication).

6) Measurements of kinesin motility using several ATP analogues reveal that the speed of motility is not related to the nucleotide hydrolysis rate (Shimizu, et al., 1991; T. Shimizu, personal communication).

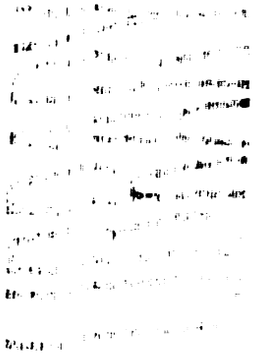



I hypothesize that the following general mechanism can account for all these points. Initially, start with both heads of a single kinesin molecule attached to the microtubule separated by a distance of 8 nm (see Fig. 6-1). The dimensions of the kinesin head are small enough to allow binding so close together. Furthermore, the dimensions of the kinesin head are such that a much greater separation is not probable. To begin, the forward head binds and hydrolyzes ATP resulting in a small conformational change in the head that levers it forward slightly. This conformational change can be much smaller than 8 nm; it must only be large enough to stretch a linkage between the two heads and create a tension on the second head. This tension induces dissociation of the trailing head from the microtubule. The key point in this model is that the trailing head must be pulled off the microtubule by tension generated by another kinesin head. In the absence of this tension, the affinity of the kinesin-microtubule binding interaction is strong enough to hinder dissociation from the microtubule even in the presence of nucleotide. The rate limiting step then becomes the detachment of the kinesin head from the microtubule.

Released from its binding site on the microtubule, the trailing head now seeks another binding site by a diffusional search. The cost in energy for the trailing head to return to its previous binding site is now high because it must stretch the spring linking the two heads together to do so. The linkage between the two heads might have the properties of an elastic band; the linkage is easily collapsible but tension increases when the band is stretched. Thus, more

energetically favorable binding sites lie forward of its previous site. Hence directionality is assured; the trailing kinesin head now binds to a binding site forward of the previously leading head and the cycle repeats.

An important corollary to the requirement for the leading kinesin head to pull off the trailing head is that a genetically engineered single-headed kinesin molecule ought not to move in a single motor assay. To date, low density motility assays with such engineered constructs have not been successful (S. Block, personal communication). A single-headed construct does move in a high density assay. The interpretation of this latter experiment is not straightforward, though, because the stiff microtubule can potentially also serve to transmit a force generating event to a neighboring kinesin head.

As described, the model can account for the characteristics of the high resolution measurements. The conformational change driving forward movement can be much smaller than the spacing between kinesin binding sites and consequently well below the resolution of the single motor records. Although the kinesin head searches for its next binding site by a diffusional search, the scope of the search is limited by the attachment of the other head, and thus few if any backward translations would occur. Finally, the movement would appear smooth since translation is mostly driven by forward diffusion of the kinesin head.

Now let us speculate how this model can account for the several findings laid out above.

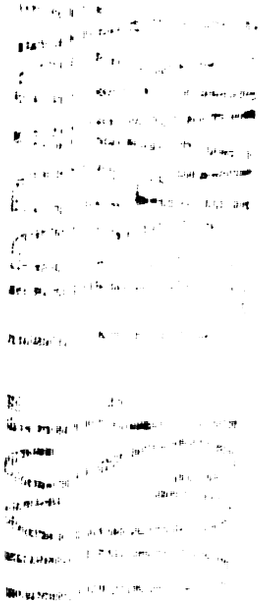

Finding #1 : Kinesin moves along the microtubule in only one direction.

As described in the preceding paragraph, the forward "ratcheting" motion of the leading head makes it energetically unfavorable to seek binding sites in the backwards direction. The magnitude of the displacement occurring during the ratcheting motion can be very small. If kinesin interacts with its binding site through ionic interactions, then when the trailing head is pulled less than 1 nm (a Debeye length) away from its binding site, it will be out of range of any electrostatic binding interaction. A conformational change on the order of 1-3 nm is more likely than one of 8 nm (spanning the entire distance between microtubule binding sites) for a protein domain whose dimensions are 9 by 3 nm (Hirokawa, et al., 1989).

Finding #2 : A single kinesin molecule can remain attached to a microtubule for 99.99% of the time, yet each head must detach in order to move forward.

This model makes detachment reliant on attachment of a the second head. Thus detachment of both heads simultaneously becomes unlikely.

Finding #3 : The velocity of microtubule translocation is constant regardless of the number of motors acting on the microtubule.

This phenomenon is unique to the kinesin motor; myosin does not behave this way. A computer simulation of kinesin motility (Pate and Cooke, 1991) based on the Huxley model (Huxley 1957) found that the only way to keep velocity independent of motor number is to set the detachment rate of the motor equal to the attachment rate. Making the detachment of the trailing head

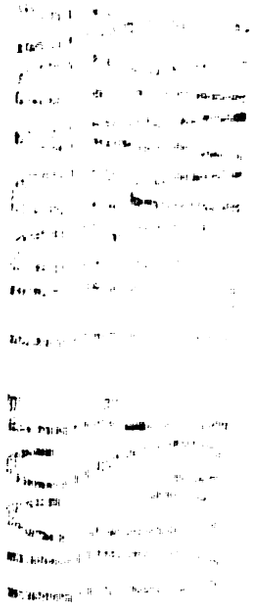

dependent on attachment of the leading head is one mechanism to explain this finding. Thus, each motor internally regulates its velocity and speed remains constant as more motors are added. Furthermore, if one kinesin head always maintains its attachment to the microtubule via a viscous coupling then as the velocity increases so does the restoring force.

Finding #4 : A 45 kD proteolytic fragment of the kinesin head has a 5 fold increased ATPase and a ten fold increased microtubule affinity.

This observation is surprising because it implies that the isolated kinesin head hydrolyzes ATP faster while still remaining strongly bound to the microtubule. One interpretation is that the kinesin head is undergoing several ATP hydrolysis cycles without detaching from the microtubule and therefore not performing any work. The proteolytic kinesin fragment is no longer coupled to another kinesin head. In this case, there is no tension applied to the kinesin head and as the model implies, the kinesin head remains attached to the microtubule.

Finding #5 : An E. Coli expressed motor fragment has an ATPase rate higher than the native molecule in BRB80, yet in this buffer, release from the microtubule is minimal in contrast to the native molecule. Optimal release requires upwards of 300 mM salt in addition to ATP.

Again, the force generating domain of kinesin in isolation has a higher affinity for the microtubule in the presence of ATP. This case is similar to the previous finding. While a trivial explanation of these findings is that the force

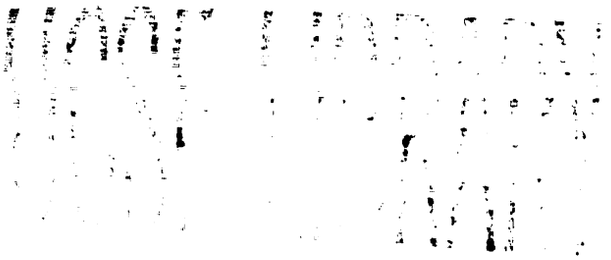

generating domain is not fully active. it is interesting to note that head fragments obtained by two different means have similar properties.

Finding #6 : Measurements of kinesin motility using several ATP analogues reveal that the speed of motility is not related to the nucleotide hydrolysis rate.

This finding implies again that nucleotide hydrolysis can take place without generating force. The explanation for this finding might be found in the myosin structure. In myosin as well as other ATPases, the nucleotide binds in a cleft of the protein and the energy of binding probably forces the cleft to close. This conformation change probably drives subsequent events in force generation. Different nucleotide analogues might bind to the cleft with less energy, hydrolyze early, and prevent the cleft from reaching its full closure. If the cleft does not completely close before nucleotide hydrolysis occurs, then perhaps the motor would not be able to generate sufficient force to pull the other kinesin head off the microtubule.

This proposed model is currently speculative, although based on careful consideration of different aspects of kinesin motility. It provides a framework for the conceptualization of kinesin motility and suggests experiments with which to test these ideas. For example, by engineering a spacer between the kinesin head and the stalk, one might be able to reduce the effectiveness with which the two heads are coupled together. This spacer should cause the biochemical properties of the altered two-headed kinesin to more resemble those of the single-headed species, and the effect should be dependent on the length of

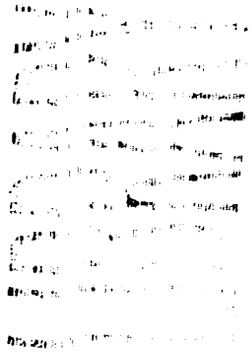

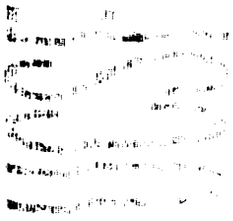

the linker. More careful examination of the number of single headed kinesin molecules required for microtubule motility, may also be useful.

FUTURE DIRECTIONS

The microscope developed for these studies of kinesin motility can be further used to examine the motile properties of other microtubule motors. Some dynein motors move much faster than kinesin and in the presence of vanadate bind the microtubule in an unusual fashion, allowing the microtubule to undergo one dimensional diffusion in the axis along its length.

As it is possible to bacterially express kinesin in an active form, the microscope could be used to look at the motile properties of mutant kinesin proteins. Also with the addition of a pulsed UV laser, one can rapidly uncage ATP and ask how quickly does kinesin begin move, possibly revealing whether force generation occurs early or late in the kinesin ATPase cycle. Finally, the addition of a laser force trap to the microscope might facilitate measurements of single motor force production (Ashkin, et al., 1990; Block, 1992).

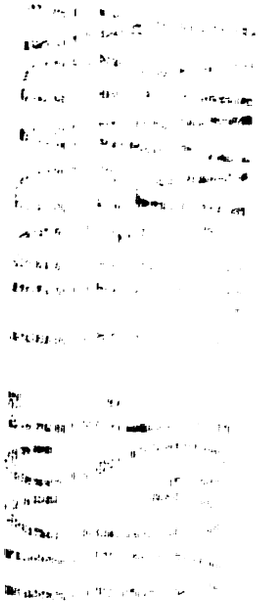

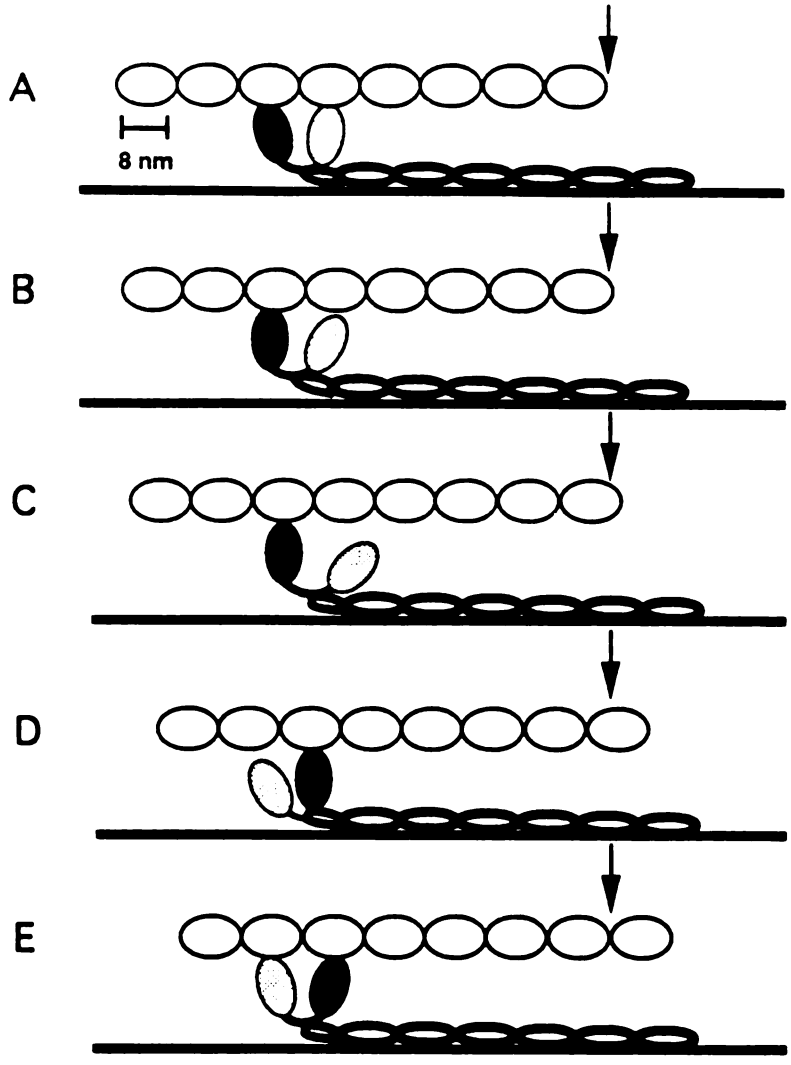

Fig. 6-1. A model for kinesin-based motility. The arrow indicates a stationary reference point for the movement of the microtubule. Both kinesin heads initially are bound to adjacent tubulin dimers on a protofilament. The forward head undergoes a small conformational change (here depicted as a forward rotation) which creates a strain on the partner head and pulls it from its binding site. The dissociated head undergoes a diffusional search for a new microtubule binding site; attachment to the forward site is favored over the previous site, since the latter case would require straining the linkage between the two heads. Upon rebinding if the second head, the microtubule moves forward to balance tensions on the two heads.

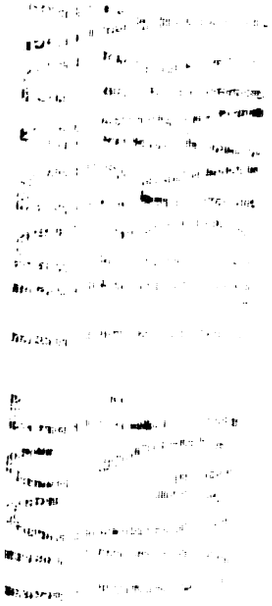

REFERENCES

Allen, R. D., Allen, N. S. and Travis, J. L. (1981). **Video-enhanced differential interference contrast (AVEC-DIC) microscopy: A new method capable of analyzing microtubule-related movement in the reticulopodial network of *Allogromia laticollaris*.** Cell Motil. *1*, 291-302.

Ashkin, A., Schulze, K., Dziedzic, J. M., Euteneur, U. and Schliwa, M. (1990). **Force generation of organelle transport measured in vivo by an infared laser trap.** Nature *348*, 346-348.

Becker, R.A., Chambers, J.M., and Wilks, A.R. (1989) **The new S language.** Wadsworth Inc., Pacific Grove, CA.

Block, S. M. (1992). **Making light work with optical tweezers.** Nature *360*, 493-495.

Block, S. M., Goldstein, L. S. and Schnapp, B. J. (1990). **Bead movement by single kinesin molecules studied with optical tweezers.** Nature *348*, 348-352.

Brady, S. T. (1985). **A novel brain ATPase with properties expected for the fast axonal transport motor.** Nature *317*, 73-75.

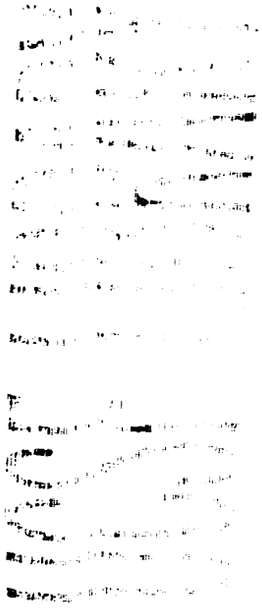

Cooke, R. (1986). **The mechanism of muscle contraction.** CRC Crit. Rev. Biochem. *21*, 53-118.

Cooke, R., Croder, M. S., Wendt, C. H., Barnett, V. A. and Thomas, D. D. (1984). **Muscle cross-bridges: do they rotate?** In Contractile mechanisms in muscle, G. H. Pollack and H. Sugi, ed., Plenum Publishing Corporation, pp. 413-427.

Cordova, N. J., Ermentrout, B. and Oster, G. F. (1992). **Dynamics of single-motor molecules: the thermal ratchet model.** Proc. Natl. Acad. Sci., USA *89*, 339-343

Eisenberg, E. and Greene, L. (1980). **The relation of muscle biochemistry to muscle physiology.** Ann. Rev. Physiol. *42*, 293-309.

Eisenberg, E. and Hill, T.L. (1985). **Muscle contraction and free energy transduction in biological systems.** Science *277*, 999-1006.

Gelles, J., Schnapp, B. J. and Sheetz, M. P. (1988). **Tracking kinesin-driven movements with nanometre-scale precision.** Nature *331*, 450-453.

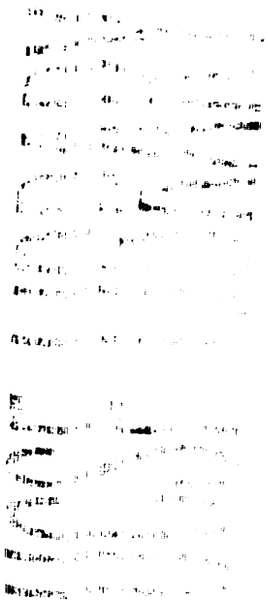

Gittes, F., Mickey, B., Nettleton, J., Howard, J. (1993). **Flexural rigidity of microtubules and actin filaments measured from thermal fluctuations in shape.** J. Cell Biol. *120*, 923-934.

Goldman, Y. E., Hibberd, M. G. and Trentham, D. R. (1984). **Initiation of active contraction by photogeneration of adenosine-5'-triphosphate in rabbit psoas muscle fibres.** J. Physiol. *354*, 605-624.

Hackney, D. D. (1988). **Kinesin ATPase: Rate-limiting ADP release.** Proc. Natl. Acad. Sci. USA *85*, 6314-6318.

Hackney, D. D., Malik, A.-S. and Wright, K. W. (1989). **Nucleotide-free kinesin hydrolyzes ATP with burst kinetics.** J. Biol. Chem. *264*, 15943-15948.

Harada, Y., Noguchi, A., Kishino, A. and Yanagida, T. (1987). **Sliding movement of single actin filaments on one-headed myosin filaments.** Nature *326*, 805-808.

Harrison, B.C., Marchese-Ragona, S.P., Gilbert, S.P., Cheng, N., Steven, A.C., Johnson, K.A. (1993). **Decoration of the microtubule surface by one kinesin head per tubulin heterodimer.** Nature, *362*, 73-75.

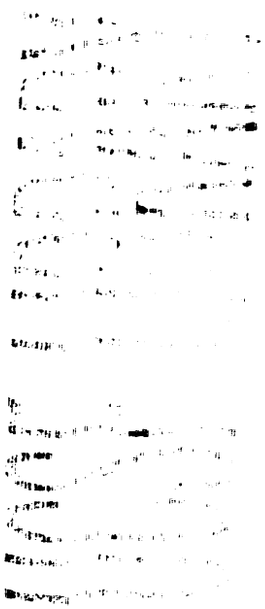

Hirokawa, N., Pfister, K. K., Yorifuji, H., Wagner, M. C., Brady, S. T. and Bloom, G. S. (1989). **Submolecular domains of bovine brain kinesin idenfied by electrom microscopy and monoclonal antibody decoration.** Cell 56, 867-878.

Holmes, K.C., Popp, D., Gebhard, W., Kabsch, W. (1990). **Atomic model of the actin filament.** Nature *347*, 44-49.

Howard, J. and Hudspeth, A. J. (1987). **Mechanical relaxation of the hair bundle mediates adaption in mechanoelectrical transduction by the bullfrog's saccular hair cell.** Proc. Natl. Acad. Sci. USA *84*, 3064-3068.

Howard, J., Hudspeth, A. J. and Vale, R. D. (1989). **Movement of microtubules by single kinesin molecules.** Nature 342, 154-158.

Huxley, A. F. (1957). **Muscle structure and theories of contraction.** Prog. Biophys. Chem. 7, 255-318.

Huxley, A. F. and Simmons, R. M. (1971). **Proposed mechanism of force generation in striated muscle.** Nature 233, 533-538.

Huxley, H. E. (1969). **The mechanism of muscular contraction.** Science *164*, 1356-1364.

MOST LIBRARY

Hyman, A., Dreschel, D., Kellogg, D., Salser, S., Sawin, K., Steffen, P., Wordeman, L. and Mitchison, T. (1991). **Preparation of modified tubulins.** Meth. Enzym. *196*, 478-485.

Ishijma, A., Doi, T., Sakurada, K. and Yanagida, T. (1991). **Sub-piconewton force fluctuations of actomyosin in vitro.** Nature *352*, 301-306.

Kabsch, W., Mannherz, H.G., Suck, D., Pai, E.F., Holmes, K.C. (1990). **Atomic structure of the actin:DNase I complex.** Nature, *347*, 37-44.

Kamimura, S. and Kamiya, R. (1989). **High-frequency nanometre-scale vibration to 'quiescent' flagellar axonemes.** Nature *340*, 476-478.

Kamimura, S. and Mandelkow, E. (1992). **Tubulin protofilaments and kinesin-dependent motility.** J. Cell Biol. *118*, 865-875.

Kerwin B., Bandman E. (1991). **Assembly of avian skeletal muscle myosins: evidence that homodimers of the heavy chain subunit are the thermodynamically stable form.** J. Cell Biol., *113*, 311-20.

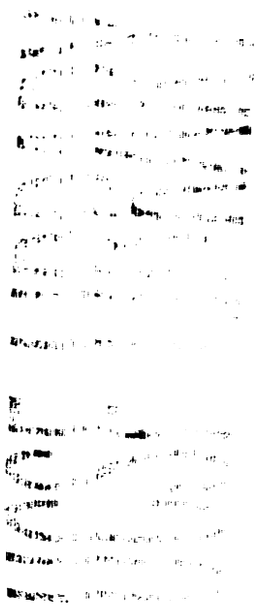

Kron, S. J. and Spudich, J. A. (1986). **Fluorescent actin filaments move on myosin fixed to a glass surface.** Proc. Natl. Acad. Sci. USA *83*, 6272-6276.

Kuo, S.C., Sheetz, M.P. (1993). **Force of single kinesin molecules measured with optical tweezers.** Science, *260*, 232-234.

Kuznetsov, S. A., Vaisberg, Y. A., Rothwell, S. W., Murphy, D. B. and Gelfand, V. I. (1989). **Isolation of a 45-kDa fragment from the kinesin heavy chain with enhanced ATPase and microtubule-binding activity.** J. Biol. Chem. *264*, 589-595.

Levitt, M., Sharon, R. (1988). **Accurate simulation of protein dynamics in solution.** Proc. Natl. Acad. Sci. USA *85*, 7557-7561.

Lymn, R. W. and Taylor, E. W. (1971). **Mechanism of adenosine triphosphate hydrolysis by actomyosin.** Biochemistry *10*, 4617-4624.

Mandelkow, E.-M., Schultheiss, R., Rapp, R., Muller, M. and Mandelkow, E. (1988). **On the surface lattice of microtubules: helix starts, protofilament number, seam, and handeness.** J. Cell Biol. *102*, 1067-1073.

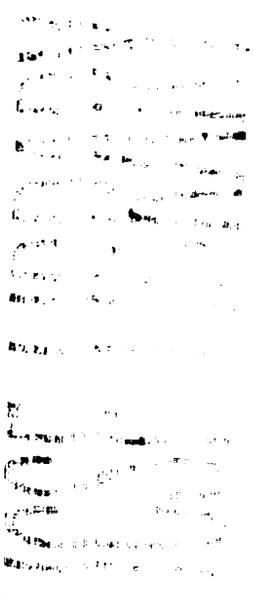

Oosawa, F. and Hayashi, S. (1986). **The loose coupling mechanism in molecular machines of living cells.** Adv. Biophys. *22*, 151-183.

Pate, E. and Cooke, R. (1991). **Simulation of stochastic processes in motile crossbridge systems.** J. Musc. Res. Cell Motil. *12*, 376-393.

Ray, S., Meyhofer, E., Milligan, R. A. and Howard, J. (1993). **Kinesin follows the microtubule's protofilament axis.** J. Cell Biol. *121*, 1083-94.

Rayment, I., Holden, H.M., Whittaker, M., Yohn, C.B., Lorenz, M., Holmes, K.C., Milligan, R.A. (1993a). **Structure of the actin-myosin complex and its implications for muscle contraction.** Science, *261*, 58-65.

Rayment, I., Rypniewski, W.R., Schmidt-Base, K., Smith, R., Tomchick, D.R., Benning, M.M., Winkelmann, D.A., Wesenberg, G., Holden, H.M. (1993b). **Three-dimensional structure of myosin subfragment-1: a molecular motor.** Science, *261*, 50-58.

Romberg, L. and Vale, R. (1993). **Chemomechanical cycle of kinesin differs from that of myosin.** Nature *361*, 168-170.

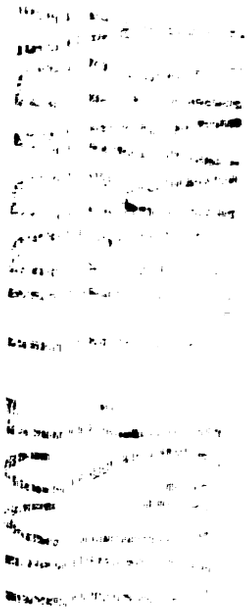

*Sadhu, A. and Taylor, E. W. (1992). **A kinetic study of the kinesin ATPase.** J. Biol. Chem. *267,* 11352-11359.

Schnapp, B. J. and Reese, T. S. (1989). **Dynein is the motor for retrograde axonal transport of organelles.** Proc. Natl. Acad. Sci. USA *86,* 1548-1552.

Scholey, J. M., Heuser, J., Yang, J. T. and Goldstein, L. S. B. (1989). **Identification of globular mechanochemical heads of kinesin.** Nature *338,* 355-357.

Schroder, R.R., Manstein, D.J., Jahn, W., Holden, H., Rayment, I., Holmes, K.C., Spudich, J.A. (1993). **Three-dimensional atomic model of F-actin decorated with Dictyostelium myosin S1.** Nature, *364,* 171-174.

Shimizu, T., Furusawa, K., Ohashi, S., Toyoshima, Y., Okuno, M., Malik, F. and Vale, R. D. (1991). **Nucleotide specificity of the enzymatic and motile activities of dynein, kinesin, and heavy meromyosin.** J. Cell Biol. *112,* 1189-1197.

Skoufias, D.A., Scholey, J.M. (1993) **Cytoplasmic microtubule-based motor proteins.** Current Opinion in Cell Biology, *5,* 95-104.

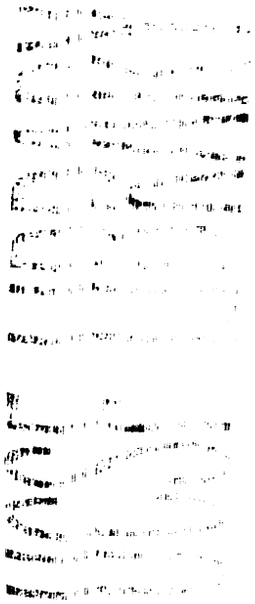

Song, Y.-H. and Mandelkow, E. (1993). **Recombinant kinesin motor domain binds to beta-tubulin and decorates microtubules with a B surface lattice.** Proc. Natl. Acad. Sci. U.S.A. *90*, 1671-1675.

Spudich JA. (1990). **Optical trapping: Motor molecules in motion.** Nature, *348*, 284-285.

Taylor, E. W. (1992). **Mechanism and Energetics of Actomyosin ATPase.** In Heart and Cardiovascular System,2, H. A. Fozzard, ed. (New York: Raven Press), pp. 1281-1293.

Titus, M.A. (1993). **Myosins.** Current Opinion in Cell Biology, *5*, 77-81.

Toyoshima YY. (1991). **Flexibility in actin-myosin motility system revealed by in vitro motility assay.** Advances in Biophysics, *27*, 213-20.

Toyoshima YY. (1991) **Bidirectional movement of actin filaments along tracks of heavy meromyosin and native thick filaments.** Journal of Cell Science. Supplement, *14*, 83-85.

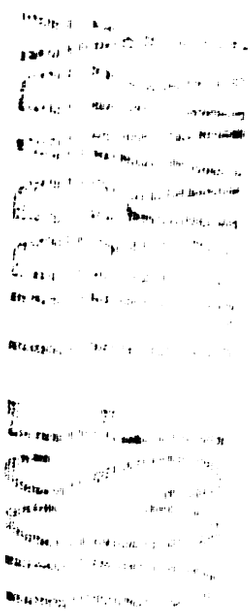

Toyoshima, Y. Y., Kron, S. J., McNallay, E. M., Niebling, K. R., Toyoshima, C. and Spudich, J. A. (1987). **Myosin subfragment 1 is sufficient to move actin filaments in vitro.** Nature *328*, 536-539.

Toyoshima, Y. Y., Kron, S. J. and Spudich, J. A. (1990). **The myosin step size: measurement of the unit displacement per ATP hydrolyzed in an in vitro assay.** Proc. Natl. Acad. Sci. USA *87*, 7130-7134.

Uyeda, T. Q., Kron, S. J. and Spudich, J. A. (1990). **Myosin step size. Estimation from slow sliding movement of actin over low densities of heavy meromyosin.** J. Mol. Biol. *214*, 699-710.

Uyeda, T. Q. P., Warrick, H. M., Kron, S. J. and Spudich, J. A. (1991). **Quantized velocities at low myosin densities in an in vitro motility assay.** Nature *352*, 307-311.

Vale, R. D. (1990a). **Microtubule-based motor proteins.** Current Opinion in Cell Biology 2, 15-22.

Vale, R. D. and Goldstein, L. S. B. (1990). **One motor, many tails: an expanding repertoire of force-generating enzymes.** Cell *60*, 883-885.

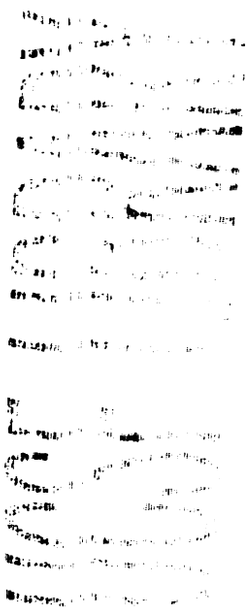

Vale, R. D. and Oosawa, F. (1990). **Protein motors and Maxwell's demons: does mechanochemical transduction involve a thermal ratchet?** Adv. Biophys. *26,* 97-134.

Vale, R. D., Reese, T. S. and Sheetz, M. P. (1985a). **Identification of a novel force-generating protein, kinesin, involved in microtubule-based motility.** Cell *42,* 39-50.

Vale, R. D., Schnapp, B. J., Mitchison, T., Steuer, E., Reese, T. S. and Sheetz, M. P. (1985b). **Different axoplasmic proteins generate movement in opposite directions along microtubules in vitro.** Cell *43,* 623-632.

Yanagida T. (1990). **Loose coupling between chemical and mechanical reactions in actomyosin energy transduction.** Advances in Biophysics, *26,* 75-95.

Yanagida, T., Arata, T. and Oosawa, F. (1985). **Sliding distance of actin filament induced by a myosin crossbridge during one ATP hydrolysis cycle.** Nature *316,* 366-369.

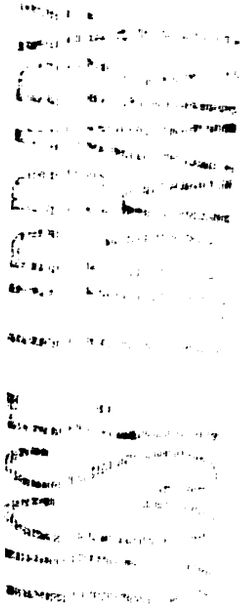

Yang, J. T., Laymon, R. A. and Goldstein, L. S. B. (1989). **A three-domain structure of kinesin heavy chain revealed by DNA sequence and microtubule binding analyses.** Cell *56*, 879-889.

Yang, J. T., Saxton, W. M., Stewart, R. J., Raff, E. C. and Goldstein, L. S. (1990). **Evidence that the head of kinesin is sufficient for force generation and motility in vitro.** Science *249*, 42-47.

NOT LIBRARY

APPENDIX

BIOCHEMICAL METHODS

KINESIN PREPARATION

The kinesin used for the motility experiments was purified from squid optic lobes by microtubule affinity (Vale, et al., 1985a) followed by sucrose gradient sedimentation. In summary, native squid tubulin is polymerized into microtubules out of a high speed optic lobe supernatent. Depleting the supernatent of ATP with apyrase and adding AMP-PNP promotes kinesin binding to the microtubules which are then pelleted out of the supernatent. Kinesin is released and separated from the microtubules by adding ATP to the microtubules, repelleting, and collecting the supernatent which now contains kinesin. A sucrose density gradient further purifies the kinesin to roughly 90% homogeneity. A byproduct of the preparation is a second motor, cytoplasmic dynein, which is collected from another part of the gradient (Schnapp and Reese, 1989).

Preparation of Squid Optic Lobe Kinesin and Dynein

Squid Buffer

K Aspartate	175 mM	Taurine	65 mM
Betaine	85 mM	Glycine	25 mM
Hepes	20 mM	$MgCl_2$	6.4 mM
EGTA	5 mM		

pH to 7.2 (room temp) with KOH

Protease Inhibitor Stocks

PMSF	100 mM (100x stock in 100% ETOH)
leupeptin	1 mg/ml (100x stock in H2O)
TAME	1 mg/ml (100x stock in DMSO)

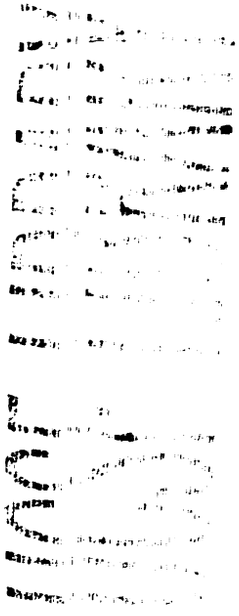

Miscellaneous Stocks

ATP	100 mM
DTT	100 mM
AMP-PNP	100 mM
Taxol	4 mM
Apyrase	Lyophylized powder

Protocol

1. Weigh about 30 g worth of squid optic lobes stored in liquid nitorgen. Add to lobes 1.5 vol/wt of squid buffer, protease inhibitors, 0.5 mM ATP, and 1 mM DTT.

2. Homogenize on ice with 20 strokes in a Dounce (B pestle) and then 20 strokes with the A pestle. Spin homogenate in a Beckman 60Ti rotor at 4 C; 55,000 rpm for 60 min.

3. Carefully remove supernatent. Discard pellet. Warm supernatent slowly to room temperature, then add 20 μM taxol (to promote microtubule formation), 100 μM AMP-PNP (to promote kinesin binding to microtubules), and 4 units/ml apyrase (to deplete ATP and also promote kinesin binding to microtubules) to supernatent. Incubate for 45 min. at room temperature. Layer supernatent over approximately an equal volume 20% sucrose (made using squid buffer) cushion containing 10 μM taxol. Spin in a Beckman 70Ti rotor at 22 C; 40,000 rpm for 60 min.

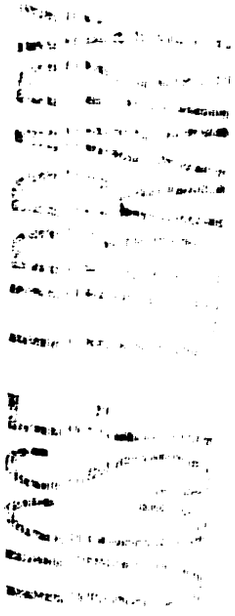

4. Remove supernatent and discard. To wash pellets, resuspend pellets in 15 mls of squid buffer, with protease inhibitors, 1 mM DTT, and 10 μM taxol added. Spin in a Beckman 70Ti rotor at 22 C; 40,000 rpm for 40 min.

5. Remove supernatent and discard. Resuspend pellets in 2 mls of squid buffer, wiht protease inhibitors, 1 mM DTT, and 10 uM taxol added. Then add 10 mM MgATP (add 10 mM $MgCl_2$ and 10 mM ATP to suspension). Incubate at room temperature for 30 minutes. Spin in Sorvall SS34 rotor at 22 C; 18,000 rpm for 30 min. If available, a Beckman TL100 tabletop ultracentrifuge can also be used with better results. Spin in TLA100 rotor at 22 C; 40,000 rpm for 20 min.

6. Pour two 5-20% sucrose gradients in squid buffer of 10 mls each in tubes for the Beckman SW41 swinging bucket rotor. Add 1 mM DTT and protease inhibitors to sucrose solutions before making gradients. Layer supernatent from previous spin (1 to 1.5 ml max) on top of gradients. Spin at 4 C; 37,000 rpm for 12 hours.

7. Fractionate gradients into 1 ml tubes, run gels and do motility assays. Aliquot, quick freeze in liquid N_2 and store in liquid N_2. The kinesin is stable for several months frozen in this manner.

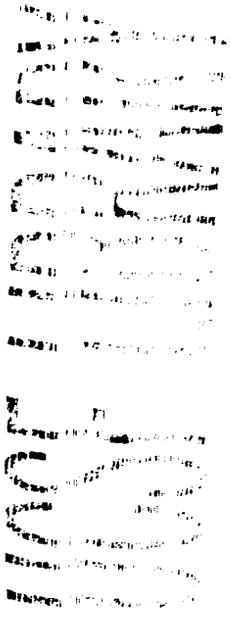

TUBULIN PREPARATION

The tubulin used in all motility experiments was prepared from bovine brain. The preparation is according to the method of Weingarten, et al. (1974) as modified by Hyman, et al. (1991).

Preparation of Bovine Brain Tubulin

MES Buffer (MB) 4L			Pipes Buffer (PB) 1L			Column Buffer (CB) 4L		
K MES	100 mM	pH 6.5	K Pipes	100 mM	pH 6.8	K Pipes	50 mM	pH 6.8
$MgCl_2$	0.5 mM		$MgCl_2$	0.5 mM		$MgCl_2$	0.2 mM	
EGTA	2 mM		EGTA	2 mM		EGTA	1 mM	
EDTA	0.1 mM		EDTA	0.1 mM		GTP	0.01 mM	

BRB80 Conversion Buffer (50 mls)
K Pipes 630 mM pH6.8
$MgCl_2$ 16.8 mM
EGTA 1 mM
Add 1 part to 20 parts CB to make BRB80.

PMSF stock = 100 mM made in 100% ETOH.

Protocol

1. Strip meninges and clots from ten fresh brains. Weigh brains and add 1.0 volume/weight of **MB** with 1 mM ATP, 0.1 mM GTP, and 1 mM PMSF. Add BME to 0.1%. Put into blender. This step will require approximately 3L of MB. Homogenize in 4x15 sec bursts. Pour into bottles for GSA rotor. You will need 5 rotors. Spin at 12000 rpm, 50 min. at 4 C. Warm Type 19 rotors to 37 C for next spin.

2. Decant supernatent into a large graduated cylinder, add glycerol (prewarm to 37 C) to 33% (1/2 vol), $MgCl_2$ to 3 mM, ATP to 1.0 mM, and GTP to

UCSF LIBRARY

0.1 mM. Pour into a 6 liter flask. Warm to 37 C under a hot running tap. Monitor temperature. Place in water bath at 37 C. Incubate for 40 min at 37 C. Polymerization in glycerol starts at 29 C.

3. Pour into tubes for Type 19 rotor. Fill all the way to the tip top, otherwise the tubes will implode upon spinning. Spin in 3 Type 19 rotors at 19,000 rpm for 2.5 hrs at 35 C. Cool ultras afterwards for next spin.

4. Resuspend pellets in 500 mls **PB** with 0.1 mM GTP and BME to 0.1%. Total volume should be less than 750 mls. Homogenize pellets with dounce and type A (tight) pestle. Place on ice for 40 minutes. Then spin at 40,000 rpm at 4 C in 2 x 45Ti rotors (Use red caps on tubes). Save supernatent (approximately 600 mls). Warm ultras for next spin.

5. Add warm glycerol to 33%, GTP to 1 mM, and $MgCl_2$ to 3 mM. Incubate as before for 40 min. at 37 C. At this point the volume is approximately 900 mls. Spin 40,000 rpm for 30 minutes in 3 x 45Ti rotors at 35 C.

6. Resuspend pellets in CB with 0.1 mM GTP and 0.1% BME to a protein concentration of approximately 20 - 30 mg/ml (between 100 - 200 mls). Dounce well and chill on ice for 40 minutes. Spin at 40,000 rpm for 30 minutes in a 45 Ti rotor.

7. Load supernatent onto a 1 x 800 ml (7.5 mm I.D.) phosphocellulose column equilibrated in CB (Load ~ 2500 mg in 160 mls). Run column at 7 mls/min. Collect flow through, this will contain the tubulin.

8. Pool peaks. Convert buffer to BRB80 and 0.1 mM GTP. Quick freeze in liquid nitrogen. Store at -80 C. Tubulin lasts for years when stored this way.

UCSF LIBRARY

LABELING TUBULIN WITH BIOTIN

The modification of tubulin with N-hydroxysuccinimide (NHS) biotin occurs at lysine residues on the surface of the tubulin dimer. Using polymerized microtubules as the substrate for the labeling reaction prevents the modification of sites on the tubulin dimer which form tubulin-tubulin contacts. Successive cycles of depolymerization and repolymerization act to separate functional tubulin from inactivated tubulin. The method described below is from Hyman, et al. (1991).

Preparation of Biotin-Modified Tubulin

1. Prepare a 100 mg/ml solution of long-chain NHS-biotin (Molecular Probes; Eugene, Ore.) in "dry" DMSO (Aldrich, Milwaukee, WI).

2. Polymerize freshly thawed monomeric tubulin (Total of 20-30 mgs of tubulin) into microtubules by adding glycerol to 33%, 5 mM $MgCl_2$, and 1 mM GTP. Warm to 37 C for 20 minutes.

3. Add long-chain NHS-biotin at 10 ul per 1 ml of MT solution. Incubate for 20 minutes at 37 C. Add Kglutamate (pH 6.8) to 10 mM to stop the reaction.

4. Sediment microtubules through about 4 mls of a 50% sucrose cushion in BRB80 (pre-warm to 35 C) by spinning in a Ti60 rotor at 50,000 rpm for 1 hour at 35 C (Pre-warm rotor and centrifuge).

UCSF LIBRARY

5. Discard supernatent. Resuspend pellet in BRB80 (see tubulin prep for buffer composition) + 20 mM Kglutamate. Collect pellets into one tube in about a fifth of the original volume. Break apart the pellet with a spatula first, then gently pass the solution through a 25 gauge needle several times to break up microtubules. Be careful not to foam the solution. Incubate on ice for 20-30 minutes to depolymerize tubulin. Centrifuge in Ti60 rotor for 20 minutes at 40,000 rpm at 4 C.

6. Collect supernatants and polymerize with 1 mM GTP, 5 mM MgCl2 and 33% glycerol final concentration. Incubate at 37 C for 20-30 minutes. Prepare a 50% sucrose cushion as described above. Centrifuge 50,000 rpm for 1 hour at 35 degrees.

7. Resuspend pellet in a tenth of the original volume of BRB80. Resuspend as before with a syringe and needle. Incubate on ice for 20 minutes.

8. Perform the final cold centrifugation with a Ti60 rotor as before or using a cold airfuge, spin for 10 minutes at maximum psi.

9. This is once-cycled biotinylated tubulin. Quick freeze in small aliquots (e.g. 4 ul) using liquid N_2 and store at -80 C. The tubulin will last indefinitely.

LABELING LATEX MICROSPHERES WITH STREPAVIDIN

The 100 nm latex microspheres used to label microtubules have a surface modified with carboxyl groups. In a two step process, the surface is activated with a bifunctional crosslinker, 1-ethyl-3-(3-dimethylaminopropyl)carbodiimide (EDC); one end of the crosslinker is bound to the surface carboxy group while the other end is protected with N-hydroxysulfosuccinimide (sulfo-NHS). Free cross linker is removed from the solution by successive centrifugation and pelleting of the microspheres. Strepavidin is then added to the surface-activated microspheres; the sulfo-NHS is displaced by strepavidin which binds to the free end of the crosslinker. By using a two step process to rinse out free crosslinker; the problem of crosslinking microspheres together is prevented. Thus, potentially damaging sonication is not needed to break up aggregates of microspheres. This improved protocol for labelling carboxy-modified latex microspheres was developed by myself with the advice of Tim Mitchison for use in these studies.

Preparation of Strepavidin Labeled Latex Microspheres

Materials

CML microspheres - Interfacial Dynamics Corp., Portland, Ore. (800 323-4810)
EDC - Pierce, Rockford, IL
sulfo-NHS - Pierce
Strepavidin - Molecular Probes, Eugene, Ore.

500 mM MES pH to 7.0 with KOH (4.88g/50mls)

Protocol

1. Add 0.1 ml 500 mM MES to 0.9 ml CML microspheres in a 1.5 ml tube.

2. Into another tube weigh out 4 mg EDC and 4 mg sulfo-NHS.

3. Rapidly put the contents of first tube into the second and rapidly mix by pipeting up and down several times. Let sit at room temperature for 20 minutes.

4. To wash microspheres, add 2 mls of 50 mM MES. Spin beads to pellet them. This can be tricky depending on the size of the bead. For 100 nanometer beads, I spin for 5 minutes at 80,000 rpm in a TLA 100.3 rotor. It is best to test what is necessary to pellet the microspheres prior to the labeling. After pelleting, resuspend beads in 3 mls 50 mM MES. Pellet again as before. Resuspend in 3 mls as before. Pellet once more and resuspend in only 1 ml 50 mM MES. This step should take less than 90 minutes.

5. Weigh into a tube 1 mg strepavidin. Add the beads to this tube rapidly, pipeting up and down several times to mix well. Let sit at room temperature for 2 hours. Pellet as before 2 times, resuspending in 50 mM MES.

6. Finally, spin beads for 5 minutes in a low speed benchtop microfuge at top speed to remove any aggregates leftover in solution. Store beads at 4 C. If desired add 0.05% azide. The beads remain useful for labeling microtubules for up to 2 months. Aggregates can be removed by occasionally repeating the previous step.

LABELING MICROTUBULES WITH LATEX MICROSPHERES

In order to label biotin modified microtubules with strepavidin labeled microspheres with high efficiency, it is essential to remove free tubulin monomers left over from the polymerization process by pelleting the microtubules through a sucrose cushion. A low speed microfuge is used because the resulting pellet is easy to resuspend, preventing microtubule breakage.

Labeling Microtubules with Strepavidin Labeled Latex Microspheres

1. In an microfuge tube mix tubulin and biotin-labeled tubulin at a 4:1 molar ratio to a final total tubulin concentration of 6 mg/ml and a volume of 20 μl. Then, add an equal volume of polymerization mix (6 mM $MgCl_2$, 20% DMSO, and 2 mM GTP in BRB80). Polymerize at 37C for 20 minutes. Return to room temperature and quickly add taxol to 20 μM.

2. In a 0.5 ml microfuge tube, layer polymerized microtubules over 100 μl of 40% sucrose in BRB80 with 10 μM taxol added. Spin in benchtop microfuge at top speed for 20 minutes. Be sure to orient tube so as to remember where the pellet will form since the pellet will be almost invisible.

3. Remove and discard supernatent. Add 100 μl BRB80 with 16 μM taxol added. The above steps remove excess unpolymerized tubulin.

4. Split microtubules into 5 aliquots of 20 μl each. The stock concentration of microspheres is most likely too high; hence, prepare aliquots of diluted microspheres. Dilute with BRB80 ranging from 1:2 to 1:100. Add 4 μl of each microsphere dilution to different microtubule aliquots.

5. After about 1 hour, assay for labeling by microscopy. The ideal labeling is to have one microsphere per microtubule. Labeled microtubules can be used for two to three days.

THE LIBRARY
University of California, San Francisco

This book is due on the last date stamped below.
Patrons with overdue items are subject to penalties.
Please refer to the Borrower's Policy for details.
For phone renewals – call (415) 476-2335
within five days **before** the due date.
All items are subject to recall after 7 days.

RETURNED
JUN 17 1996

Series 4128 R110118 10/95

For reference

Not to be taken from the room.

617362

3 1378 00617 3622

UC San Francisco LIBRARY
UNIVERSITY OF CALIFORNIA · UNIVERSITY OF CALIFORNIA